School of Chemical and Petroleum Engineering

Department of Chemical Engineering

Graphene Oxide & Graphene Based Catalysts in Photochemical Reactions

Shizhen Liu

This thesis is presented for Degree of

Master of Philosophy

of

Curtin University

May 2013

Declaration

To the best of my knowledge and belief this thesis contains no material previously published by any other person except where due acknowledgment has been made. This thesis contains no material which has been accepted for the award of any other degree or diploma in any university.

Shizhen Liu

Acknowledgement

My enthusiastic gratitude must be presented to my supervisor professor Shaobin Wang who supports me with extremely worthy instruction, patience and rigorous attitudes to complete this research work. His intelligence brings me into an absolutely novel realm with passions and supervision.

My deepest gratitude must also go to my co-supervisor professor Shaomin Liu whose knowledge always gives me inspiration. I really thank him for always paying such attention on my study and life in Australia to support me finishing my master degree.

I also want to thank Professor Ming Ang who is the chairman of my thesis. I must say without help from him I cannot have this precious opportunity to study as a researcher and such an achievement in my work.

I would like to thank Dr Hongqi Song; he looks after me like a real young brother. His diligent, conscientious attitude on research really impresses me. He helps me resolve so many problems on my study and teaches me to be a real researcher.

I also want to thank Dr Yunjin Yao who provided me support in the initial works.

I am also grateful to my colleagues and friends, particularly Guanliang, Eddy and Hussein who have helped me on various occasions for fulfillment of this thesis.

I am also thankful to all laboratory technical staff, Karen Haynes, Jason Write and Ann Carroll for their technical support.

Finally I specially thank my parents for anything they give to me, thank them to give me infinite encourage and finical support for so many years, and thank them to give me a life to see this beautiful world by my eyes.

Abstract

Graphene has impressible absorbing ability and its electron transmission capacity makes it a great prosperity in many science horizons. In this study graphene or graphite nitride has been employed as a carrier in order to modify TiO_2, ZnO and Ta_2O_5 photocatalysts.

Graphene modified TiO_2 particles were obtained by a sol-gel method from titanium isoproproxide (or P25) and reduced graphene oxide (RGO). The X-ray diffraction (XRD), Fourier transform infrared spectroscopy (FT-IR), field emission scanning electron microscopy (FE-SEM), UV-vis diffuse reflectance (UV-vis DRS) and thermo gravimetric differential thermal analysis (TG-DTA) were investigated over the samples. The diffuse reflectance spectra (DRS) studies indicate that G-TiO_2 has a significant light absorption increasing and red shift of absorption peak. G-TiO_2 photocatalyst could decompose methylene blue under visible light (> 430 nm). G-TiO_2 synthesised from titanium isoproproxide presented better activity than G-TiO_2 (P25). The catalysts could also produce $^{\bullet}OH$ and $[O_2]^-$ radicals via electron scavengers (peroxymonosulphate, peroxydisulphate and hydrogen peroxide) to enhance degradation process with visible illumination.

ZnO loaded RGO photocatalysts were synthesized through Zn powder and graphite oxide. The structural, morphological, and physicochemical properties of the samples were thoroughly investigated by XRD, FT-IR, FE-SEM, UV-visible DRS, TG-DTA, and Raman spectroscopy. Zn powder could successfully reduce GO and ZnO was obtained simultaneously by one-step hydrothermal method. RGO-ZnO photocatalysts could bleach MB under UV-vis illumination.

Three different compounds: ammonia, graphene and C_3N_4 were utilized to dope tantalum pentoxide photocatalyst. Catalysts were analyzed by X-ray diffraction, UV–vis diffuse reflectance spectra and FTIR spectroscopy. The photocatalytic behavior was thorough investigated in bleaching methylene blue under UV-visible illuminations; the modified catalysts could decompose methylene blue, showing better activity than undoped Ta_2O_5. However, only N-doped Ta_2O_5 will show activity under visible light.

Publications by author

Referred journal publications

S. Liu, H. Sun, S. Liu, S. Wang, Graphene facilitated visible light photodegradation of methylene blue over titanium dioxide photocatalysts, Chemical Engineering Journal, 214 (2013) 298-303.

Y. Yao, S. Miao, S. Liu, L.P. Ma, H. Sun, S. Wang, Synthesis, characterization, and adsorption properties of magnetic Fe_3O_4@graphene nanocomposite, Chemical Engineering Journal, 184 (2012) 326-332.

H. Sun, S. Liu, G. Zhou, H.M. Ang, M.O. Tadé, S. Wang, Reduced Graphene Oxide for Catalytic Oxidation of Aqueous Organic Pollutants, ACS Applied Materials & Interfaces, 4 (2012) 5466-5471.

H. Sun, G. Zhou, S. Liu, H.M. Ang, M.O. Tadé, S. Wang, Nano-Fe^0 Encapsulated in Microcarbon Spheres: Synthesis, Characterization, and Environmental Applications, ACS Applied Materials & Interfaces, 4 (2012) 6235-6241.

Hongqi Sun, Shizhen Liu, Shaomin Liu, Shaobin Wang, A comparative study of reduced graphene oxide modified TiO_2, ZnO and Ta_2O_5 in visible light photocatalytic/photochemical oxidation of methylene blue, Applied Catalysis, B. (accepted).

Papers in preparation

S. Liu, H. Sun, S. Liu, S. Wang, One-step hydrothermal synthesis of ZnO-reduced graphene oxide using Zn powder for photocatalysis, (in revision).

S. Liu, R. Ullah, H. Sun, S. Liu, S. Wang, Ta_2O_5 photocatalysts with graphene dopant for methylene blue decomposition, (to be submited).

Referred conference Presentation

S. Liu, H. Sun, S. Liu, S. Wang, Graphene doped TiO_2 catalysts for visible light photochemical reactions, 7th International Conference on Environmental Catalysis, Lyon, France, September 2 – 6, 2012

Contents

Figure List

1 Introduction and overview

1.1 Background

In the past decades, more and more researchers have paid much interest on development of environmentally friendly materials and treatment techniques, because of the pressure to control and prevent a variety of environmental pollutants. There mainly included three kinds of contaminations; air, water and solid pollution, which cause threat to people health, civilization development and biological environmental security.

Water contamination majorly comes from human activities, which produce a large number of industrial, agricultural and domestic wastes to be discharged into the water. At present, more than 4200 billion cubic meters of sewage water were discharged into rivers of the world annually, and about 5.5 trillion cubic meters of sewage leached into lakes polluting fresh water, which is equivalent to more than 14% of the total global fresh water storage. Organic pollutants play an important role in water pollution; it takes up more than 50% of water pollutants. The major paths of this kind of pollutant are involved in the industry of plastics, synthetic fibres, synthetic rubber, detergents, pigment, solvents synthesis, paints, pesticides, food additives, pharmaceuticals and other organic compounds. Those industries on one hand are improving the quality of human life and on the other hand they endanger human health.

The hazard of water organic pollutants is dramatical. They are considered as toxics or a contributor to human chronic diseases including the human hepatic dysfunction, carcinogenics, hindering human body development and endangering body endocrine system [1-3]. In the last decades, much studies have been paid attention to photochemical methods for water treatment, for that photocatalysis supplied a promising strategy to decompose organic contaminants directly into carbon dioxide and water without any extensive energy supply and it is totally environmentally friendly. It also supports a new path for novel technology. Numerous studies have been reported to use nano-particles as photocatalysts for

water splitting to hydrogen generation, degradation of environmental pollutants and wastewater treatment, carbon dioxide remediation, self-cleaning activity and air purification[4-6].

1.2 Photocatalysts

TiO_2 has been studied extensively because it is considered as one of the most effective photocatalysts for the degradation of organic pollutants[7]. This reputation is also attributed to its relative nontoxicity and long-term thermodynamic stability. Today, many research groups manage to enhance the photocatalytic properties and optimize to degrade various organic and inorganic pollutants[8]. The energy from solar radiation that can arrive at the surface of the earth will stimulate TiO_2 particles at less than 5% of all radiation energy ($\lambda <$ 385 nm) [9]. Novel type of titanium oxide photocatalyst could degrade pollutants effectively under this kind irradiation. TiO_2 has a narrow band gap energy (E_{bg} = 3.2 eV for anatase type TiO_2) and can be a photocatalyst for oxidation or reduction. Reactive radicals (primarily $OH^{\cdot}$ and $O_2^{\cdot}$) or direct holes are to initiate the oxidation of most organic species in water and air. For an organic molecule, the process may lead to partial oxidation or can be proceeding toward total mineralization and formation of CO_2 and mineral acids [10-12]. The overall efficiency of photon utilization by TiO_2 is, however, limited by electron–hole recombination which transforms radiation into thermal energy. Indeed photon scattering and the intrinsic physical properties of TiO_2 limit the absorption of photons to those with UV-A or greater wavelength energy[13]. Because of the reasons, photocatalyst modification has been considered as key technology toward future photo-chemistry.

1.3 Graphene and graphene oxide

The term of graphene was first appeared in 1987 to describe single sheet of graphite as the constituent of carbon film. Graphene is an one-atom-thick two-dimensional crystallite which has an aromatic like lattice as a build block for all sp^2 carbons including fullerene, carbon nanotubes, and graphite[14]. Graphene oxide (GO) is the oxidised form of graphene. Bradder et al.[15] state that the structures of graphene show significant capacity to remove inorganic gas via intercalation and reactive adsorption. The acid-base interactions with surface functional groups located at the edges of the carbon layers play a role in the mechanism of the removal process. Matsuo et al.[16] reported the removal of formaldehyde from the gas phase by silver GO contained amino groups. They found that the amount of formaldehyde adsorbed on this adsorbent was much higher than that on activated carbon. Although, activated carbon has been a simple and cost-effective material for the removal of contaminants in water, the production of activated carbon and regeneration are expensive and hard to recycle. In addition, activated carbon sometimes shows a low adsorption for some kinds of ions[15]. An important process in photocatalytic mineralization of organic substrates is the initial oxidation of organic substrate occurring on the photocatalyst surface [17]. Therefore, it was thus deduced that graphene or GO will play a role in adsorption of other compounds in water due to its hydrophilic-hydrophobic properties change and effectively acceleration to the process of catalytic reaction.

1.4 Graphene doped TiO_2 photocatalyst

The major initial steps of TiO_2 photocatalytic mechanism under visible irradiation[9] are summarized in following steps:

$$T_iO_2 + hv \rightarrow h_{vb}^{+} + e_{cb}^{-}$$

$$h_{vb}^{+} + OH^{-} \rightarrow {}^{\cdot}OH$$

$$e_{cb}^{-} + Ti^{+4}OH \leftrightarrow Ti^{+3}OH$$

$$Ti^{+3} + O_{2\,ads} \rightarrow Ti^{+4} + O_2^{-}$$

$${}^{\cdot}OH + R_{pollutant} \rightarrow CO_2 + H_2O \text{ or Actived Radical}$$

$$h_{vb}^{+} + e_{cb}^{-} \rightarrow \text{Thermal energy or Luminescence}$$

In a photochemical reaction process, conduction band electrons (e^-) and valence band holes (h^+) are generated when aqueous TiO_2 suspension is irradiated with light energy bigger than its band gap energy (Eg=3.2 eV)[18]. Graphene is a 0 eV band gap semiconductor in which the filled valence band touches the empty conduction band thus arising a new band for radical production (Figure 1.1).

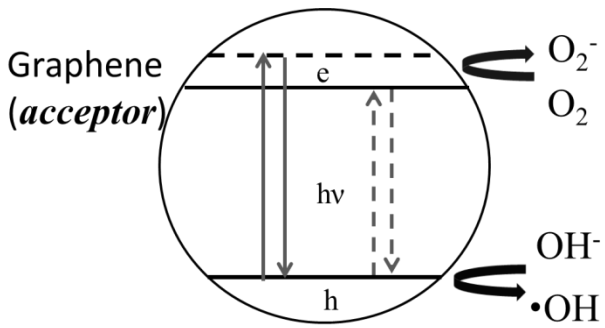

Figure 1. 1 Graphen plays as an accepter to rebuild a new conduction band in order to narrow band gap energy.

Ohtani claims that semiconductor photocatalysis is the catalysis of a photochemical reaction at the surface a solid semiconductor [19]. Zhang et al. [20] indicate that high adsorption material will support a high concentration of reactants near the TiO_2, organic compounds in many ways overlap the TiO_2 photocatalyst surface. Leary [21] indicates that the graphene

sheet is an ideal electron sinks or electron transfer bridges. Exfoliated graphene sheets have a theoretical surface area of 2600 m^2/g, making graphene highly attractive as a high-surface area 2D photocatalyst support. Furthermore, high quality graphene sheets induce ballistic transport, which means that electrons can travel without scattering at motilities exceeding 15.000 $m^2 V^{-1} s^{-1}$ at room temperature. The application of graphene in combination with TiO_2 therefore presents the opportunity to simultaneously cover all three mechanisms of photocatalytic reaction.

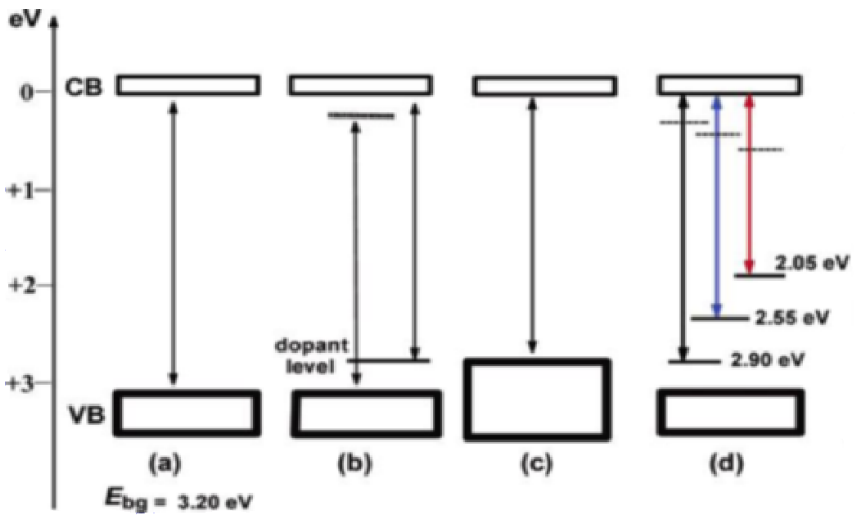

Figure 1. 2 The influence by the band gap electronic structure of anatase TiO_2 Doping on organic material [22].

The above diagram was proposed by Serpone [22], which logically demonstrates the influence of the changes that might occur to the band gap and electronic structure of anatase TiO_2 on doping with various organic elements (Figure 1.2) The presence of localized states near the valence band edge has been proposed to be at the origin of the visible-light activity of anion-doped TiO_2, the narrowed band gap energy could utilize the modification of TiO_2 in photo-property such as red shift in radiation which can improve the quantity of solar energy or lower trigger energy of photo-reaction.

1.5 Scope and objectives of this thesis

The main objective of this research is to synthesize new kind of photocatalysts by using graphene oxide or reduced graphene oxide for visible light radiation. The new carbon material, graphene oxide or graphene will be used as a support to synthesize photocatalyst composites. New method will be tested to synthesize graphene oxide, reduced graphene oxide (RGO) and new sol-gel method will be utilized to produce light responsive nano-photo-particle which will be evaluated in dye degradation. In this research, the comparison between RGO doped commercial TiO_2 (P25) and RGO doped home-made TiO_2 will be carried out. Also graphene modified ZnO and Ta_2O_5 systems will be synthesised and tested in dye degradation.

1.6 Structure of thesis

In this thesis, a novel carbonaceous nanomaterial, graphene, has been synthesized in order to modify several light active semiconductors to decompose methylene blue dye in aqueous system with ultraviolet or visible illumination. There are six sections in this thesis. Firstly the background of graphene or graphene oxide and photocatalysis has been introduced, graphene as a new kind of film-like material possess very special electronic properties and other physical and chemical properties. It has potentials to play as a carrier to accept photo-electron and reduce the time of pair recombination. In second part, more detail has been demonstrated about graphene, which includes the history of graphene and the development of modern technology to synthesise vast surface graphene sheets. Photocatalysis is also a kind of new technology; it has multifocal future on hydrogen energy generation, pollution treatment and so on, however, the existence photocatalysts have drawbacks such as high cost, low efficiency, high electron-hole pair combination speed and UV-radiation response only. Now

many researches reveal that graphene or graphite oxide dopant could enhance the photocatalyst properties in numerous functions. In the following chapters, our major work has been presented, graphene doped TiO_2 particles successfully degrade MB under visible radiation, G-TiO_2 sample could efficiently create •[OH] radicals from water with electron scavengers. The ZnO - RGO photocatalyst has been synthesized by Zn powder and graphite oxide suspension via hydrothermal methodology, which could decompose MB with artificial solar radiation. In part five of the thesis, graphene and graphene like inorganic material "graphite nitride" have been studied as dopants to modify commercial Ta_2O_5 particle; the results indicate that graphene has strong ability to absorb pollutants and g-C_3N_4-Ta_2O_5 could decompose MB under visible radiation gradually. At last conclusion and work for future are presented.

1.7 References

[1] I. Arslan, I. Balcioglu, T. Tuhkanen, D. Bahnemann, H2O2/UV-C and Fe2+/H2O2/UV-C versus TiO2/UV-A Treatment for Reactive Dye Wastewater, Journal of Environmental Engineering, 126 (2000) 903-911.

[2] M. Rani, N. Gupta, B. Pal, Superior photodecomposition of pyrene by metal ion-loaded TiO2; catalyst under UV light irradiation, Environmental Science and Pollution Research, 19 (2012) 2305-2312.

[3] E. Forgacs, T. Cserháti, G. Oros, Removal of synthetic dyes from wastewaters: A review, Environment International, 30 (2004) 953-971.

[4] F.B. Li, The enhancement of photodegradation efficiency using Pt-TiO2 catalyst, Chemosphere, 48 (2002) 1103.

[5] F. Wang, K. Zhang, Reduced graphene oxide–TiO2 nanocomposite with high photocatalystic activity for the degradation of rhodamine B, Journal of Molecular Catalysis A: Chemical, 345 (2011) 101-107.

[6] H. Sun, R. Ullah, S. Chong, H.M. Ang, M.O. Tadé, S. Wang, Room-light-induced indoor air purification using an efficient Pt/N-TiO2 photocatalyst, Applied Catalysis B: Environmental, 108–109 (2011) 127-133.

[7] S. Klosek, D. Raftery, Visible Light Driven V-Doped TiO2 Photocatalyst and Its Photooxidation of Ethanol, The Journal of Physical Chemistry B, 105 (2001) 2815-2819.

[8] K. Woan, Pyrgiotakis, G. and Sigmund, W., Photocatalytic Carbon-Nanotube–TiO2 Composites, Advanced Materials, (2009) 2233–2239.

[9] C. Chen, X. Li, W. Ma, J. Zhao, H. Hidaka, N. Serpone, Effect of Transition Metal Ions on the TiO2-Assisted Photodegradation of Dyes under Visible Irradiation: A Probe for the

Interfacial Electron Transfer Process and Reaction Mechanism, The Journal of Physical Chemistry B, 106 (2001) 318-324.

[10] E. Felizzetti, The role of colloidal particles in the photodegradation of organic compounds of environmental concern in aquatic systems, Advances in colloid and interface science, 32 (1990) 271.

[11] C.K. Grätzel, Decomposition of organophosphorus compounds on photoactivated TiO2 surfaces, Journal of molecular catalysis, 60 (1990) 375.

[12] S.T. Martin, Chemical mechanism of inorganic oxidants in the TiO2/UV process: increased rates of degradation of chlorinated hydrocarbons, Environmental science & technology, 29 (1995) 2567.

[13] B. Gao, G.Z. Chen, G. Li Puma, Carbon nanotubes/titanium dioxide (CNTs/TiO2) nanocomposites prepared by conventional and novel surfactant wrapping sol-gel methods exhibiting enhanced photocatalytic activity, Applied Catalysis B: Environmental, 89 (2009) 503-509.

[14] C. Chen, Q.-H. Yang, Y. Yang, W. Lv, Y. Wen, P.-X. Hou, M. Wang, H.-M. Cheng, Self-Assembled Free-Standing Graphite Oxide Membrane, Advanced Materials, 21 (2009) 3007-3011.

[15] P. Bradder, S.K. Ling, S. Wang, S. Liu, Dye Adsorption on Layered Graphite Oxide, Journal of Chemical & Engineering Data, 56 (2010) 138-141.

[16] Y. Matsuo, Removal of formaldehyde from gas phase by silylated graphite oxide containing amino groups, Carbon, 46 (2008) 1162.

[17] E. Pelizzetti, Mechanism of the photo-oxidative degradation of organic pollutants over TiO2 particles, Electrochimica Acta, 38 (1993) 47.

[18] I.K. Konstantinou, TiO2-assisted photocatalytic degradation of azo dyes in aqueous solution: kinetic and mechanistic investigations:: A review, Applied catalysis. B, Environmental, 49 (2004) 1.

[19] B. Ohtani, Preparing Articles on Photocatalysis—Beyond the Illusions, Misconceptions, and Speculation, Chemistry Letters, 37 (2008) 217.

[20] X. Zhang, M. Zhou, L. Lei, Preparation of photocatalytic TiO2 coatings of nanosized particles on activated carbon by AP-MOCVD, Carbon, 43 (2005) 1700-1708.

[21] R. Leary, A. Westwood, Carbonaceous nanomaterials for the enhancement of TiO2 photocatalysis, Carbon, 49 (2011) 741-772.

[22] N. Serpone, Is the Band Gap of Pristine TiO2 Narrowed by Anion- and Cation-Doping of Titanium Dioxide in Second-Generation Photocatalysts? The Journal of Physical Chemistry B, 110 (2006) 24287-24293.

2

2 Literature review

2.1 Introduction

In 1967, a photocatalytic reaction was firstly reported by Professors Fujishima and Honda at the University of Tokyo of Japan, which grips a great interest onward novel energy, photo-electric property, photo-semiconductor, water treatment and so on. In their study, it was found that water could be hydrolysed on the surface of titanium single crystal electrode under certain wavelength radiation, this phenomena revealing the possibility to produce hydrogen gas from solar radiation energy, and it was widely acknowledged as the Honda-Fujishima Effect [1]. When the surface of the rutile TiO_2 electrode was irradiated by light constantly at wavelengths shorter enough than TiO_2 band gap, which is about 415 nm (3.1 eV), photocurrent from the platinum electrode to the TiO_2 electrode through an external redox circuit occurred. Water can be decomposed using UV radiation without the application of external voltage, according to the following scheme.

$$TiO_2 + hv \rightarrow e^- + h^+$$

$$2H_2O + 4h^+ \rightarrow O_2 + 4H^+$$

$$2H^+ + e- \rightarrow H_2$$

The overall reaction is:

$$2H_2O + 4hv \rightarrow O_2 + 2H_2$$

Ever since, people develop more and more technologies to utilize solar energy into extensive areas. Now it is well known that TiO_2 or other semiconductors and their modified particles can be adapted. Kim et al. employed TiO_2 with anatase crystal for sterilization of food-borne pathogenic bacteria[2]. TiO_2 nanoparticles with near ultraviolet radiation (UV-A) can produce electronic holes (h^+) inward its valence band, it reinforced conduction hydroxyl

radical (OH^-) produced by the oxidation of water which can decompose the bio-cell efficiently and eliminate bacteria. As a conclusion, the photocatalyst played a significant role in a heterogeneous system, same as UV radiation.

Zou et al. have considered SiO_2 as a support to load TiO_2 nano-particles for air pollution treatment especially for volatile organic compounds (VOCs) [3]. They suggested that photocatalytic oxidation to remove toxic air pollutants from electrical, electronic, agricultural, textile, petrochemical, metallurgical and many other industries is a very promising process. SiO_2 can create bigger surface area of TiO_2-SiO_2 particles at 274.1 – 421.1 m^2/g, which is much higher than commercial titanium dioxide (Degussa P25, 50.4 m^2/g). Meanwhile SiO_2 can enhance the adsorption of VOCs reinforcing photocatalysis of VOCs into carbon dioxide and water. Kim and Hong reported a study in acetone, methanol, toluene degradation by TiO_2 semiconductor thin film under 254 nm UV radiations at temperature of 45 ℃ [4]. The experiment proved that water vapour could enhance the photocatalytic degradation rate of toluene, but the catalytic activity was inhibited for acetone because water vapour eventually seemed to hinder the adsorption of acetone molecules on the catalyst surface. It also has been proved that the UV - Ozone oxidation technology could oxidize the organic matters in water system, such as chloroform, hexachlorobenzene, carbon tetrachloride, benzene, to make them into harmless CO_2 and H_2O. This technology can effectively be used for environmental deodorant or air pollution treatment. Several reports demonstrate that the titanium dioxide is widely used for air purification, deodorant, sterilization, anti-fouling, and demister[5] because the cooperation of photocatalyst, sunlight irradiation and water evaporation can produce OH^-, O_3^+ radicals with high redox potential.

Since the late of 1960s, photocatalysis technology was utilized in water treatment. Fujishima has begun to investigate the photo-electrolysis in water system[6] in the first time, he selected

a single crystal n-type TiO_2 (rutile) semiconductor electrode as an oxidant which has a sufficiently positive valence band edge to oxidize water to oxygen. TiO_2 is also an extremely stable material, even in the presence of aqueous electrolyte solution, much more than other types of semiconductor that have been tested. The possibility of solar photoelectrolysis was demonstrated for the first time in 1969 with the system shown below (Figure 2.1), the reactor was exposed to near – UV light, and was connected to a platinum black counter electrode through an electrical load. This report attracted the attention of not only electrochemists but also many scientists in a broad area, and numerous related studies were reported in the 1970s.

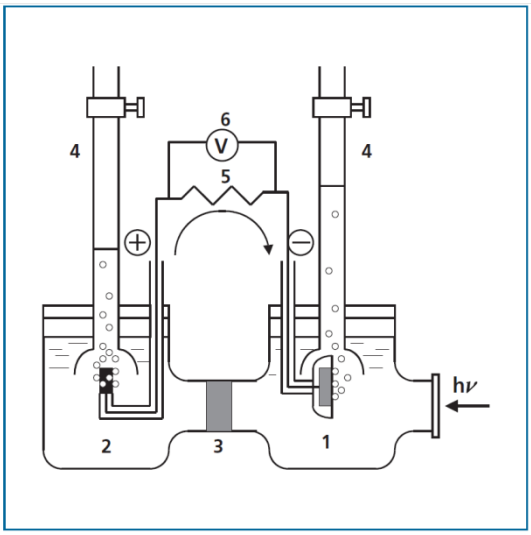

Figure 2. 1 Schematic diagram of electrochemical photocell. (1) n-type TiO_2 electrode; (2) platinum black counter electode; (3) ionically conducting separator; (4) gas buret; (5) load resistance; (6) voltmeter

One mechanism has been wildly accepted that near-UV irradiation on TiO_2 particulates generates conduction-band electrons (e_{CB}^-) and valence-band holes (h_{VB}^+). These charge carriers either stay inside the crystal or migrate to the surface to react with the available adsorbents, such as OH^- . The highly oxidative h_{VB}^+ (E_0= +2.7 V) may directly react with the surface-absorbed organic molecules, or indirectly oxidize the organic compounds via formation of $^{\bullet}OH$ radicals. It is well known that $^{\bullet}OH$ radicals are the primary oxidation species to initiate the degradation reaction in the photocatalysis of various organic substrates

because in the process hydrogen peroxide has been detected[7]. It has been considered that there is a high oxidation electrode potential between conduction-band electrons and valence-band holes. The light energy can be efficiently used in redox chemistry reactions which include organic pollutant decomposition in water.

2.2 Water organic pollutants

In a long history, human beings are magnifically affecting the earth environment; in turn the environment conversely affects human life; living, health, generation, evolution. However, there is an increasing tendency in pollutant emissions including inorganic and organic pollutants. According to the World Health Organization (WHO), 1.8 millions of people die of diarrhoea per year and 88% of these cases are related to the ingestion of contaminated water, lack of sanitation and bad hygiene practice (WHO, 2006). Furthermore, almost 1/6 of World's population do not have access to safe drinking water, most of them in the third World.

For chemical engineering, environmental problem attracts great interests. The pollutants from textile, paper, and plastic industries are always threats to human life. These industries contaminate the environment by releasing the toxic, cancerogenic and coloured waste water [8-10]. Phenol, dye stuff and aromatic liked compounds [11-13] are the main organic water pollutants due to high toxicity and high chemical stability. Generating hydroxyl radicals to capture the hydrogen atoms from the carbon atoms of straight-chain alkanes, will result in degradation of ketones, alkenes, aldehydes, alcohols and others. These compounds other than alkanes are more easily degradable by micro-organisms in the water environment. Yue et al. reported decomposition of crude oil absorbed into expanded graphite/TiO_2/NiO composites[14]. In the study, TiO_2 loaded NiO photocatalyst was supported on expanded

graphite which is considered to have high adsorption capacity to heavy oils in water. FT-IR spectra indicated that most of organic functional groups such as C–H, C–S and C–C decreased because of photo-decomposition with solar energy. After an intensive study, TiO_2 is considered to have a wide-energy band gap which is a limitation to extract more radiation energy under the visible light wavelength. Most of light sensitive semiconductor materials have the drawbacks of low quantum yields and the lack of visible-light utilization[11]. Photocatalysis has not been widely applied to treat wastewater in industry, as its reaction speed is not high enough, which is widely considered due to a quick recombination of charge pairs and the radiation energy will totally waste into thermal energy[15].

2.3 Photocatalytic water treatment

Photo-degradation of organics is referred to organic matters such as aromatics, alkanes, lipids, organic acids, etc being gradually oxidized to low molecular weight intermediates and eventually into CO_2, H_2O and other anions such as NO^{3-}, PO_4^{3-}, Cl^{1-} with radiation [16].

Heterogeneous nano-photo-catalysts are referred as particles with 20 – 200nm with photo sensitivity and high surface area. Because the particles have the ultra-small size and the super surface area, electronic property of the particle is totally different from bulk system. Over its structure the element atoms of surface ligand is often insufficiency and dislocation, which will result in an increase in dot position. The activation of catalyst surface is much higher than the regular semiconductor. The quantum size affects discrete energy levels [17, 18], the potential of conduction band becomes more negative, and the energy gap is wider. Therefore, nano-semiconductor

particles have a stronger oxidizing or reducing potential which leads to much easier participation into photo-electronic reaction. TiO_2 particles with nano-size have a high photocatalytic activity, low cost, non-toxicity. As well-known that a wide band gap energy makes catalysts to be stimulated under ultraviolet light, and this illumination energy only occupies 4% of incoming solar energy, thus rendering the overall process impractical[19]. Thus development of semiconductor nano-particle to harvest as more as visible light energy (wavelength more than 380 nm, which occupied 43% incoming solar) attracts more and more interest of researchers in the last decades.

2.4 Ion doping method to modify photocatalysts

Heteroatom doping technology to modify property of a photocatalyst is considered as one of the effective ways to extend light absorption in visible region of the photocatalyst. It is reducing the recombination rate of photo-induced electrons/holes. At the same time the doping ion can impose structure defects to capture electronic carrier and extend its lifespan. The heteroatom in the crystal lattice will lead to structure distortion and different ion size, breaking the symmetry of the crystal. This phenomenon is also beneficial in improving the photo-induced electron and hole separation. For instance, Fe^{3+} is always considered as the most acceptable dopant on TiO_2 modification because of its unique 3d atomic orbitals with half-filled electron and moderate molecular energy [20]. Zhu et al. claim that Fe^{3+} can be successfully doped into TiO_2 lattice by sol-gel method under different calcination conditions. DRS spectra and Raman diffraction indicate the Fe^{3+} doped TiO_2 particle can narrow the band gap. The crystal structure of TiO_2 plays a very important role and anatase TiO_2 is much more efficient than rutile lattice in organic pollutant degradation.

Non-metal dopants are considered to be more beneficial to catalyst modification because Fermi electronic energy level in non-metal atoms is discrete or quasi-continuous, which will narrow the semiconductor band gaps. Comparing with metal dopants, non-metal elements increase surface area and adjust the pH value of surface for enhancing the pollutant adsorption process[21]. Yang et al. introduced carbon and nitrogen into TiO_2 lattice and concluded that the visible light sensitivity was enhanced by the narrowing of the band gap due to mixing N 2p and O 2p states and that carbon dopant played a significant role to enhance the separation of photo-excited phase [22] and weaken recombination. The N-C doped TiO_2 photocatalyst has a good performance in degradation of "what chemical" at visible irradiation.

Zou et al. presented a brilliant result about TiO_2 with heteroatom doping technology[19]. They developed nickel-indium-tantalum-oxide with nickel and in doping. During 400-hours experiment the catalyst samples remained quite stable under visible light irradiation. The band gap is between 2.3-2.6 eV. The band structure of NiO at Ni 3d orbits can absorb ultraviolet-visible irradiation even more at 420 to 520 nm.

2.5 Semiconductor combination modification method

Different from ion doping, semiconductor cooperation provides new covalence band or conduction band to initial photocatalyst directly. There are many researches indicating that semiconductor cooperation is not only to modify mixture absorption peek of particle to red shift in all illumination but also to arise the ability of photo-reaction and improve photocatalystic behaviour, this phenomena can be ascribed to better electron transfer between different semiconductors. Furth more combination of crystal will create more defects and nano porous structure which will positively

enhance surface activation. For instance, metal oxidation can postpone electronic transforming of TiO_2 from anatase phase to rutile phase; it is also good at enhancing the TiO_2 in the absorption of the visible wavelength. It is well known that the order of capability of material absorption performance strength is Pt/WO_3-TiO_2 > Cu/WO_3-TiO_2 > Ag/WO_3-TiO_2 > Ni/WO_3-TiO_2.

Abe et al. synthesised platinum, tantalum, tungsten, iodine, oxygen, nitrogen multiple element complex photocatalyst for water splitting and hydrogen production.This novel system has catalytic response under visible light and high efficiency for hydrogen production from water. Pt-TaON particle has a band gap about 2.5 eV, the conduction band and valence band edges are -0.3 and +2.2 V respectively. This system has enough negative normal hydrogen electrode (NHE) to reduce H_2O to hydrogen gas. In contrast, Pt-WO_3 system is good at oxidation whose NHE of valence band is much higher than H_2O to oxidise water. In a two-step (Figure 2.2) photo-excitation combined with a redox circuit between IO^{3-} and I^-. The prompt reduction of IO^{3-} to I^- over Pt–WO_3 particle maintains a very low concentration of IO^{3-} in the solution during the photoreaction, effectively suppressing the undesirable backwards reaction of IO^{3-} reduction to I^- onto Pt–TaON particale[23].

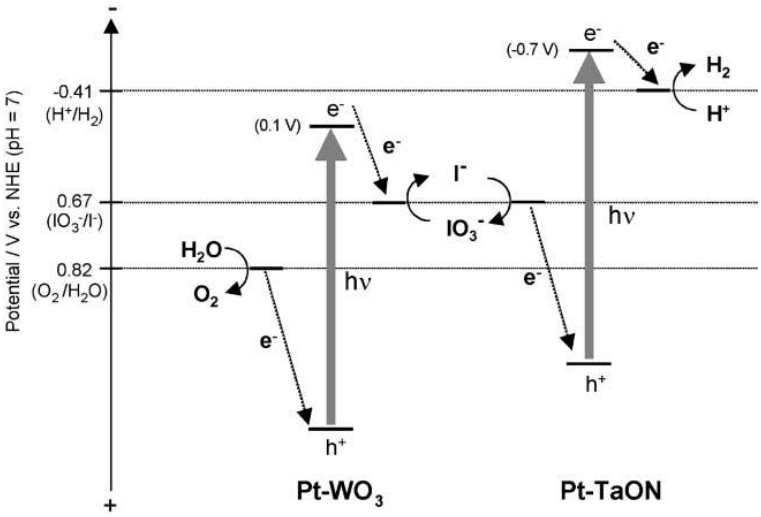

Figure 2. 2 The combination function of Platinum doped WO_3 semiconductor; platinum doped TaON semiconductor and intermediary agent I-/IO_3- for photo water split [23]

Photoactive sensitization compounds are the chemicals with high photo stimulating factor and easy adsorption onto the surface of the photocatalyst. When such a chemical possesses visible illumination energy, these optically active substances directly absorb photon into photoelectronic material and transform photo current into photocatalyst vacant state. Thereby the whole photo-electron system will temporarily obtain expanded excitation wavelength range, and the photocatalytic reaction efficiency will be enhanced. There are several requirements for dye sensitization:

(1) It is required to be tightly adsorbed on the photocatalyst surface, or the dye molecules include polar groups such as carboxyl, hydroxyl;

(2) It shows good absorption of visible light in solar light spectrum;

(3) The compound should have a more negative reduction potential than the oxidation potential of the electrolyte and more negative oxidation reduction potential;

(4) The compound should have a good chemical stability with long-term irradiation;

(5) The compound oxidation state and excited states have stability;

(6) The compound and photocatalyst should have a match relationship which is utilized for excited electron injection quickly;

(7) The compound molecule can be dissolved in the solvent.

Many kinds of photosensitizing agent are employed for photocatalyst modification, for instance; cyanine dyes, phthalocyanine, coumarin, chlorophyll, eosin, bipyridine ruthenium. Stergiopoulos et al. [24] investigated commercial organic ruthenium N3 and other two new dyes, Ru (dcmpp) (debpy) CI (PF6) (abbreviated as Ru-CI), and Ru (dcmpp) (debpy) NCS (PF6) (abbreviated as Ru-NCS). The results indicate that these three dye sensitizers have good absorption under visible light. The absorption wavelength of TiO_2 /Dye system has expanded to more than 700 nm. Some reports also indicate that Ruthenium (Ru) bipyridine, Osmium (Os) bipyridine, phthalocyanine and phthalocyanine, porphyrin , chlorophyll and its derivatives can usually be utilized as a photosensitizing dye[25-27]. However the dye sensitizer will be easily degraded[28].

Although the dye-sensitized TiO_2 system demonstrated the ability to decompose pollutants using visible light, the photoreaction efficiency was very low due to the much slower interfacial electron transfer between substrates and the back electron transfer to the oxidized sensitizer. Bae et al.[29] investigated a $Ru^{II+}L_3$ sensitizer with Pt-TiO_2 particles (Figure 2.3). They found carbon tetrachloride （CCl_4） could be decomposed in to Cl^- under visible light irradiating but the fast initial dechlorination on Pt/TiO_2/$Ru^{II+}L_3$ stopped after 30-minute irradiation. The durability of Pt/TiO_2/$Ru^{II+}L_3$ photocatalysts remains to be solved.

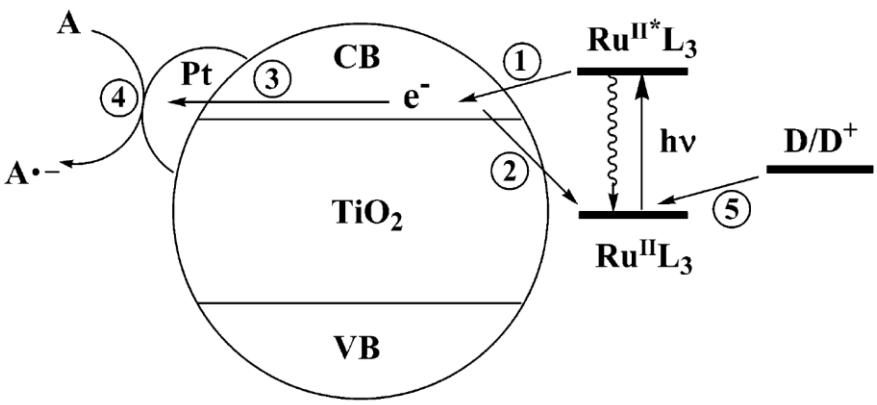

Figure 2. 3 Visible light-induced reductive degradation of perchlorinated compounds (Cl_3CX = Cl for CCl_4, X = CO_2- for CCl_3CO_2-) on Pt/TiO_2RuII+L3 particles; ① Electron injection from the excited sensitizer to CB; ② Back electron transfer to the oxidized sensitizer (RuIIL3); ③ Electron migration and trapping in Platinum deposits; ④ Interfacial electron transfer to a perchlorinated molecule on Platinum; ⑤ Sensitizer regeneration by electron donors[29].

2.6 Graphene structure and properties

In the early century, it was believed that one-atom layered 2-dimentional material does not exist in the word. Some famous scientists claimed that, in the strict sense, two-dimensional crystal is thermodynamically unstable, because thermal fluctuations will destroy the atoms by the long-range order in the two-dimensional crystals in any limited temperature. In other words, the vibration of atoms displacement by the thermal divergence fluctuations is bigger than atom space; it will lead material to self-decomposition or aggregation out of two-dimensional lattice. However, in 2004 Geim and Novoselov from Manchester University successfully prepared one layer graphene sheet by “Tear tape/microfolitation” method, which is currently considered the world's thinnest material with only one carbon atom layer. Different from all other known materials, graphene is not only highly stable but also its electrical conductivity is very high. In addition, one layer graphene sheet can be employed as a heat conductor because it has much stronger thermal effects than any other materials.

Graphene as a novel carbonaceous nanomaterial has impressively theoretical surface area of 2600 m^2/g [30], making it highly attractive as a high-surface area 2D photocatalyst support. It has high mechanical strength (1060 GPa), high thermal conductivity (~3000 $Wm^{-1}K^{-1}$). In addition, high quality graphene sheets permit ballistic transport, meaning that electrons can travel without scattering at motilities exceeding 15,000 m^2 V^{-1} s^{-1} at room temperature, making them potentially ideal electron transfer bridges[31-34]. Because graphene has a hexagonal honeycomb network structure, the sp^2-bonded carbon lattice can have numerous outstanding electronic and spacious delocalized π-bonds which enhance its structural stability and current conductivity capacity [35]. Because of those characteristics, graphene recently attracts many people in theory and application fields to investigate its chemical, structural and electrical properties.

Graphene has outstanding electronic conduction contributed by its huge delocalized π bond; the internal carrier concentration is as high as 10^{13} cm^{-2}. When the carrier concentration (electron and hole) of graphene becomes zero, a metallic quantum conductance e^-/h^+ can still be measured. This phenomenon reveals that even the carrier concentration is zero, graphene remained metal property. It was previously considered by the special structure in graphene, however in recent years, the attention about the disorder and other reasons led to the existence of the minimum quantum of conductance. At Fermi level of graphene the carrier (election and hole) shows a linear chromatic dispersion, the electrons velocity is about 1/300 of the speed of light. The electronic behaviour of the Dirac equation in quantum mechanics describes that the electron effective quality is zero. Thus graphene is a unique quality of Dirac in condensed matter physics[36]. In fact, graphene is not a 2-dimensional flat material [37]. Wang et al. stated that corrugation and scrolling (Fig 2.4 (A)) are part of the intrinsic nature of grapheme nanosheets (GNS), because the 2D membrane structure becomes thermodynamically stable via bending[38]. Calculations show that, for limited

systems, the long-range ordered structure of graphene will fluctuate in 3-dimensional space in order to dissipate some of the energy fluctuation (Fig 2.4 (B)).

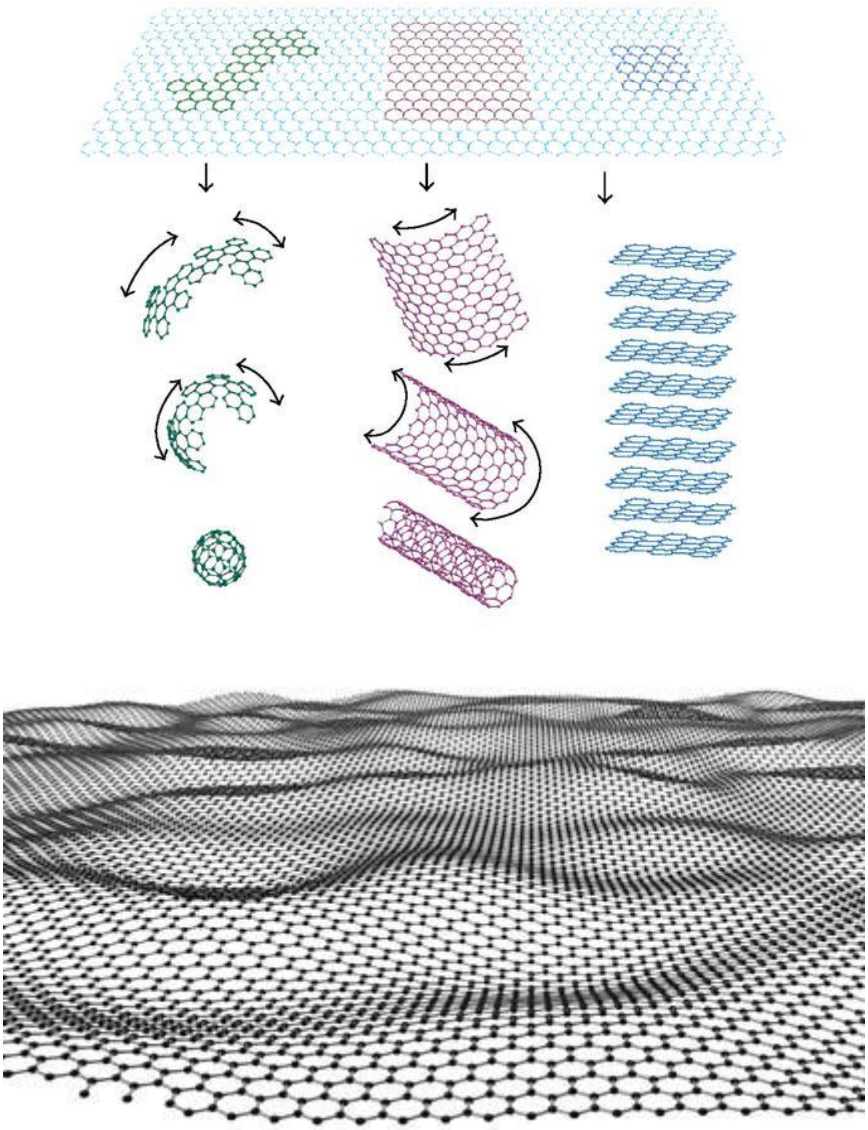

Figure 2. 4 (A)One atomic lay graphene can be considered as the element of carbon nano-tube and Fullerene[39]. (B) graphene sheet with surface vibration.

Currently there are many methods to produce single graphene sheet: (a) micromechanical cleavage, which can produce graphene sheets in very limited quantities, (b) epitaxial growth of graphene films, and (c) chemical processing to synthesize graphene, which involved graphite oxidation, exfoliation and GO reduction. Among them, the chemical approach is

usually thought as the most suitable method toward producing graphene sheets in a large quantity. In addition, graphite powders are usually used as raw materials for bulk production of graphene sheets[38]. Initially Andre and Novoselov adopted microfolitation method to split single graphene sheet from graphite crystal surface[31], they adopted mechanical force to peel graphene layers and transferred to the carrier on the silicon oxide crystal surface. This method can prepare micron size graphene, however, it is difficult to achieve large-scale synthesis because the unpredictable control process. In 2004, Heer [40] make an achievement of epitaxial growth of graphene structure on the SiC surface. This sort of loaded graphene can be created directly through the lithography process in electronic devices[41]. However the SiC crystal surface will prone to reconstruction in the high-temperature heating process which leads more complex of surface structure. So the large scale and uniform thickness graphene is different to obtain through this method. In contrast, chemical vapour deposition method (CVD) is one efficient method to produce and control structure of single layer graphene [42]. It selects metal single crystal or metal film as a substrate, on its surface carbon compounds can be absorbed and decomposition under high-intensity thermal treatment, in which carbon compounds play as graphene precursors. Many infections such as substruction selection, growth temperature and different carbon precursors can adjust the graphene production, so CVD graphene process attracted more and more researchers. In laboratory, Hummer method is the most common way to obtain graphene particle, graphite is oxidised by strong oxidants such as concentrated sulphuric acid, potassium permanganate or sodium nitrate in an aqueous system to be graphene oxide (GO) suspension (Fig 2.5 (A)). Under ultrasonic treatment, GO has the tendency to change to single layer graphene much easily (Fig 2.5 (B) because oxygen functional groups graft onto the graphene surface[43]. In addition the oxidation time for GO

synthesis simply affects the proportion distribution of graphene sheets of different oxygenation levels[44].

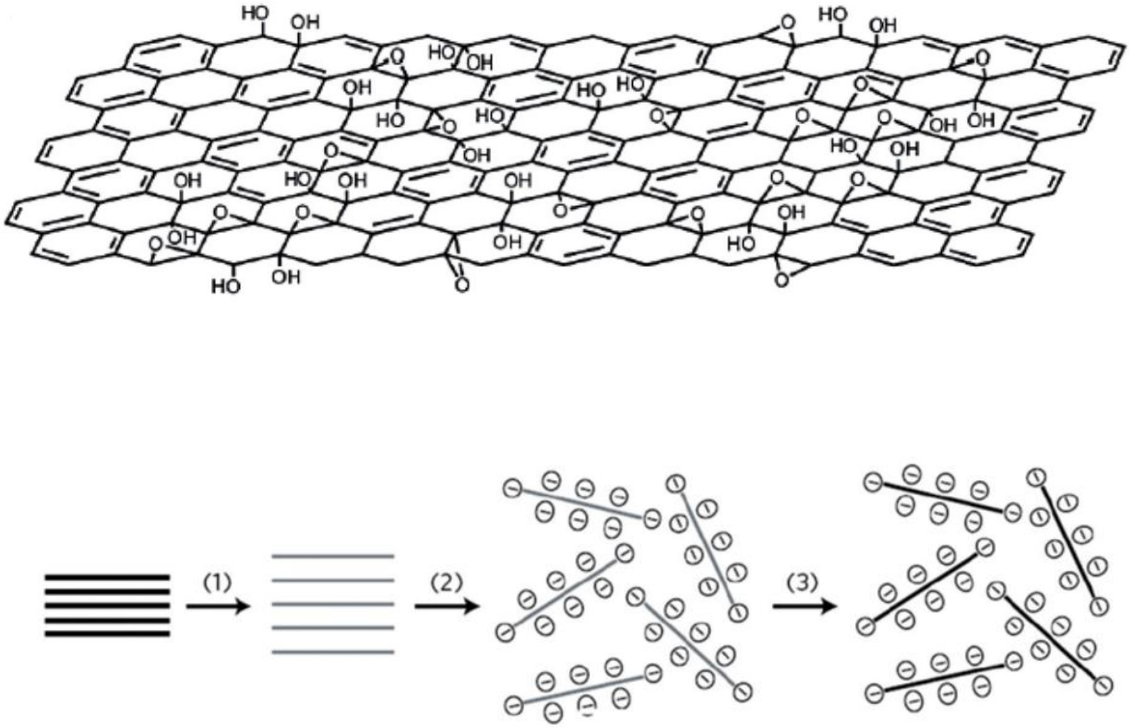

Figure 2. 5 (A)Graphene oxide (GO) sheet; (B) Epoxy and hydroxyl will be utilized for “exfoliation” process[44].

Graphite oxide, formerly referred as graphitic oxide or graphitic acid, is a compound of carbon, oxygen, and hydrogen in variable ratios. In fact, GO has a layered structure and various functional groups such as epoxy and hydroxyl groups which are attached to the basal planes and carboxylic on the edge planes[45]; it can also be used as an adsorbent. Seredych and Bandosz investigated the removal of ammonia in gas by GO via its intercalation and reactive adsorption[46]. They believed that the acid-base interactions with surface functional groups located at the edges of the carbon layers can remove ammonia and present the basic property. Matsuo et al. found that the amount of formaldehyde adsorbed on this adsorbent was much higher than that on activated carbon[47], although water molecules were pre-

adsorbed before. Thus GO will also be good at adsorption of other compounds in water due to its hydrophilic/hydrophobic change. Graphene oxide has obvious different electronic conductivity comparing with naked graphene. Based on the theoretic calculation from Ito et al., graphene has 0 eV band gap but graphene oxide can converse its gap band by oxygen contented ratio [44, 48, 49]. Graphene oxide with the oxygen uptake increasing from 0 to 0.5 ML (O / C = 50%), its band gap has changed from 3.39 eV (semi-metal transition) to complete more than 5 eV (insulator). When the O/C ratio is 25% graphene oxide has transformed from a conductor to insulator[50]. The environment also can modify graphene electronic property, H_2O and NO_2 accept electrons from the graphene resulting in p-type doping of graphene [51]. Although some researches indicate that the band gap of graphene is also influenced by its nanoribbons width, there will be a decline in semiconductor gap[52]. Previously the change of optical property has been suggested as a partial restoration of the network within the carbon structure and has been observed through chemical reduction of the GO sheets[53].

The electronic property of GO has been widely studied. Yeh et al. studied graphene oxide as a semiconductor showing photocatalytic activity[44]. Based on XPS, optical absorption spectra, electrochemical measurements, it was explicitly indicated that graphene oxide as a semiconductor is ascribed by the oxygen functionalities which reduced the symmetry of the π-π^* system to open the gap. The top energy level of the valence band was changed to the O 2p orbitals. The band energy is eligible for water splitting (the conductor band energy is from -0.71 to -0.75 and the valence band energy is from 1.6 to 0.75). Although graphene oxide is a p-semiconductor, the gap energy is modifiable because oxygen content can be changed. The Fermi level of the GO specimens shows a positive shift with the population of oxygen functionalities on the graphene layers. After illumination the oxygen functional groups will dislocate. The electronic and photocatalytic analysis of GO demonstrated that GO has a

conversable feature for its electronic properties and can serve as an effective media for photosynthetic reactions including water splitting[49].

In a recent study it was found that GO has a magnetic property. The magnetism is not common for the light p-block elements [52]. Some reports have predicted ferromagnetic ordering could exist among various defects on graphene structures, such as vacancy, topological defects or frustration, and hydrogen chemisorption or perhaps the edge. Graphene-like character [54] originates from the carbon π-electron system rather than from possible d-element impurities. An alternative approach considers the effects of edges of graphene nanostructures which can be conveniently modeled using one-dimensional periodic strips of graphene. Such models are commonly referred to as graphene nanoribbons. There are two high-symmetry crystallographic directions in graphene, armchair and zigzag[55] in Figure 2.6. Graphene nanoribbons were theoretically predicted and experimentally confirmed to exhibit semiconductivity if they had narrow widths and smooth edges.[56, 57]

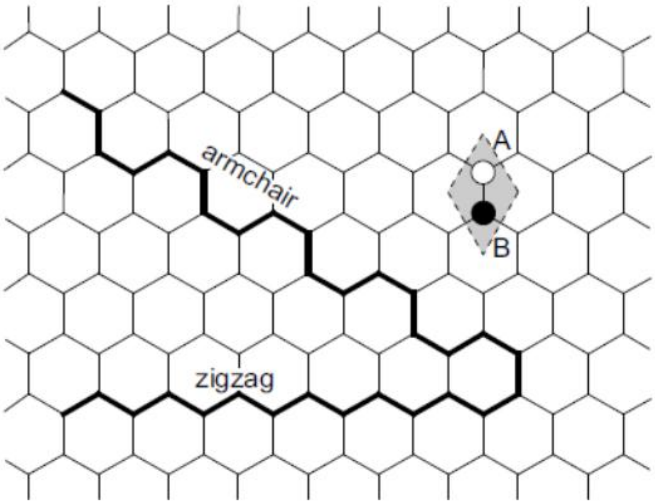

Figure 2. 6 Two kinds of defect overlap graphene sheet: zigzag and armchair

Son et al. predicted that external electric fields induce half-metality in zigzag graphene nanoribbons. The intriguing magnetic properties of graphene nanostructures may find applications in spintronics[58]. This kind of magnetic behavior may be ascribed to itinerant electron magnetism rather than superexchange magnetic coupling interaction between spins like molecule-based magnets[55]. This property makes carbon nanomaterials promising for transport of spin-polarized currents and for spin-based quantum information processing[59]. In addition, some researches indicated there is less trivial over hexagonal fragments with edges cutting along the same zigzag direction. It has been shown theoretically that above the critical size the system undergoes a transition into a broken-symmetry antiferromagnetic state[60]. The low-energy states are localized at the edge and decay quickly in the bulk graphene. High density of low-energy electronic states supported a possibility of magnetic ordering. Recently many of reports have pointed out that even untreated graphite exhibits ferromagnetism[61] .

2.7 Graphene -TiO_2 (ZnO) for photo-catalytic degradation of dyes

Numerous studies have been reported in the last decades on the photo degradation of organic compounds using semiconductor particles as photocatalysts[62, 63]. However, less than 5% of the solar energy (λ < 385 nm) can be used, the fraction of this energy harvest is quite limited by current photocatalytic materials. To utilize more effectively the inexpensive and inexhaustible energy of solar radiation reaching the surface of the earth, low cost and nontoxic photocatalysts with more efficient photocatalytic activity and high stability are sought, however, no such a material or system currently satisfy all these requirements [30].

It is well known, two challenges restrict the development of photo-catalyst technology; firstly most of sensitive semiconductors have slow quantum efficiency, in other words, the ratio of IPCE (Monochromatic Incident Photon-to-Electron Conversion Efficiency) is extremely low which can be attributed to high recombination speed between photon and electron on conduction band and valence band. Secondly, majority of semiconductors can only be triggered under short wavelength illumination due to the high band gap between conduction bands and valence bands. However, a carbonaceous nanomaterial, graphene, can modify the light sensitive particles.

Many researchers indicate that graphene, graphene oxide or reduced graphene oxide (RGO) can be adopted as coupling or doping compounds with the photo sensitive semiconductors such as TiO_2, ZnO and so on[12, 28, 45, 53, 63-75]. TiO_2 particles are well known to be one of the highest effective photocatalyst in degradation of dye pollutants and other organic pollutants, however its high trigger photo energy and high recombination ratio impede its utilization[76]. So visible light responsive modification to TiO_2 through GO/graphene is an attractive route to treat water pollution [77].

The mechanism of inorganic element dopants such as graphene with ability to enhance the visible light sensitivity is not yet well known. The valence and conduction bands of TiO_2 are mainly formed due to the major contribution by completely filled oxygen 2p orbital and the empty Ti 3d orbital, respectively. Some studies and literature on hetero-atom doped TiO_2 support the observation that, due to energy equality, the 2p orbital of the doped carbon atom are significantly interacting with O 2p orbital and contributing to the valence band formation, thereby the band width of the valence band decreases significantly[78-80]. The enhancement was also ascribed to the giant two-dimensional planar graphene structure favouring adsorption, which can suppress electron–hole recombination due to the high electrical

conductivity. Enhancement was also attributed to extension of light absorption to longer wavelengths in the visible range due to the high transparency and band-gap narrowing resulted from the presence of Ti–O–C bonds similar to the case of C-doped TiO_2 (Figure 2.7) [30, 68].

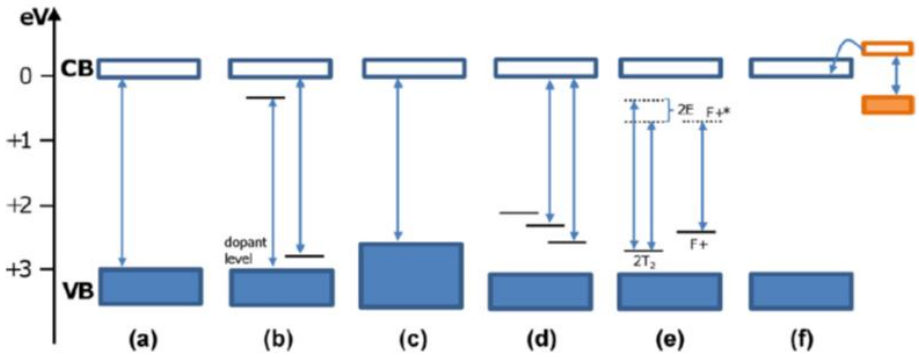

Figure 2. 7 Schemes illustrating the possible changes that might occur to the band- gap electronic structure of TiO_2 on doping with carbon (or other non-metals). (a) band-gap of pure TiO_2, (b) doped TiO_2 with localised dopant levels near the VB and the CB, (c) band-gap narrowing resulting from boarding of the VB, (d) localised dopant levels and electronic transitions to the CB, (e) electronic transitions from localised levels near the VB to their corresponding excited states for Ti+3 and F+ colour centres, (f) sanitization by smaller band-gap semiconductor [30].

Although some theories indicate that the cooperation between graphene and TiO_2 makes band-gap narrowing occurring, leading to a red-shift in photoactive wavelengths, there are currently other different interpretations of the role of the carbon atoms, and the manner and magnitude by which the band-gap is reduced, as well as the magnitude of carbon doping induced shift in absorption threshold to vary from as little as 0.1 to as much as 1.05 eV[30].

The bridged 2D graphene sheets as highly conducting materials have an excellent electronic conduction in flat and can well serve as the acceptor and transporter of the photo-excited electrons in the graphene sheet loading TiO_2. This function of the graphene decreased the charge-transfer resistance and consequently improved the photo-electrochemical performance of the Graphene-TiO_2 particles [41, 68, 81, 82]. Similarly, in graphene oxide loaded TiO_2 composites the excited electron from TiO_2 can quickly transfer from the conduction band of TiO_2 to the GO/graphene, the electrons have more opportunity to expose to pollutants and

keep stable condition with high potentials, which effectively suppresses the recombination of photo-generated charge carriers and transforms into high energy radicals in the same time leaving more charge carriers to form highly reactive species and promote the degradation of dyes [68]. It is accepted that graphene has a function which enables an easy and fast transfer of conduct band electron of TiO_2, similar to that of noble metal in TiO_2 lattice[83]. Valentin et al. [84] claimed that under conditions of low oxygen concentration, C substitution for oxygen (C@O) and formation of oxygen vacancies is favoured, whereas oxygen rich conditions favour interstitial C atoms and/or substitution for titanium (C@Ti). Yang et al. [85] also found that the variation in the band-gap for C@O substitution in TiO_2, and the introduction of spin-polarized gap states of C 2p orbital. For C@Ti, spin-polarized states were not introduced, but the band-gap was reduced by 0.18 eV and 0.3 eV in anatase and rutile TiO_2, respectively.

The reduction of graphene oxide can lead to surface defects on the 2-dimentional graphene sheets, those defects are assumed to increase the amount of hole in composite which can adjust the percentage of hole and electron, reducing the recombination speed between them. Additionally the defects can destruct the crystal surface and produce a tendency as formulated below:

$$O_2^{2-} + h^+ \rightarrow O^-$$

$$O^- + h^+ \rightarrow O^{\cdot}$$

$$O^- (ads) + \ \rightarrow O^{\cdot}$$

$$O^- (ads) + H_2O \rightarrow O^{\cdot} (ads) + OH^-(ads)$$

Thus, the absorption capability of the catalyst onto dissociative oxygen atoms and aromatic organic contamination will be increased [68, 86].

It is proposed that graphene-based photocatalysts can be prepared at fairly low temperatures Jiang et al.[45], investigated azo dye degradation on a TiO_2-graphene composite. $(NH_4)_2TiF_6$

was adopted as a TiO_2 precursor and H_3BO_3 was employed as a reductant. However, graphene has low solubility in water and polar organic solvents and the strong van der Waals force makes graphene aggregating [38, 87, 88]. The hydrophobic/hydrophilic incompatibility between graphene and inorganic compounds (especially metal oxides) makes it difficult to directly deposit metal oxides on graphene[45, 89]. Graphene oxide with oxygen-containing groups can interact with titanium hydroxide by hydrogen bonds [90], leading to self-assembling of TiO_2 particles to anchor on graphene oxide surface. XPS analyses found that there is new bond between graphene and TiO_2 particle. Calcination temperature affects the photocatalytic activity of graphene loading TiO_2 composites. When the calcination temperature is increased from 100 to 200 ℃ there is a weak tendency of degradation ability whereas the activity is higher at 250 ℃. In general cases the calcination temperature is much higher [91]. It is believed that high temperature will result in the partial combustion of graphene oxide, causing partial destruction of the composite structure which is unmerited for photo-degradation[45]. However, the black graphene oxide sheets in the composite will increase photo absorbing and scattering, leading to a weak photocatalytic activity of the composites when the graphene oxide content was too high. In general, graphene oxide based TiO_2 composite exhibited excellent photocatalytic ability for the oxidative degradation of organic pollutants such as methyl red, orange G, methyl blue, methyl orange, furthermore it also showed a strong photocatalytic activity for the reduction of toxic Cr(VI) to Cr(III).

Hou et al.[92] reported a novel 3-D hydrogenated photocatalyst within titanium dioxide (P25) graphene and carbon nanotube (Figure 2.8). In this procedure the authors employed L-ascorbic acid and hydrazine for RGO production, which could gradually restored strong π-π^* interaction among the reduced graphite oxide sheets[93]. During the reduction, the π-π^* conjugated structures of reduced GO sheets are increased and the amount of the π-π stacking increases. The particle overlaps or coalesces of flexible graphene sheets form the 3D

structures. The cooperation could dramatically enhance photo degradation organic pollutants [94]. In this TiO_2–C composite, graphene could play a role as an acceptor of the photogenerated electrons and ensure fast charge transfer (to suppress charge recombination) in view of its high conductivity, leading to an enhancement in the photocatalytic performance[95]. Carbon doping strongly affects the light absorption of photocatalysts and there is a red shift in the absorption edge from 385 to 405 nm of P25 sample, which plays an important role in the visible light photocatalysis. These functional groups on the edges of graphene oxide can act as anchor sites[96] and metallic ions will be adsorbed onto the surfaces of GO sheets due to their bonding with the oxygen atoms of the negatively charged.

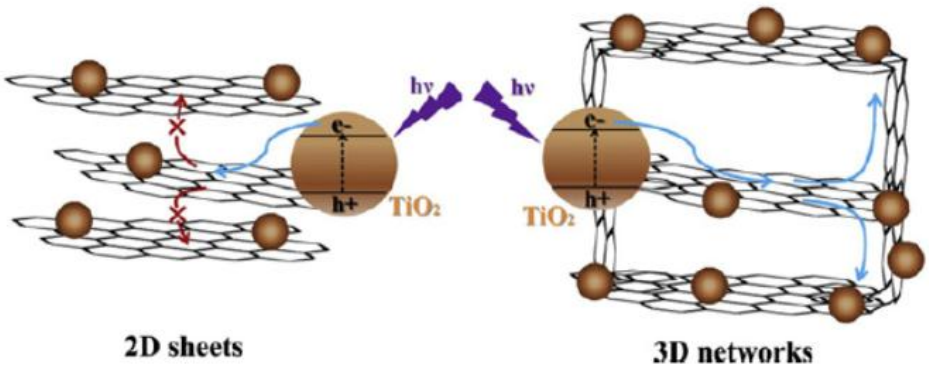

Figure 2. 8 Schematic diagrams for illumination the charge behaviour at interfaces in 2D P25-graphene sheet and 3D-graphene network [92]

Same as TiO_2, zinc oxide is also a photocatalyst because of its strong oxidizing power, non-toxic instinct, and low cost. ZnO is a wide band-gap semiconductor (3.37 eV) with a conduction band edge located at approximately the same level as that of TiO_2. More attractively, the electron mobility of ZnO has been proven to be higher than that of TiO_2 [97]. Graphene doped ZnO nanoparticles are useful to extend the light absorption or suppress the electron–hole recombination [98].

Li et al. [96] synthesised a system of flower-like ZnO nanoparticles anchoring on GO sheets and utilized for photocatalytic degradation of organic dyes in aqueous system with visible

light. In a typical process, ZnCl with exfoliated GO suspension was mixed in ethanol and sodium hydroxide solution, and then the particles were annealed at 400 ℃. In the UV-spectrum analysis, the ZnO/GO composite shows absorption in the whole visible region (Figure 2.9).

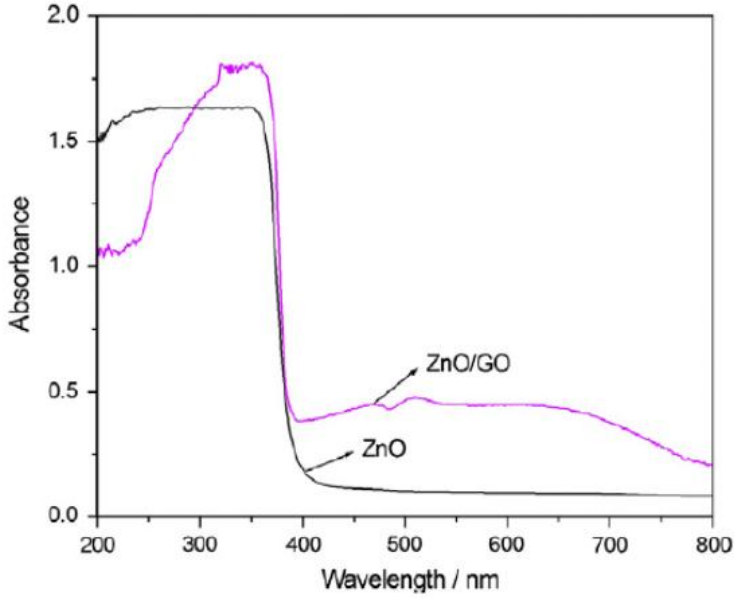

Figure 2. 9 UV-Vis diffuse reflection spectra of pure ZnO and ZnO/GO nanocomposite

ZnO/GO nanocomposite was found to exhibit very prominent photocatalytic efficiency, and 98.1% of MB was photodegraded from the aqueous solution after visible-light irradiation for 40 to 60 min (MB initial concentration, 5.0 $\times 10^{-5}$ mol/L; 100 mL). GO as electron collector and transporter is responsible for the enhanced photocatalytic performance under visible light. If GO sheets were used as photocatalysts, however, very slow reaction rate was observed.

ZnO containing graphene photocatalyst can be incorporated with magnetic material. In this way, the catalyst could possess high photocatalystic behaviour with magnetic separation in a suspension system. Fu and Wang [99] prepared $ZnFe_2O_4$ nanocrystals coupling onto graphene sheets by a one-step hydrothermal method. In a typical process, GO powder, absolute ethanol, $Zn(NO_3)_2 \cdot 6H_2O$ and $Fe(NO_3)_3 \cdot 3H_2O$ were vigorously stirred together to synthesise a stable bottle-green homogeneous emulsion, under hydrothermal treatment at

180℃. Different proportions of particles were collected by filtration. In this case, GO was reduced to RGO without strong interaction with ZnO and Fe_2O_3, O 2p orbitals in ZnO and Fe 3d vacancy orbitals were assumed to attribute to photoexcitation. The UV-visible diffuse reflectance spectra showed an absorption sharp edge at 700 nm and band gap energy was estimated to be 1.90 eV. As a result, the significant enhancement in photoactivity can be ascribed to the efficient separation of photogenerated carriers in the $ZnFe_2O_4$-graphene coupling system, and graphene plays an important role as a supporter and carrier.

Ji et al. [100] proposed the dye with photo-electronic property is usually easier to excite than ZnO at upper wavelength 420 nm. Photo–electron will transfer to the conduction band of ZnO. The electron is trapped by surface to generate various reactive oxidations, which accelerates the dye self-degradation [101]. Li et al. [102] generated a ZnO@GO photocatalyst using raw GO and $Zn(AcO)_2{\cdot}3H_2O$. The excited dye can inject electrons to graphene or graphene derivatives. In photocatalytic degradation of RhB under UV-visible light irradiation, the degradation process was completed within 120 min on the naked ZnO particle. However, the degradation of RhB was completed within 60 min in the presence of the ZnO@GO.

Ta_2O_5 as a semiconductor has been intensively studied. Recently it has been investigated as an efficient photocatalyst for decomposition of VOCs, water splitting into H_2 and O_2, and CO_2 reduction. Ta_2O_5 and derivatives have been thought as new photocatalysts with a redox potential at 2.8 eV. Murase et al.[103] calcined Ta_2O_5 particle in NH_4OH in order to dope nitrogen element into Ta_2O_5 lattice. Nitrogen substituted the oxygen element and the nitrogen-doped $Ta_2N_xO_{5-x}$ could have photo-excitation under visible radiation. In UV-Vis

absorption spectra, it was found that N-dopant could affect the band gap energy and shift location of sharp edge (Figure 2.10).

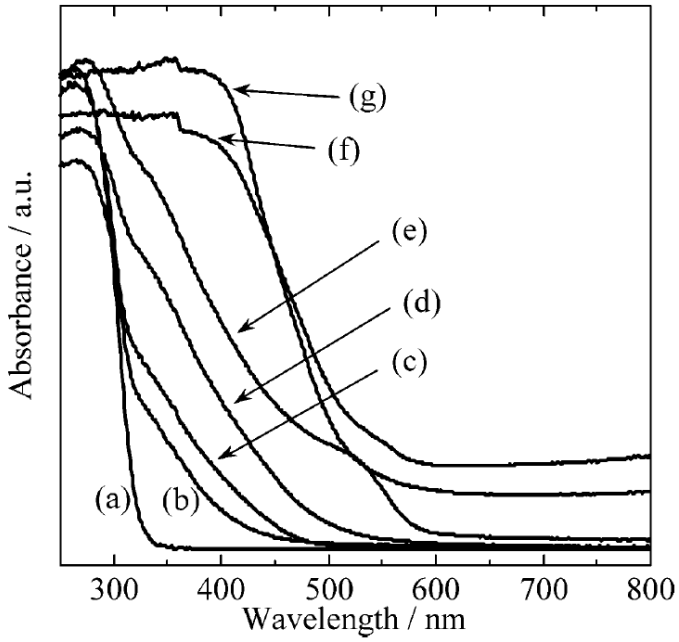

Figure 2. 10 UV-Vis absorption spectra of Ta_2O_5, Ta_2O_5-xNx, and TaON powders. (a) x = 0 (600 °C, air), (b) x = 0.10 (600 °C, NH3), (c) x =0.17 (620 °C, NH3), (d) x = 0.24 (650 °C, NH3), (e) x = 0.35 (700 °C,NH3), (f) mixture of TaON and Ta2O5 (800 °C, NH3), and (g) TaON phase, TaO1.40N0.60 (850 °C, NH3)[103].

Furthermore nitrogen-doped Ta_2O_5 can decompose organic compounds under UV and Vis light irradiations. It is potential that Ta_2O_5 could also be modified by graphene oxide. However, no such investigation has been reported.

2.8 Conclusion

Organic water pollutants have threatened humans. Novel photo-degradation technology provides an alternative method to resolve this problem by using photo-sensitive semiconductors and solar energy, which could decompose organic compounds into CO_2 and H_2O. However, most photo-catalysts possess high band gap energy and low efficiency, which could be attributed to low surface area of catalyst, low absorption ability, unstable electronic structure of corrosion.

Many strategies to modify a photocatalyst in order to increase its light absorption capacity, stabilization, and photoreaction efficiency, for instance: ion doping, dye sensitization, noble metal doping, and electron scavenger and so on. It is believed that organic or inorganic materials can be used to adjust the band gap energy of a photocatalyst.

Graphene is a new carbonaceous nanomaterial with one carbon layer structure, and with special photo and electric property. Because of special electronic properties, high surface area, and super stability, graphene doped photocatalysts are good at visible light absorption, low recombination of electron-hole pair and adsorption of a pollutant. Graphene doped photocatalysts can be used in water purification for organic depollution.

2.9 References

[1] A. Fujishima, K. Honda, Electrochemical Photolysis of Water at a Semiconductor Electrode, Nature, 238 (1972) 37-38.

[2] B. Kim, D. Kim, D. Cho, S. Cho, Bactericidal effect of TiO2 photocatalyst on selected food-borne pathogenic bacteria, Chemosphere, 52 (2003) 277-281.

[3] L. Zou, Removal of VOCs by photocatalysis process using adsorption enhanced TiO2-SiO2 catalyst, Chemical engineering and processing, 45 (2006) 959.

[4] S.B. Kim, S.C. Hong, Kinetic study for photocatalytic degradation of volatile organic compounds in air using thin film TiO2 photocatalyst, Applied Catalysis B: Environmental, 35 (2002) 305-315.

[5] A. Fujishima, T.N. Rao, D.A. Tryk, Titanium dioxide photocatalysis, Journal of Photochemistry and Photobiology C: Photochemistry Reviews, 1 (2000) 1-21.

[6] K. Hashimoto, TiO2 photocatalysis: a historical overview and future prospects, AAPPS Bulletin, 17 (2007) 12.

[7] T. Hirakawa, Properties of O2-and OH formed in TiO2 Aqueous Suspensions by Photocatalytic Reaction and the Influence of H2O2 and Some Ions, Langmuir, 18 (2002) 3247.

[8] I. Arslan, I. Balcioglu, T. Tuhkanen, D. Bahnemann, H2O2/UV-C and Fe2+/H2O2/UV-C versus TiO2/UV-A Treatment for Reactive Dye Wastewater, Journal of Environmental Engineering, 126 (2000) 903-911.

[9] M. Rani, N. Gupta, B. Pal, Superior photodecomposition of pyrene by metal ion-loaded TiO₂ catalyst under UV light irradiation, Environmental Science and Pollution Research, 19 (2012) 2305-2312.

[10] E. Forgacs, T. Cserháti, G. Oros, Removal of synthetic dyes from wastewaters: A review, Environment International, 30 (2004) 953-971.

[11] F.B. Li, The enhancement of photodegradation efficiency using Pt-TiO2 catalyst, Chemosphere, 48 (2002) 1103.

[12] F. Wang, K. Zhang, Reduced graphene oxide–TiO2 nanocomposite with high photocatalystic activity for the degradation of rhodamine B, Journal of Molecular Catalysis A: Chemical, 345 (2011) 101-107.

[13] H. Sun, R. Ullah, S. Chong, H.M. Ang, M.O. Tadé, S. Wang, Room-light-induced indoor air purification using an efficient Pt/N-TiO2 photocatalyst, Applied Catalysis B: Environmental, 108–109 (2011) 127-133.

[14] X. Yue, R. Zhang, F. Zhang, L. Wang, Decomposition of crude oil absorbed into expanded graphite/TiO2 /NiO composites, Desalination, 252 (2010) 163-166.

[15] A.L. Linsebigler, G. Lu, J.T. Yates, Photocatalysis on TiO2 Surfaces: Principles, Mechanisms, and Selected Results, Chemical Reviews, 95 (1995) 735-758.

[16] A.L. Linsebigler, G. Lu, J.T. Yates Jr, Photocatalysis on TiO2 surfaces: Principles, mechanisms, and selected results, Chemical Reviews, 95 (1995) 735-758.

[17] I. Robel, Quantum dot solar cells. Harvesting light energy with CdSe nanocrystals molecularly linked to mesoscopic TiO2 films, Journal of the American Chemical Society, 128 (2006) 2385.

[18] K.L. Schulte, P.A. DeSario, K.A. Gray, Effect of crystal phase composition on the reductive and oxidative abilities of TiO2 nanotubes under UV and visible light, Applied Catalysis B: Environmental, 97 (2010) 354-360.

[19] Z.G. Zou, Direct splitting of water under visible light irradiation with an oxidesemiconductor photocatalyst, Nature, 414 (2001) 625.

[20] J. Zhu, Nanocrystalline Fe/TiO2 Visible Photocatalyst with a Mesoporous Structure Prepared via a Nonhydrolytic Sol-Gel Route, The journal of physical chemistry. C, 111 (2007) 18965.

[21] Di Li, Li, Visible-light-driven NF-codoped TiO2 photocatalysts. 2. Optical characterization, photocatalysis, and potential application to air purification, Chemistry of Materials, 17 (2005) 2596.

[22] X. Yang, Synthesis of visible-light-active TiO2-based photocatalysts by carbon and nitrogen doping, Journal of Catalysis, 260 (2008) 128.

[23] R. Abe, T. Takata, H. Sugihara, K. Domen, Photocatalytic overall water splitting under visible light by TaON and WO3 with an IO3-/I- shuttle redox mediator, Chemical Communications, (2005) 3829-3831.

[24] T. Stergiopoulos, Binary polyethylene oxide/titania solid-state redox electrolyte for highly efficient nanocrystalline TiO2 photoelectrochemical cells, Nano letters, 2 (2002) 1259.

[25] S. Arounaguiri, B.G. Maiya, “Electro-Photo Switch” and “Molecular Light Switch” Devices Based on Ruthenium (II) Complexes of Modified Dipyridophenazine Ligands: Modulation of the Photochemical Function through Ligand Design, Inorganic chemistry, 38 (1999) 842-843.

[26] E.M. Kober, B.P. Sullivan, T.J. Meyer, Solvent dependence of metal-to-ligand charge-transfer transitions. Evidence for initial electron localization in MLCT excited states of 2, 2'-bipyridine complexes of ruthenium (II) and osmium (II), Inorganic chemistry, 23 (1984) 2098-2104.

[27] T. Tsujioka, Y. Hamada, K. Shibata, A. Taniguchi, T. Fuyuki, Nondestructive readout of photochromic optical memory using photocurrent detection, Applied Physics Letters, 78 (2001) 2282-2284.

[28] E. Bae, Highly enhanced photoreductive degradation of perchlorinated compounds on dye-sensitized metal/TiO2 under visible light, Environmental science & technology, 37 (2003) 147.

[29] E. Bae, W. Choi, J. Park, H.S. Shin, S.B. Kim, J.S. Lee, Effects of Surface Anchoring Groups (Carboxylate vs Phosphonate) in Ruthenium-Complex-Sensitized TiO2 on Visible Light Reactivity in Aqueous Suspensions, The Journal of Physical Chemistry B, 108 (2004) 14093-14101.

[30] R. Leary, A. Westwood, Carbonaceous nanomaterials for the enhancement of TiO2 photocatalysis, Carbon, 49 (2011) 741-772.

[31] K.S. Novoselov, Electric field effect in atomically thin carbon films, Science, 306 (2004) 666.

[32] K.A. Mkhoyan, Atomic and electronic structure of graphene-oxide, Nano letters, 9 (2009) 1058.

[33] D. Graf, Spatially resolved Raman spectroscopy of single-and few-layer graphene, Nano letters, 7 (2007) 238.

[34] L. Liu, Graphene oxidation: Thickness-dependent etching and strong chemical doping, Nano letters, 8 (2008) 1965.

[35] J.H. Hwang, K.S. Lee, H.S. Bang, D.C. Choo, T.W. Kim, J.M. Lee, W.I. Park, Enhancement of the Hole Injection Current in Polymer Light-Emitting Devices Fabricated Utilizing a Graphene Layer, Journal of The Electrochemical Society, 158 (2011) J273-J275.

[36] K.S. Novoselov, Two-dimensional gas of massless Dirac fermions in graphene, Nature, 438 (2005) 197.

[37] J.C. Meyer, A.K. Geim, M.I. Katsnelson, K.S. Novoselov, T.J. Booth, S. Roth, The structure of suspended graphene sheets, Nature, 446 (2007) 60-63.

[38] G. Wang, Synthesis and characterisation of hydrophilic and organophilic graphene nanosheets, Carbon, 47 (2009) 1359.

[39] N.J. Coville, S.D. Mhlanga, E.N. Nxumalo, A. Shaikjee, A review of shaped carbon nanomaterials, South African Journal of Science, 107 (2011) 01-15.

[40] W.A. De Heer, H. de, Epitaxial graphene electronic structure and transport, Journal of physics. D, Applied physics, 43 (2010) 374007.

[41] C. Berger, Electronic confinement and coherence in patterned epitaxial graphene, Science, 312 (2006) 1191.

[42] J. Wintterlin, Graphene on metal surfaces, Surface Science, 603 (2009) 1841.

[43] W.S. Hummers Jr, Hummers, Preparation of graphitic oxide, Journal of the American Chemical Society, 80 (1958) 1339.

[44] T.F. Yeh, Graphite Oxide with Different Oxygenated Levels for Hydrogen and Oxygen Production from Water under Illumination: The Band Positions of Graphite Oxide, The journal of physical chemistry. C, 115 (2011) 22587.

[45] G. Jiang, Z. Lin, C. Chen, L. Zhu, Q. Chang, N. Wang, W. Wei, H. Tang, TiO2 nanoparticles assembled on graphene oxide nanosheets with high photocatalytic activity for removal of pollutants, Carbon, 49 (2011) 2693-2701.

[46] M. Seredych, Mechanism of ammonia retention on graphite oxides: role of surface chemistry and structure, The journal of physical chemistry. C, 111 (2007) 15596.

[47] Y. Matsuo, Y. Nishino, T. Fukutsuka, Y. Sugie, Introduction of amino groups into the interlayer space of graphite oxide using 3-aminopropylethoxysilanes, Carbon, 45 (2007) 1384-1390.

[48] J. Ito, Semiconducting nature of the oxygen-adsorbed graphene sheet, Journal of applied physics, 103 (2008) 113712.

[49] T.F. Yeh, Graphite oxide as a photocatalyst for hydrogen production from water, Advanced functional materials, 20 (2010) 2255.

[50] D.W. Boukhvalov, Modeling of graphite oxide, Journal of the American Chemical Society, 130 (2008) 10697.

[51] T.O. Wehling, Molecular doping of graphene, Nano letters, 8 (2008) 173.

[52] O.V. Yazyev, Emergence of magnetism in graphene materials and nanostructures, Reports on progress in physics, 73 (2010) 056501.

[53] G. Williams, B. Seger, P.V. Kamat, TiO2-Graphene Nanocomposites. UV-Assisted Photocatalytic Reduction of Graphene Oxide, ACS nano, 2 (2008) 1487-1491.

[54] J. Barzola Quiquia, Experimental evidence for two-dimensional magnetic order in proton bombarded graphite, Physical review. B, Condensed matter and materials physics, 76 (2007) 161403.

[55] Y. Wang, Room-temperature ferromagnetism of graphene, Nano letters, 9 (2009) 220.

[56] Q. Yan, Intrinsic current-voltage characteristics of graphene nanoribbon transistors and effect of edge doping, Nano letters, 7 (2007) 1469.

[57] X. Li, Chemically derived, ultrasmooth graphene nanoribbon semiconductors, Science, 319 (2008) 1229.

[58] Y.W. Son, Half-metallic graphene nanoribbons, Nature, 444 (2006) 347.

[59] J. Wu, Graphenes as potential material for electronics, Chemical Reviews, 107 (2007) 718.

[60] J. Fernández Rossier, Magnetism in graphene nanoislands, Physical review letters, 99 (2007) 177204.

[61] P. Esquinazi, Induced magnetic ordering by proton irradiation in graphite, Physical review letters, 91 (2003) 227201.

[62] M. Qamar, M. Muneer, A comparative photocatalytic activity of titanium dioxide and zinc oxide by investigating the degradation of vanillin, Desalination, 249 (2009) 535-540.

[63] D. Fu, The synthesis and properties of ZnO–graphene nano hybrid for photodegradation of organic pollutant in water, Materials Chemistry and Physics, 132 (2012) 673.

[64] W. Zou, J. Zhu, Y. Sun, X. Wang, Depositing ZnO nanoparticles onto graphene in a polyol system, Materials Chemistry and Physics, 125 (2011) 617-620.

[65] J. Zhu, Y. Li, Y. Chen, J. Wang, B. Zhang, J. Zhang, W.J. Blau, Graphene oxide covalently functionalized with zinc phthalocyanine for broadband optical limiting, Carbon, 49 (2011) 1900-1905.

[66] Y. Zhang, TiO2-Graphene Nanocomposites for Gas-Phase Photocatalytic Degradation of Volatile Aromatic Pollutant: Is TiO2-Graphene Truly Different from Other TiO2- Carbon Composite Materials?, ACS nano, 4 (2010) 7303.

[67] Y. Yang, T. Liu, Fabrication and characterization of graphene oxide/zinc oxide nanorods hybrid, Applied Surface Science, 257 (2011) 8950-8954.

[68] H. Zhang, P25-graphene composite as a high performance photocatalyst, ACS nano, 4 (2010) 380.

[69] D.-H. Yoo, T.V. Cuong, V.H. Pham, J.S. Chung, N.T. Khoa, E.J. Kim, S.H. Hahn, Enhanced photocatalytic activity of graphene oxide decorated on TiO2 films under UV and visible irradiation, Current Applied Physics, 11 (2011) 805-808.

[70] G. Williams, Graphene− Semiconductor Nanocomposites: Excited-State Interactions between ZnO Nanoparticles and Graphene Oxide†, Langmuir, 25 (2009) 13869.

[71] V. Stengl, TiO2-Graphene Nanocomposite as High Performance Photocatalysts, The journal of physical chemistry. C, 115 (2011) 25209.

[72] T.S. Sreeprasad, S.M. Maliyekkal, K.P. Lisha, T. Pradeep, Reduced graphene oxide–metal/metal oxide composites: Facile synthesis and application in water purification, Journal of Hazardous Materials, 186 (2011) 921-931.

[73] J. Shen, One step hydrothermal synthesis of TiO2-reduced graphene oxide sheets, Journal of Materials Chemistry, 21 (2011) 3415.

[74] G.H. Jeong, Direct synthesis of noble metal/graphene nanocomposites from graphite in water: photo-synthesis, Chemical communications (London. 1996), 47 (2011) 12236.

[75] H. Hu, X. Wang, F. Liu, J. Wang, C. Xu, Rapid microwave-assisted synthesis of graphene nanosheets-zinc sulfide nanocomposites: Optical and photocatalytic properties, Synthetic Metals, 161 (2011) 404-410.

[76] S. Klosek, D. Raftery, Visible Light Driven V-Doped TiO2 Photocatalyst and Its Photooxidation of Ethanol, The Journal of Physical Chemistry B, 105 (2001) 2815-2819.

[77] C. Chen, X. Li, W. Ma, J. Zhao, H. Hidaka, N. Serpone, Effect of Transition Metal Ions on the TiO2-Assisted Photodegradation of Dyes under Visible Irradiation: A Probe for the Interfacial Electron Transfer Process and Reaction Mechanism, The Journal of Physical Chemistry B, 106 (2001) 318-324.

[78] M. Sathish, Characterization and photocatalytic activity of N-doped TiO2 prepared by thermal decomposition of Ti–melamine complex, Applied catalysis. B, Environmental, 74 (2007) 307.

[79] S. Sato, Photocatalysts Sensitive to Visible Light, Science, 295 (2002) 626-627.

[80] R. Asahi, T. Morikawa, T. Ohwaki, K. Aoki, Y. Taga, Visible-Light Photocatalysis in Nitrogen-Doped Titanium Oxides, Science, 293 (2001) 269-271.

[81] N. Yang, Two-dimensional graphene bridges enhanced photoinduced charge transport in dye-sensitized solar cells, ACS nano, 4 (2010) 887.

[82] K.K. Manga, Multilayer hybrid films consisting of alternating graphene and titania nanosheets with ultrafast electron transfer and photoconversion properties, Advanced functional materials, 19 (2009) 3638.

[83] Y.J. Yu, Tuning the graphene work function by electric field effect, Nano letters, 9 (2009) 3430.

[84] C. Di Valentin, Theory of carbon doping of titanium dioxide, Chemistry of Materials, 17 (2005) 6656.

[85] K. Yang, Density functional characterization of the visible-light absorption in substitutional C-anion-and C-cation-doped TiO2, The journal of physical chemistry. C, 113 (2009) 2624.

[86] J. Zhang, Increasing the Oxygen Vacancy Density on the TiO2 Surface by La-Doping for Dye-Sensitized Solar Cells, The journal of physical chemistry. C, 114 (2010) 18396.

[87] Y. Wang, X. Chen, Y. Zhong, F. Zhu, K.P. Loh, Large area, continuous, few-layered graphene as anodes in organic photovoltaic devices, Applied physics letters, 95 (2009) 063302.

[88] T.N. Murakami, Y. Fukushima, Y. Hirano, Y. Tokuoka, M. Takahashi, N. Kawashima, Surface modification of polystyrene and poly(methyl methacrylate) by active oxygen treatment, Colloids and Surfaces B: Biointerfaces, 29 (2003) 171-179.

[89] S.M. Paek, Enhanced cyclic performance and lithium storage capacity of SnO2/graphene nanoporous electrodes with three-dimensionally delaminated flexible structure, Nano letters, 9 (2009) 72.

[90] J.V. Stark, Nanoscale metal oxide particles/clusters as chemical reagents. Unique surface chemistry on magnesium oxide as shown by enhanced adsorption of acid gases (sulfur dioxide and carbon dioxide) and pressure dependence, Chemistry of Materials, 8 (1996) 1904.

[91] B. Jiang, In Situ Growth of TiO2 in Interlayers of Expanded Graphite for the Fabrication of TiO2–Graphene with Enhanced Photocatalytic Activity, Chemistry - A European Journal, 17 (2011) 8379.

[92] C. Hou, Q. Zhang, Y. Li, H. Wang, P25–graphene hydrogels: Room-temperature synthesis and application for removal of methylene blue from aqueous solution, Journal of Hazardous Materials, 205–206 (2012) 229-235.

[93] Z. Sui, X. Zhang, Y. Lei, Y. Luo, Easy and green synthesis of reduced graphite oxide-based hydrogels, Carbon, 49 (2011) 4314-4321.

[94] Z. Tang, S. Shen, J. Zhuang, X. Wang, Noble-Metal-Promoted Three-Dimensional Macroassembly of Single-Layered Graphene Oxide, Angewandte Chemie, 122 (2010) 4707-4711.

[95] H. Zhang, X. Lv, Y. Li, Y. Wang, J. Li, P25-Graphene Composite as a High Performance Photocatalyst, ACS Nano, 4 (2009) 380-386.

[96] B. Li, ZnO/graphene-oxide nanocomposite with remarkably enhanced visible-light-driven photocatalytic performance, Journal of Colloid and Interface Science, 377 (2012) 114.

[97] K. Keis, C. Bauer, G. Boschloo, A. Hagfeldt, K. Westermark, H. Rensmo, H. Siegbahn, Nanostructured ZnO electrodes for dye-sensitized solar cell applications, Journal of Photochemistry and Photobiology A: Chemistry, 148 (2002) 57-64.

[98] H. Zhang, X. Lv, Y. Li, Y. Wang, J. Li, P25-graphene composite as a high performance photocatalyst, ACS nano, 4 (2010) 380-386.

[99] Y. Fu, X. Wang, Magnetically Separable ZnFe2O4–Graphene Catalyst and its High Photocatalytic Performance under Visible Light Irradiation, Industrial & Engineering Chemistry Research, 50 (2011) 7210-7218.

[100] P. Ji, J. Zhang, F. Chen, M. Anpo, Study of adsorption and degradation of acid orange 7 on the surface of CeO2 under visible light irradiation, Applied Catalysis B: Environmental, 85 (2009) 148-154.

[101] M.J. Allen, V.C. Tung, R.B. Kaner, Honeycomb Carbon: A Review of Graphene, Chemical Reviews, 110 (2009) 132-145.

[102] B. Li, H. Cao, ZnO@graphene composite with enhanced performance for the removal of dye from water, Journal of Materials Chemistry, 21 (2011) 3346-3349.

[103] T. Murase, H. Irie, K. Hashimoto, Visible light sensitive photocatalysts, nitrogen-doped Ta2O5 powders, The Journal of Physical Chemistry B, 108 (2004) 15803-15807.

3

3 Graphene facilitated visible light photodegradation of methylene blue over titanium dioxide photocatalysts

Abstract

Graphene-TiO_2 composites (G-TiO_2) were synthesized by a sol-gel method using titanium isoproproxide (or P25) as Ti-precursors, and reduced graphene oxide (RGO). The structural, morphological, and physicochemical properties of the samples were thoroughly investigated by means of X-ray diffraction (XRD), Fourier transform infrared spectroscopy (FT-IR), field emission scanning electron microscopy (FE-SEM), UV-vis diffuse reflectance (UV-vis DRS) and thermogravimetric differential thermal analysis (TG-DTA). The diffuse reflectance spectra (DRS) studies demonstrated that there is an enhanced absorption of light absorption by G-TiO_2 compared with that of naked TiO_2. The photocatalytic activity in methylene blue bleaching for G-TiO_2 under visible light (> 430 nm) is much enhanced. G-TiO_2 synthesised from titanium isoproproxide presented higher activity than that of G-TiO_2 (P25).

3.1 Introduction

Photocatalytic decomposition of various organic compounds in aqueous solutions has been widely studied and many nanomaterials have been developed as photocatalysts for this technology [1-4]. TiO_2 has been intensively investigated as a photocatalyst for environmental clean-up and solar energy conversion. However, TiO_2 can only decompose aromatic organics into CO_2 and H_2O under UV-illumination whereas it cannot absorb visible light with wavelength longer than 387 nm due to a large band gap of 3.2 eV. Thus, TiO_2 can only utilize 3–5% of the solar energy that can reach onto the earth surface. The common strategies for extending the absorption threshold of TiO_2 to visible light region include doping, coupling or anchoring with other organic or inorganic elements such as nitrogen, carbon, halogen, and metals into the titania lattice [5-9].

Combination of different types of carbon with TiO_2 has been suggested as a promising method for an enhanced photocatalytic performance [10, 11]. In the past a few years, graphene as a novel carbonaceous nanomaterial has attracted more and more interests due to its chemical, structural and electrical properties. Graphene is considered as a single sheet of graphite which has impressively theoretical surface area of 2600 m^2/g [10]. Because it has a hexagonal honeycomb network structure, the sp^2-bonded carbon lattice can have numerous outstanding electronic and spacious delocalized π-bonds which enhance its structure stability and current conductivity capacity [12].

Several attempts in using graphene oxide (GO) or reduced graphene oxide (RGO) for modification of TiO_2 for photocatalytic degradation of organics have been reported[13, 14]. Zhang et al. [15] used a commercial TiO_2 (P25) and GO to obtained TiO_2-graphene nanocomposite. Thuy-Duong et al. [16] prepared a TiO_2 (P25)-GO composite using a simple colloidal blending method. Liang et al. [17] reported a graphene/TiO_2 nanocrystals hybrid

fabricated by directly growing TiO_2 nanocrystals on graphene oxide (GO) sheets. The reported graphene/TiO_2 nanocrystals hybrid has a superior photocatalytic activity over other TiO_2 materials in the degradation of a dye of rhodamine B. Chen et al. [18] also investigated GO/TiO_2 composites via a self-assembly method on GO using $TiCl_3$ as Ti-precursor. However, using P25 to deposit on GO usually resulted in aggregation of TiO_2. In addition, exfoliated GO exhibits poor electronic conductivity because of the interruption of the π system by substitution with oxygen functional groups. Therefore, a form of graphene/TiO_2 composite with high interfacial contact with graphene surface without aggregating will be highly in demand for an improved photocatalytic performance. The unique structure will facilitate the charge separation and electron transfer from TiO_2 to graphene upon irradiation[19].

we report a preparation of G-TiO_2 composite using a reduced graphene oxide and a titanium precursor by a sol-gel method. For comparison, a G-TiO_2(P25) was synthesized. These photocatalysts were tested in photocatalytic degradation of a dye, methylene blue, under simulated sunlights and visible lights.

3.2 Experimental

1. Materials and reagents

Natural graphite powders (AF99, 325 mesh, 99.995% carbon content) were used for GO synthesis. All other reagents, sulphuric acid (95–98%, Shcarlau), $KMnO_4$ (Fluka), H_2O_2 (30%, Biolab), were used as received. Titanium (IV) isopropoxide (TTIP) was used as a Ti-precursor and supplied by Aldrich Chemicals with a purity of 97%. A reference material of TiO_2-P25 was received from Degussa, Germany.

2. Preparation of TiO_2 and G-TiO_2 samples

Graphene oxide (GO) was prepared by a modified Hummers method [20, 21] and reduction of exfoliated GO was obtained by hydrothermal solvation using hydrazine hydrate. Typically, GO (100 mg) was loaded in a 250 mL round bottom flask with 100 mL deionized water and subjected to ultrasonic treatment for 2 h, yielding a homogeneous yellow-brown dispersion. Hydrazine hydrate (1.00 mL) was then added in and the solution was heated at 100 ℃ for 24 h. The reduced GO (RGO) was gradually precipitated as a black solid. This product was separated by filtration and washed with ethanol and water several times and then dried at 80 ℃.

For synthesis of G-TiO_2, RGO powder, hexadecyltrimethylammonium bromide (CTAB, 0.5 g) and 30 mL ethanol were placed in a 100 mL beaker with stirring. After 30 min, titanium isoproproxide was dropwised into the reactor. Then 20 mL DI water was added into the mixture. The suspension was stirred for 8 h and dried at 80 ℃. The solid was calcined in a muffle furnace at 500 ^{o}C from environment temperature, then keep it for 5 min and cool down in air immediately. In G-TiO_2 samples, graphene loading was kept at 1, 3, 5, and 7 wt%. The synthesis process is shown in Figure 3.1. Graphene loaded commercial titanium oxide (TiO_2-P25) was also prepared by a similar method as described above using P25 powders. The graphene loading was kept at 3 wt%.

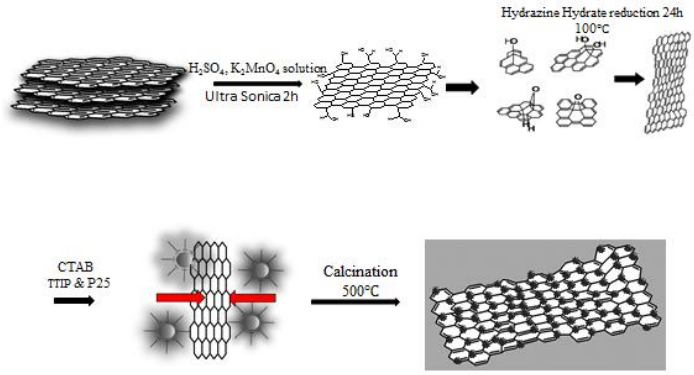

Figure 3. 1 Procedures of G-TiO_2 composite synthesis.

3. Characterization of materials

The crystalline structure of samples was analyzed by powder X-ray diffraction (XRD) using a Bruker D8-Advance X-Ray diffractometer with Cu Kα radiation (λ = 1.5418 Å) operated at 40 kV and 30 mA, respectively. FTIR analysis was performed on a Perkin-Elmer Model FTIR-100 with a MIR detector. UV–vis diffuse reflectance spectra (DRS) of samples were recorded on a JASCO V670 spectrophotometer with an Ø 60 mm integrating sphere, and $BaSO_4$ as a reference material. Field emission scanning electron microscopy (FE-SEM), performed on Zeiss Neon 40EsB, was used to evaluate the morphology, size and texture information of the samples. Thermogravimetric-differential thermal analysis (TG-DTA) was carried out on a TGA/DSC 1 instrument of Mettler-Toledo under air flow at a heating rate of 10 ºC/min.

4. Photocatalytic tests

Photocatalytic performances of various catalysts were evaluated by the photodegradation of methylene blue (MB) under either artificial solar light or visible light. In a typical process, aqueous solution of MB (10 mg/L, 200 mL) and the photocatalysts (100 mg) were put into a 1- L double-jacket cylindrical reactor with cycled cooling water (25 ℃) and stirring. The

photoreaction vessel was positioned 30 cm away from the radiation source with a cut-off filter. Two light sources were applied. One is UV-vis light with intensities at 2.31 $\mu W/cm^2$ (220-280 nm), 6.94 mW/cm^2 (315-400 nm), and 129.3 mW/cm^2 (400-1050 nm). The other is visible light with an intensity of 84 mW/cm^2 at 400-1050 nm. The reaction solution was firstly kept in dark and stirred for 30 min. The photocatalytic reaction was started by turning on the halogen lamp. At given time intervals, the dispersion was centrifuged and the MB solution was analyzed by a JASCO UV-vis spectrophotometer at a wavelength of 664 nm.

3.3 Results and Discussion

Figure 3.2 shows XRD patterns of various TiO_2 and G-TiO_2 samples. G-TiO_2 and G-P25 showed different patterns owing the different crystalline structures of G-TiO_2 (anatase) and G-P25 (30% rutile and 70% anatase). For synthesized TiO_2 and G-TiO_2, X-ray diffraction at 25.4, 37.8, 48.0, 54.3, and 62.7º corresponded to characteristic peaks of crystal planes (101), (101), (004), (200), (211), (204) of anatase, respectively [22], suggesting a pure anatase phase of TiO_2. Meanwhile, P25 and G-P25 showed mixed crystalline phases of anatase and rutile. A comparison of P25 and G-P25 suggests that addition of graphene can not change crystalline structure of TiO_2. The Scherrer equation[24] was used to estimate the size of crystallites of G-TiO_2 samples and the particle diameter was obtained at about 86 - 91 nm.

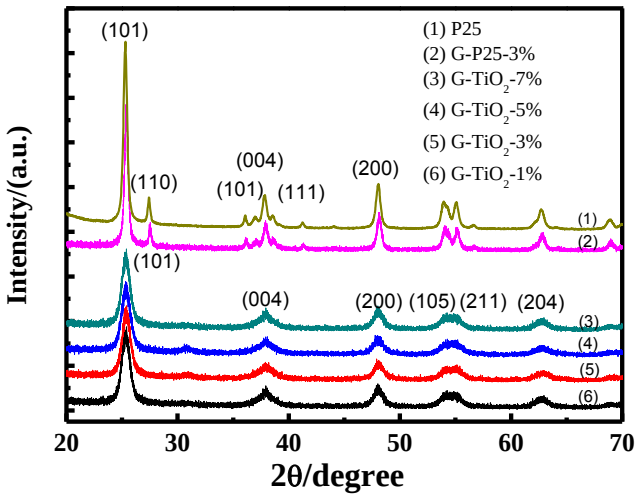

Figure 3. 2 XRD patterns of P25, G-TiO_2 and G-P25.

FTIR spectra of GO, graphene, G-TiO_2-3% before and after calcination were presented in Figure 3.3 the characteristic peaks of GO, including O–H stretching at 3000 cm^{-1}, C-O stretching at 1030 cm^{-1}, and C-OH stretching at 1165 cm^{-1}, were clearly observed, which suggest the presence of hydroxyl, carboxyl and oxygenation function groups. For the RGO sample, the bands associated with the oxygen functional groups were entirely eliminated. The OH band also disappeared due to thermal treatment and hydrophobic surface of graphene [25, 26]. However a new absorption band at 1500 cm^{-1} could be identified, which was attributed to the skeletal vibration of the graphene sheets [27]. For G-TiO_2-3% skeletal ring vibrations of domains are observed around 1616 cm^{-1}, which indicates the presence of Ti-O-C stretching [28-30].

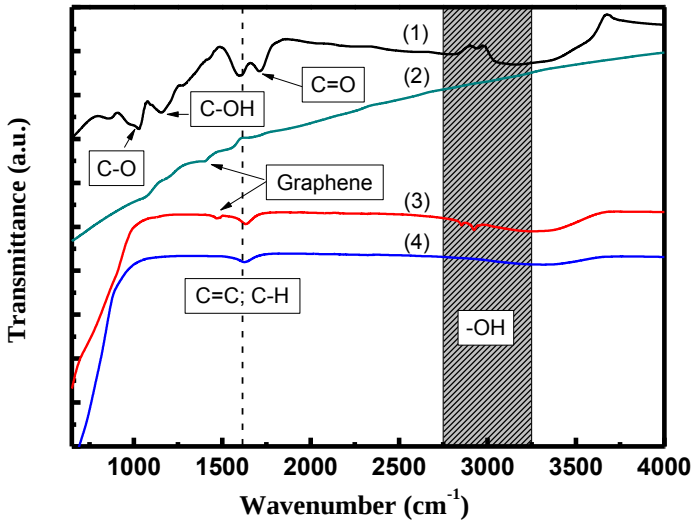

Figure 3. 3 FTIR spectra of GO (1), RGO (2), G-TiO_2-3% before calcination (3) and G-TiO_2-3% after calcination (4).

Figure 3.4 shows the TG-DTA curves of GO, RGO, G-TiO_2-3% before and after calcination. Weight loss below 110℃ was observed, contributed to desorption of water. The hydrophilic property of carbon hexagonal network would be destroyed, and hydroxide functional groups in titanium dioxide would be decomposed since 80 ℃. TG results exhibited two obvious steps of mass loss, the first one was due to the removal of oxygen-containing groups accompanied by the liberation of CO_X and H_2O species from about 300℃ to 550℃[31], and the second was owing to carbon combustion with a sharp exothermic peak at 580 ℃ in DTA curve. The RGO decomposition temperature is much higher than graphene oxide. The poor stability of GO was attributed to the hydroxyl and carboxyl groups that may reduce the oxidation activation energy surrounding the signal graphene sheet.

G-TiO_2-3% dried gel did not show such clear steps of mass loss compared with the graphene oxide. Two weak exothermic peaks were observed at 160 and 300 ^{o}C, respectively, due to desorption of water, ethanol, hydroxyl groups and decomposition of organic precursors from hydrolysis. The exothermic peak at about 450 ℃ was due to the combustion of organics. The broad peak at about 580 ^{o}C arose from decomposition of graphene. For RGO@TiO_2-3%

sample, the mass loss was much less than the associated dried gel. The weight content of reduction of graphene oxide in the composite was evaluated to be 3.8%. The chemical bonds formed via the calcination were expected to play an important role in the photo degradation [32].

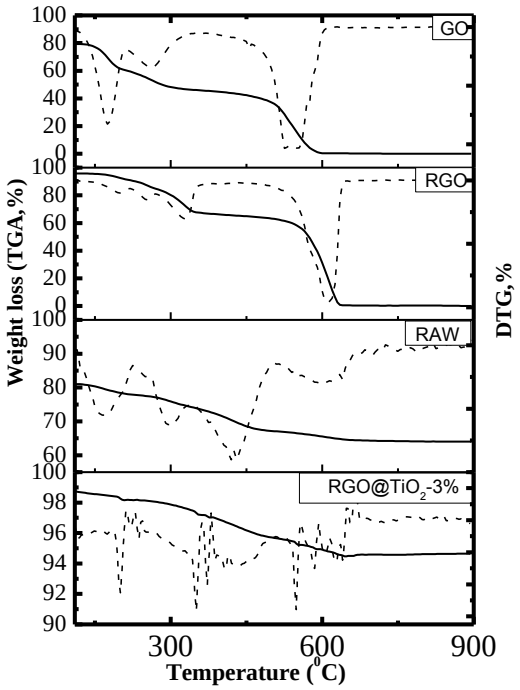

Figure 3. 4 TG-DTA spectra of GO, RGO, G-TiO_2-3% before and after calcination.

Figure 3.5 displays the SEM images of RGO, G-P25-3% and G-TiO_2-3% to evaluate their morphologies. It was found many layers of graphene sheets appear in RGO. For G-P25-3%, it was observed that titania nanoparticles were attached onto the surface of RGO sheets and they were intercalated between the graphene “Sandwich” constructed in an aggregation. P25 nanoparticles are in a diameter of 20–40 nm. No single RGO sheet was observed in G-P25-3%. For G-TiO_2-3%, large aggregated TiO_2 particles with diameter of 100-200 nm were cooperated on graphene sheets. That is because Ti precursor was much easier to be absorbed onto the RGO sheet surface than P25.

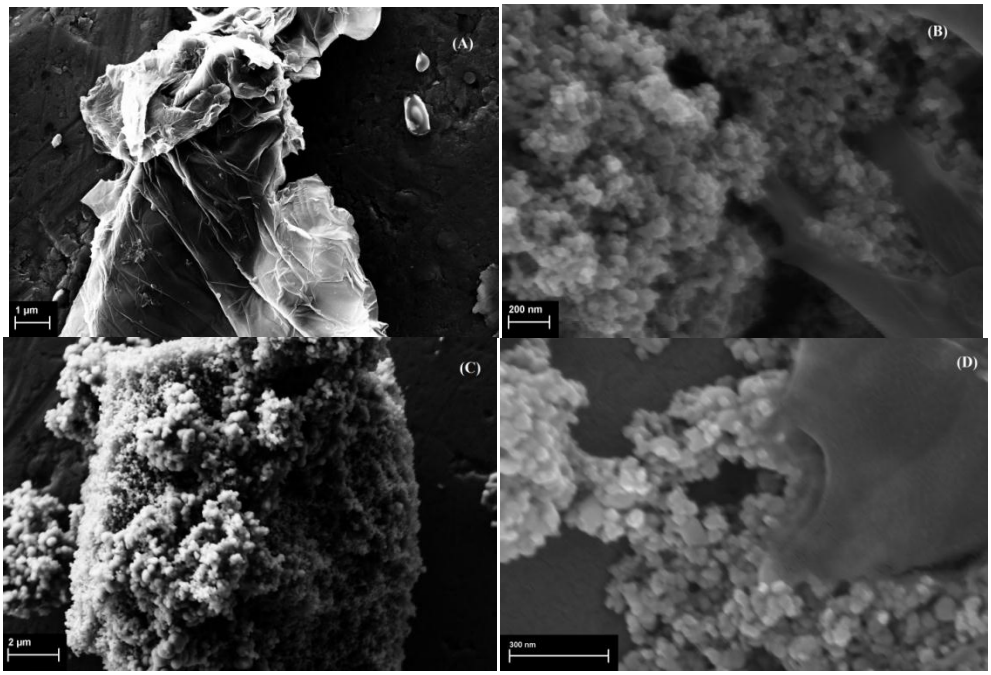

Figure 3. 5 SEM images of (A) RGO sheet (B)G-P25-3% (C)G-TiO_2-3% in 2 µm (D)G-TiO_2-3% in 300 nm

Diffuse reflectance spectra of P25, synthesized TiO_2, G-P25-3% and G-TiO_2-3% are shown in Figure 3.6. After integration of RGO, the thresholds of G-TiO_2-3% and G-P25-3% photocatalyst were extended visible light region. The Kubelka-Munk equation, $\alpha h\nu = B\ (h/\lambda - Eg)\ n$ ($n = 0.5$ for indirect transition), was used to estimate the band gap energies. When $h\nu$ extrapolated to $(\alpha h\nu)\text{-}n = 0$ represents the absorption band gap energy. The band gap of P25 is 3.15 eV, compared to the prepared anatase TiO_2 of 3.19 eV. The band gap was significantly narrowed to 2.98 eV and 2.80 eV by the two types Graphene modified sample. The greater band gap narrowing is possibly attributed to the Ti-O-C bonds from hydrolysis of Ti-precursor which built new molecular orbital and narrowed the band gap [33, 34].

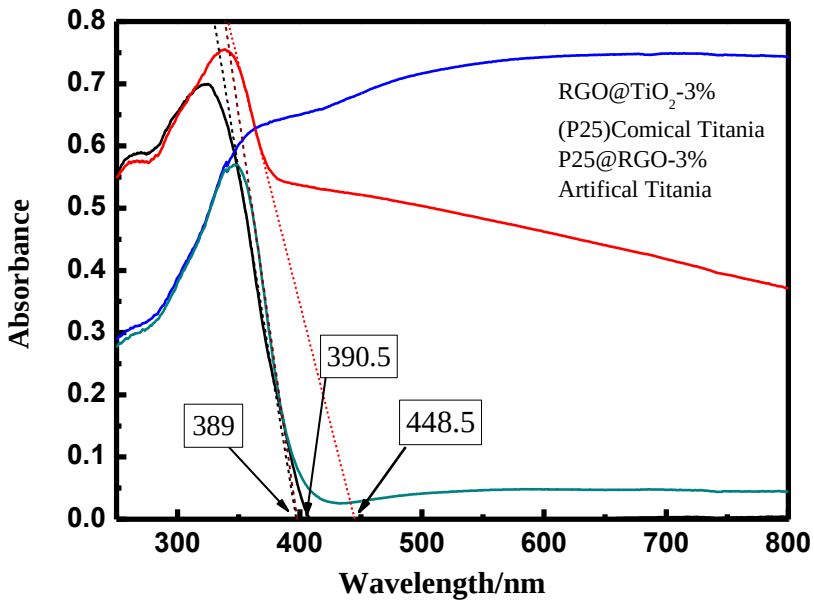

Figure 3. 6 UV-vis diffuse reflectance spectra of P25, TiO_2, G-TiO_2-3% and G-P25-3%.

Figure 3.7 shows the efficiencies of various photocatalysts in MB degradation under either UV-visible or pure visible light irradiations. Under UV-vis lights, the artificial titanium dioxide demonstrated a high activity in MB degradation. 98% MB degradation was achieved at 90 min. Meanwhile, G-TiO_2 (P25) showed a high adsorption of MB and it exhibited higher activity than TiO_2 prepared. The MB degradation would be at 100% at 80 min. For G-TiO_2 catalysts, G loading significantly influenced their catalytic activities. G-TiO_2-3% could decompose MB at 100% in 110 min while G-TiO_2-5% could reach 100% MB decomposition at 90 min.

Generally, the graphene modified TiO_2 photocatalysts exhibited excellent performance in decomposition MB under visible light (wavelength longer than 420 nm). During the adsorption process, G-TiO_2 (P25)-3% composition demonstrated significant MB adsorption with about 30% reduction while other catalysts showed little MB adsorption. Under the

visible light radiation, P25 presented little MB degradation, due to its low visible absorption. G-TiO_2(P25)-3% showed MB degradation with MB reduction from 70% to 40% in 90 min. For G-TiO_2, decomposition of MB depended on graphene loading. G-TiO_2-1% showed about 10% MB degradation in 90 min, while other G-TiO_2 showed similar MB degradation. In 90 min, about 69% MB has been degraded. In extended time, G-TiO_2-3% could achieve 95% MB degradation in about 150 min. Fig.3.7 showed that G-TiO_2-3% presented strong visible light absorption and the band gaps was reduced to 2.78 eV, therefore, resulting in high catalytic activity in MB degradation.

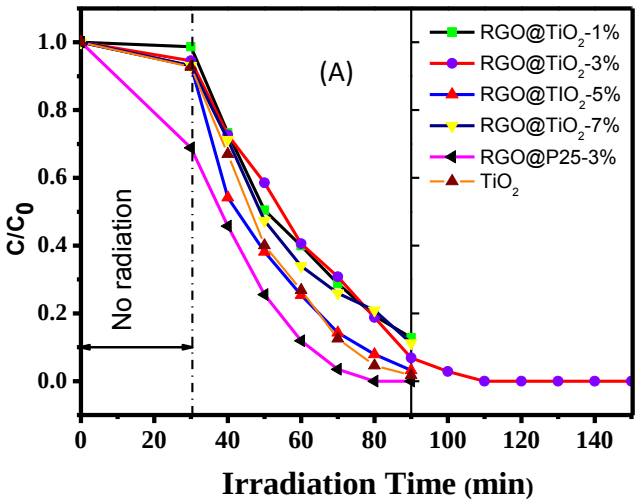

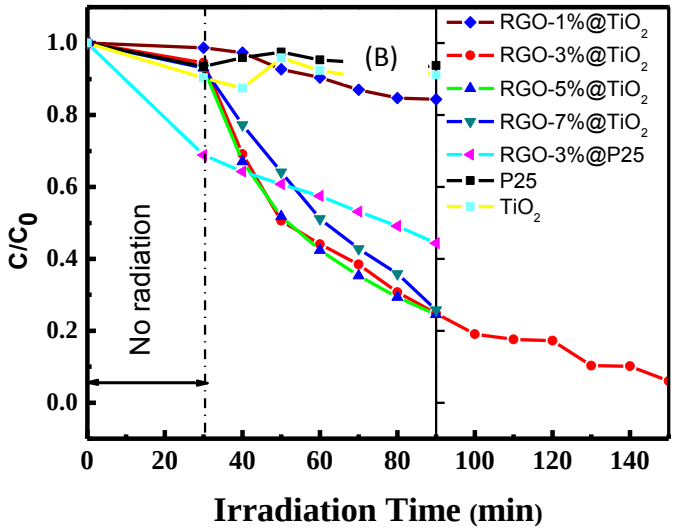

Figure 3. 7 Photodegradation of methylene blue solutions under solar irradiations (A) and visible light (B).

Increase catalyst absorptivity. MB molecules could transfer from the solution to the catalysts' surface and be adsorbed with offset face-to-face orientation via π-π conjugation between MB and aromatic regions of the graphene (Figure 3.8), and therefore, the absorptivity of dyes increases compared to bare TiO_2. Extend light absorption. The chemical bonds of Ti-O-C and good transparency of graphene render a red shift in the photo responding range and facilitate a more efficient utilization of light for the catalyst. Suppress charge recombination. Graphene could act as an acceptor of the photo generated electrons by titanium dioxide particle and ensure fast charge transportation in view of its high conductivity, and therefore, an effective charge separation can be achieved[13, 32].

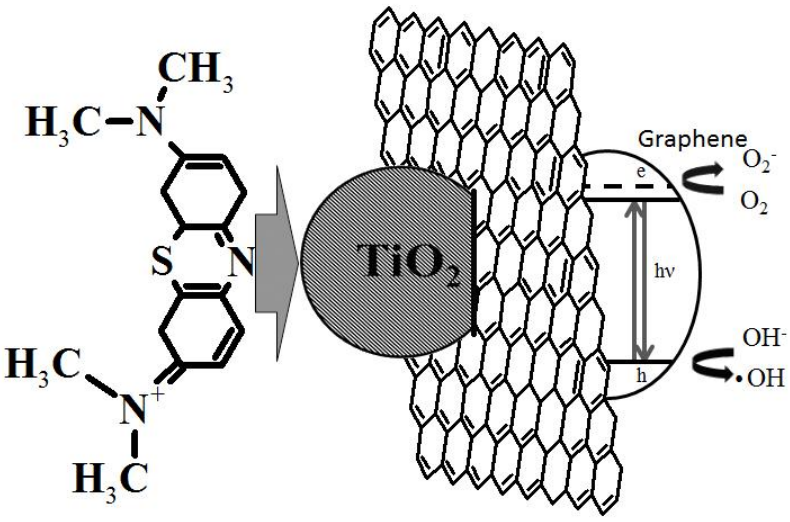

Figure 3. 8 Graphene enhanced MB adsorption and decomposition

Electronic scavenger technology is widely utilized in water treatment to enhance the photo-redox process. The photo-excited G-TiO_2 sample was further tested with electronic scavenger assistance. Three different kinds of electronic scavengers were adopted: peroxymonosulphate (PMS), Peroxydisulphate (PDS) and hydrogen peroxide (H_2O_2). Figure 3.9 demonstrate all scavengers could enhance the reaction. After adsorption and desorption equilibrium (30 min), PDS contented system could decompose all MB in 125 min which is faster than pure G-TiO_2 decomposition behave by 15 min. PMS system could mineralize all MB in about 90 min. H_2O_2 assistance has the best consequence which can degrade all MB in 20 min.

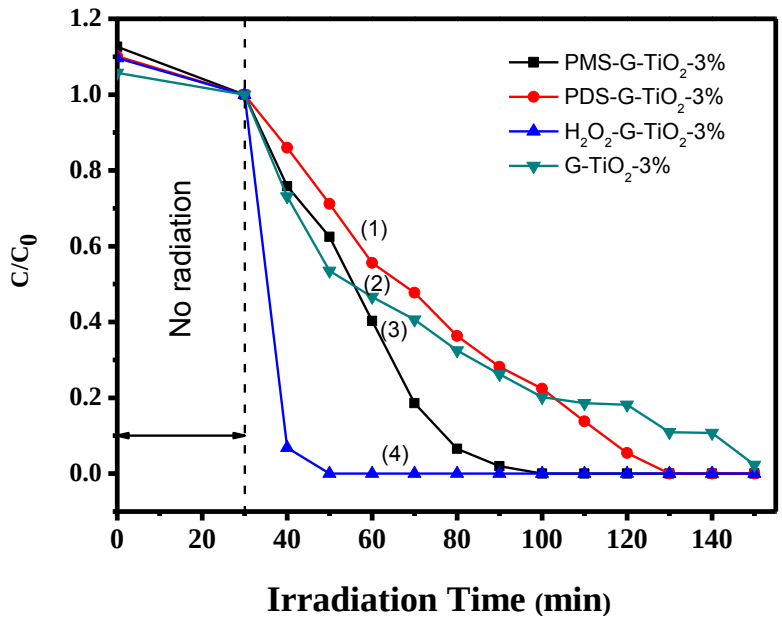

Figure 3. 9 Scheme of photodegradation by G-TiO2-3% with electron scavenger assistance under visible irradiation. (1) PDS; (2) G-TiO_2-3% only; (3) PMS; (4) H_2O_2.

H_2O_2 is one of the used green oxidants, relevant for organic decomposition. In common cases a catalyst pursued to activate H_2O_2 to generate more reactive oxidizing intermediates. In a first step of oxygen reduction reaction (ORR), the moderate oxidant $^{\cdot}O_2$ is produced by the reaction of dissolved O_2 with a first photoinduced electron. $[H^+]$ is important in the second step, where it helps to transfer a second electron to form H_2O_2 (eqn (1) and (2)). H_2O_2 could be further activated to the most reactive .OH by accepting a third photoinduced electron from Fenton agents due to its band positions (eqn (3)) which can mineralize organic pollutants.

$$O_2 + e^- \rightarrow \cdot O_2^- \qquad (1)$$

$$\cdot O_2^- + 2H^+ + e^- \rightarrow H_2O_2 \qquad (2)$$

$$H_2O_2 \rightarrow \cdot OH + OH^- \qquad (3)$$

G-TiO_2-3% then has been examined to react with different quantity of H_2O_2 into the hydroxyl radical (.OH), which could decompose MB dye (Figure 3.10). The system showed no reaction without G-TiO_2-3% and visible light illumination, there was a weak decline when

illumination and H_2O_2 exist together. At all H_2O_2 concentration, MB degradation achieve at faster rate and 7 mL H_2O_2 methylene blue degradation will achieve 100% in 20 min.

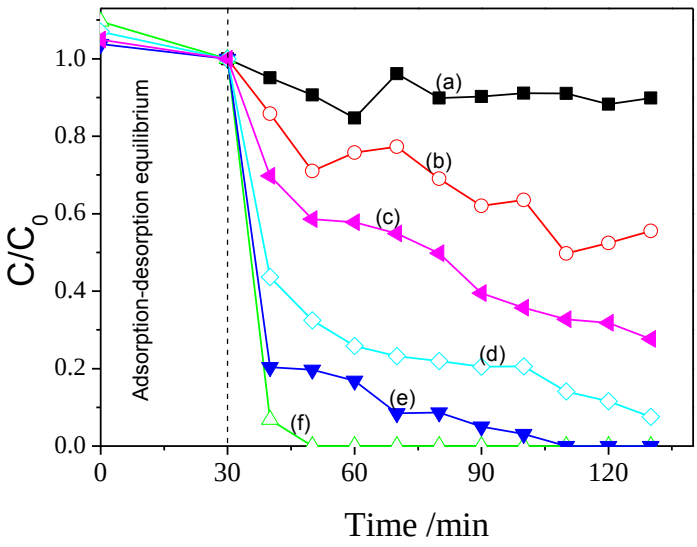

Figure 3. 10 Scheme of photodegradation by 0.1 gram G-TiO_2-3% with H_2O_2 assistance under visible irradiation in different volume (a) 7 ml H_2O_2; (b) 7 ml H_2O_2 & illuminant ; (c) 1 ml H_2O_2, illuminant & catalyst; (d) 3 ml H_2O_2, illuminant & catalyst; (e) 5 ml H_2O_2, illuminant & catalyst; (f) 7 ml H_2O_2, illuminant & catalyst.

3.4 Conclusion

In this study novel graphene contented TiO_2 photocatalyst been successfully synthesized. Graphene doped tatiana with highly photocatalytic performance under the radiation in the range over 410 nm. A clear red shift and obvious band gap narrow can be observed in UV-vis diffuse reflectance; as a result the TiO_2 visible light absorption capability has been enhanced. The G/TiO2 catalysts exhibit high efficiency to mineralize dye methylene blue under visible illumination. Using Ti precursor in sol-gel synthesis will produce a better G-TiO_2 photocatalyst than G-TiO_2 (P25).

3.5 References

[1] O.M. Alfano, D. Bahnemann, A.E. Cassano, R. Dillert, R. Goslich, Photocatalysis in water environments using artificial and solar light, Catalysis Today, 58 (2000) 199-230.

[2] M.N. Chong, B. Jin, C.W.K. Chow, C. Saint, Recent developments in photocatalytic water treatment technology: A review, Water Research, 44 (2010) 2997-3027.

[3] S. Malato, P. Fernandez-Ibanez, M.I. Maldonado, J. Blanco, W. Gernjak, Decontamination and disinfection of water by solar photocatalysis: Recent overview and trends, Catalysis Today, 147 (2009) 1-59.

[4] R. Ullah, H. Sun, S. Wang, H.M. Ang, M.O. Tade, Wet-Chemical Synthesis of InTaO4 for Photocatalytic Decomposition of Organic Contaminants in Air and Water with UV-vis Light, Industrial & Engineering Chemistry Research, 51 (2012) 1563-1569.

[5] H. Sun, S. Wang, H.M. Ang, M.O. Tade, Q. Li, Halogen element modified titanium dioxide for visible light photocatalysis, Chemical Engineering Journal, 162 (2010) 437-447.

[6] S.G. Kumar, L.G. Devi, Review on Modified TiO2 Photocatalysis under UV/Visible Light: Selected Results and Related Mechanisms on Interfacial Charge Carrier Transfer Dynamics, Journal of Physical Chemistry A, 115 (2011) 13211-13241.

[7] F. Han, V.S.R. Kambala, M. Srinivasan, D. Rajarathnam, R. Naidu, Tailored titanium dioxide photocatalysts for the degradation of organic dyes in wastewater treatment: A review, Applied Catalysis a-General, 359 (2009) 25-40.

[8] J. Zhang, Y. Wu, M. Xing, S.A.K. Leghari, S. Sajjad, Development of modified N doped TiO2 photocatalyst with metals, nonmetals and metal oxides, Energy & Environmental Science, 3 (2010) 715-726.

[9] H. Sun, R. Ullah, S. Chong, H.M. Ang, M.O. Tade, S. Wang, Room-light-induced indoor air purification using an efficient Pt/N-TiO2 photocatalyst, Applied Catalysis B-Environmental, 108 (2011) 127-133.

[10] R. Leary, A. Westwood, Carbonaceous nanomaterials for the enhancement of TiO2 photocatalysis, Carbon, 49 (2011) 741-772.

[11] S. Sakthivel, H. Kisch, Daylight Photocatalysis by Carbon-Modified Titanium Dioxide, Angewandte Chemie International Edition, 42 (2003) 4908-4911.

[12] J.H. Hwang, K.S. Lee, H.S. Bang, D.C. Choo, T.W. Kim, J.M. Lee, W.I. Park, Enhancement of the Hole Injection Current in Polymer Light-Emitting Devices Fabricated Utilizing a Graphene Layer, Journal of The Electrochemical Society, 158 (2011) J273-J275.

[13] Q. Xiang, J. Yu, M. Jaroniec, Graphene-based semiconductor photocatalysts, Chemical Society reviews, 41 (2012) 782-796.

[14] X. An, J.C. Yu, Graphene-based photocatalytic composites, Rsc Advances, 1 (2011) 1426-1434.

[15] H. Zhang, X. Lv, Y. Li, Y. Wang, J. Li, P25-Graphene Composite as a High Performance Photocatalyst, ACS nano, 4 (2009) 380-386.

[16] N.-P. Thuy-Duong, P. Viet Hung, E.W. Shin, P. Hai-Dinh, S. Kim, J.S. Chung, E.J. Kim, S.H. Hur, The role of graphene oxide content on the adsorption-enhanced photocatalysis of titanium dioxide/graphene oxide composites, Chemical Engineering Journal, 170 (2011) 226-232.

[17] Y.Y. Liang, H.L. Wang, H.S. Casalongue, Z. Chen, H.J. Dai, TiO2 Nanocrystals Grown on Graphene as Advanced Photocatalytic Hybrid Materials, Nano Res., 3 (2010) 701-705.

[18] C. Chen, W. Cai, M. Long, B. Zhou, Y. Wu, D. Wu, Y. Feng, Synthesis of Visible-Light Responsive Graphene Oxide/TiO2 Composites with p/n Heterojunction, ACS nano, 4 (2010) 6425-6432.

[19] S.D. Perera, R.G. Mariano, K. Vu, N. Nour, O. Seitz, Y. Chabal, K.J. Balkus, Hydrothermal Synthesis of Graphene-TiO2 Nanotube Composites with Enhanced Photocatalytic Activity, ACS Catalysis, (2012) 949-956.

[20] W.S. Hummers Jr, Hummers, Preparation of graphitic oxide, Journal of the American Chemical Society, 80 (1958) 1339.

[21] J.Y. Jang, M.S. Kim, H.M. Jeong, C.M. Shin, Graphite oxide/poly(methyl methacrylate) nanocomposites prepared by a novel method utilizing macroazoinitiator, Composites Science and Technology, 69 (2009) 186-191.

[22] G. Jiang, X. Zheng, Y. Wang, T. Li, X. Sun, Photo-degradation of methylene blue by multi-walled carbon nanotubes/TiO2 composites, Powder Technology, 207 (2011) 465-469.

[23] D. Wang, L. Xiao, Q. Luo, X. Li, J. An, Y. Duan, Highly efficient visible light TiO2 photocatalyst prepared by sol–gel method at temperatures lower than 300 °C, Journal of Hazardous Materials, 192 (2011) 150-159.

[24] A.L. Patterson, The Scherrer formula for X-ray particle size determination, Physical review, 56 (1939) 978.

[25] Y. Wang, X. Chen, Y. Zhong, F. Zhu, K.P. Loh, Large area, continuous, few-layered graphene as anodes in organic photovoltaic devices, Applied physics letters, 95 (2009) 063302.

[26] T.N. Murakami, Y. Fukushima, Y. Hirano, Y. Tokuoka, M. Takahashi, N. Kawashima, Surface modification of polystyrene and poly(methyl methacrylate) by active oxygen treatment, Colloids and Surfaces B: Biointerfaces, 29 (2003) 171-179.

[27] C. Nethravathi, M. Rajamathi, Chemically modified graphene sheets produced by the solvothermal reduction of colloidal dispersions of graphite oxide, Carbon, 46 (2008) 1994-1998.

[28] T.-D. Nguyen-Phan, V.H. Pham, E.W. Shin, H.-D. Pham, S. Kim, J.S. Chung, E.J. Kim, S.H. Hur, The role of graphene oxide content on the adsorption-enhanced photocatalysis of titanium dioxide/graphene oxide composites, Chemical Engineering Journal, 170 (2011) 226-232.

[29] K.H. Liao, Aqueous Only Route toward Graphene from Graphite Oxide, ACS nano, 5 (2011) 1253.

[30] J. Shen, One step hydrothermal synthesis of TiO2-reduced graphene oxide sheets, Journal of Materials Chemistry, 21 (2011) 3415.

[31] S. Stankovich, Synthesis of graphene-based nanosheets via chemical reduction of exfoliated graphite oxide, Carbon, 45 (2007) 1558.

[32] H. Zhang, P25-graphene composite as a high performance photocatalyst, ACS nano, 4 (2010) 380.

[33] N. Serpone, Is the Band Gap of Pristine TiO2 Narrowed by Anion- and Cation-Doping of Titanium Dioxide in Second-Generation Photocatalysts?, The Journal of Physical Chemistry B, 110 (2006) 24287-24293.

[34] Daylight Photocatalysis by Carbon-Modified Titanium Dioxide, Angewandte Chemie (International ed.), 42 (2003) 4908-4911.

4

4 One-step hydrothermal synthesis of ZnO-reduced graphene oxide using Zn powder for photocatalysis

Abstract

Zn powder was utilized as a reducing agent and ZnO precursor for one-step synthesis of reduced graphene oxide (RGO)-ZnO photocatalysts. Two RGO-ZnO composites were synthesised with or without a surfactant. The structural, morphological, and physicochemical properties of the samples were thoroughly investigated by X-ray diffraction (XRD), Fourier transform infrared spectroscopy (FT-IR), field emission scanning electron microscopy (FE-SEM), UV-vis diffuse reflectance (UV-vis DRS), thermo-gravimetric-differential thermal analysis (TG-DTA), and Raman spectroscopy. Zn powder could effectively reduce GO to graphene and transformed to ZnO. RGO-ZnO photocatalysts can successfully decompose MB under UV-vis illumination, better than ZnO.

4.1 Introduction

Graphene as a novel carbonaceous nanomaterial has a single or mutiple carbon atom layer with two dimensional aromatic structure, which has Young's modulus (~1100 GPa), fracture strength (125 GPa), thermal conductivity (~5000 $Wm^{-1}K^{-1}$), specific surface area (theoretical value of 2630 m^2g^{-1}), magnetism and fascinating transport properties [1]. Those remarkable characteristics have stimulated wide interest in both experimental and theoretical investigation as well as application [1-5]. Currently, the methods for a large scale production of graphene have been established based on chemical reduction of graphene oxide (GO) using hydrazine[6], dimethylhydrazine, sodium borohydride or strong alkaline solution such as NaOH, KOH, NH_4OH with pH value more than 10 [7]. Obviously these chemical reagents are toxic or harmful to the environment or human health. Wu et al. demonstrated that high-quality graphene can be obtained by vacuum reducing GO at around 1000℃ in H_2 gas. However this method will consume carbonaceous material at high temperature [8]. This process can also be used as the efficient method to synthesise graphene sheet in a large scale[9] but the quality of reduced GO(RGO) is relied on the experimental conditions[10].

Semiconductors for photocatalysis are often modified by noble metals in order to improve electron transfer process. In this way the light absorption will be extended and the band gap will be narrowed to suppress the electron-hole recombination. The dopant can improve the stabilization of catalyst surface[1]. Zinc oxide as a typical semiconductor material can absorb ultraviolet (UV) light to yield photoelectrons and holes to effectively degrade organic pollutants [11-14].

Currently RGO functionalised ZnO has been reported because RGO possesses the ability to accept the electrons, and favour adsorption of aromatic compounds due to π- π conjunction

[15]. Most of investigations reported to adopt zinc salts or commercial zinc oxide to incorporate RGO sheets [16-18]. Fan et al. have suggested to use iron powder for reduction of graphene oxide in acid solution [19]. Mei & Ouyang have reduced GO by zinc powder with ultrasonication assistance in HCl solution[9]. Many reports indicated that metal assistance for GO reduction is more effective than the other reduction process [20]. In addition, advanced hydrothermal method has been used to obtain ZnO particles with narrow size distribution, less defect crystallization, without agglomeration and phase homogeneity [21, 22]. It was also been stated that graphene is poorly soluble in water and polar organic solvents that is easily aggregates owing to strong van der Waals force, The hydrophobic/hydrophilic incompatibility between graphene and inorganic compounds (especially metal oxides) also makes it difficult to directly deposit metal oxides on graphene. Thus a dispersant is usually needed to solve these problems [22, 23].

Herein we presented a one-step hydrothermal approach to prepare RGO-ZnO composites, using Zn powder with a cationic surfactant, cetyltrimethylammonium bromide (CTAB) or without the surfactant. The photocatalysts were tested for degradation of methylene blue (MB) as a water organic pollutant under ultraviolet and visible radiation (UV-vis light). It was found that synthesis of RGO-ZnO composite could be achieved using Zn powder and GO as precursors. Additionally, RGO-ZnO exhibits enhanced photocatalytic performance as comparing with naked ZnO.

4.2 Experimental

4.2.1 Materials and reagents

Graphite powder (purity 99.9995%), sulphuric acid (95–97%), cetyltrimethyl ammonium bromide (CTAB) was obtained from Sigma–Aldrich Corporation. Hydrogen peroxide (30%)

was purchased from Chem-Supply. Methylene Blue (MB), potassium permanganate, hydrochloric acid (32%, analytical grade) was obtained from Biolab. Zinc powder was obtained from Australian Metal Powders Supplies.

4.2.2 Synthesis of Graphene-ZnO particles

Graphene oxide (GO) was prepared by the Hummers method [23, 24]. Then GO (0.0112 g/mL) was dispersed in aqueous solution in ultrasonics for 2 h. Two ZnO/RGO samples were prepared. In a typical synthesis, For 15% graphene contented G-ZnO-CTAB sample, 2 g zinc powder were mixed with 40 mL GO suspension (pH = 2.2), then CTAB powder was gradually added into the solution with its final concentration at 0.1 M. The solution was magnetically stirred for 2 h then transferred into a Teflon-lined stainless steel autoclave (80 mL). Hydrothermal reactions were carried out at 195℃ for 24 h. Black sediment was collected and cleaned with ethanol and distilling water several times and then dried in air at 60℃. This is referred as G-ZnO-CTAB. The synthesis diagram is presented in Figure 4.1. The other G-ZnO sample was synthesised in the same method without using CTAB.

The possible processes for ZnO nanoparticle formation under hydrothermal conditions can be represented as follows:

$$Zn + GO_xH_y \rightarrow Zn^{2+} + \frac{y}{2}H_2 \uparrow + GO_x^{y-}$$

$$Zn + H_2O \rightarrow Zn^{2+} + H_2 \uparrow + OH^-$$

$$Zn^{2+} + GO^{z-} + OH^- \rightarrow (GOZn)^{z+}z(OH)^- + Zn(OH)_4^{2-} \rightarrow G(ZnO) + ZnO + H_2O$$

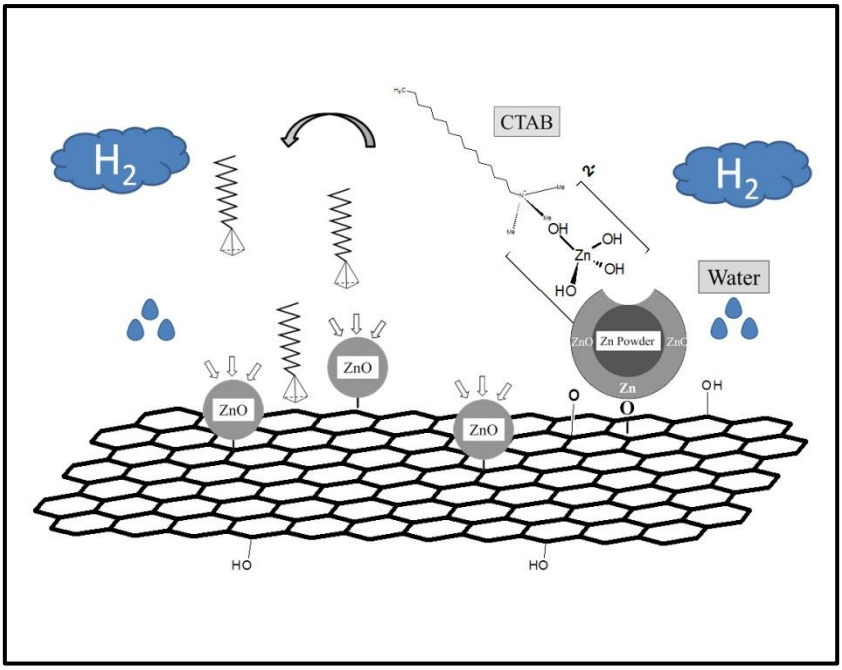

Figure 4. 1 Procedures of G-ZnO-CTAB composite synthesis.

4.2.3 Characterization of materials

UV–visible diffuse reflectance spectra (DRS) of samples were recorded on a JASCO V 670 spectrophotometer with an Ø 60 mm integrating sphere, and $BaSO_4$ was used as a reference material. The crystalline structure of samples was analysed by powder X-ray diffraction (XRD) using a Bruker D8-Advance X-Ray diffractometer with Cu Kα radiation (λ = 1.5418 Å). Field Emission Scanning Electron Microscopy (FE-SEM), performed on Zeiss Neon 40EsB, was used to evaluate the morphology, size and texture information of the samples. Raman spectra were recorded on a Dilor Labram 1B dispersive Raman spectrometer by adopting a laser of 633 nm as incident light. TGA analyses were conducted on a TGA/DSC 1 Thermo-gravimetric analyser supplied by the Mettler-Toledo Instrument.

4.2.4 Photocatalytic activity of composites

Photocatalytic activities of G-ZnO samples were evaluated in decomposition of MB with ultraviolet and visible light irradiations. A high pressure Hg lamp was utilized as radiation source. The average intensities of the lamp were measured to be 21.31 $\mu W/cm^2$, 6.941×10^3 $\mu W/cm^2$ and 129.6×10^3 $\mu W/cm^2$ at 220-280 nm, 315-400 nm and 400-1050 nm, respectively. In the typical process, 200 mL, 10 ppm MB solution with 0.05 g photocatalyst particles were continuously stirred in a 1000 mL double-jet cylindrical quartz vessel reactor, which was placed 20 cm away from light source and irradiated under UV-visible light without a filter. The reaction temperature was controlled by recycled cooling water at 25 ℃ in a water bath. Concentration of MB was measured by the absorption spectroscopic technique. In a regular interval, 4 mL aliquots were taken from the reactor and separated from catalyst particles in a centrifuge at 4700 rpm for 10 min and the absorbance was determined at λ=664 nm with a UV-visible spectrophotometer.

4.3 Characterization of Photocatalyst

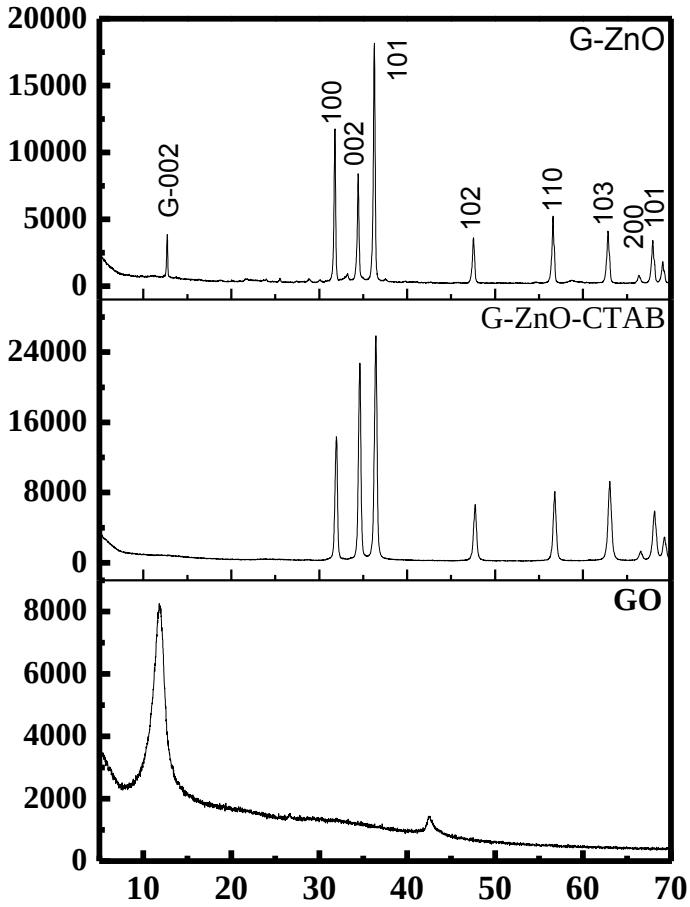

Figure 4. 2 XRD patterns of GO, G-ZnO,and G-ZnO-CTAB samples

Figure 4.2 shows XRD patterns of G-ZnO, G-ZnO-CTAB and GO. G-ZnO and G-ZnO-CTAB demonstrated similar patterns. The reflections of ZnO in hexagonal wurtzite lattice (JCPDS 75-0576, a =0.3249 nm, c=0.5205 nm) can be observed. CTAB assisted hydrothermal method produced greater XRD intensity for ZnO[22, 25]. In addition, graphene oxide has been reduced dramatically because no (002) peak of graphene can be observed at 2θ between 10 to 15 degree in G-Zn-CTAB sample, suggesting that CTAB is

able to separate graphene sheet and prevent agglomeration[26]. However, (002) diffraction of GO was observed on G-ZnO and the position is shifted. It suggests that there is a strong interaction between ZnO particle and graphene [27].

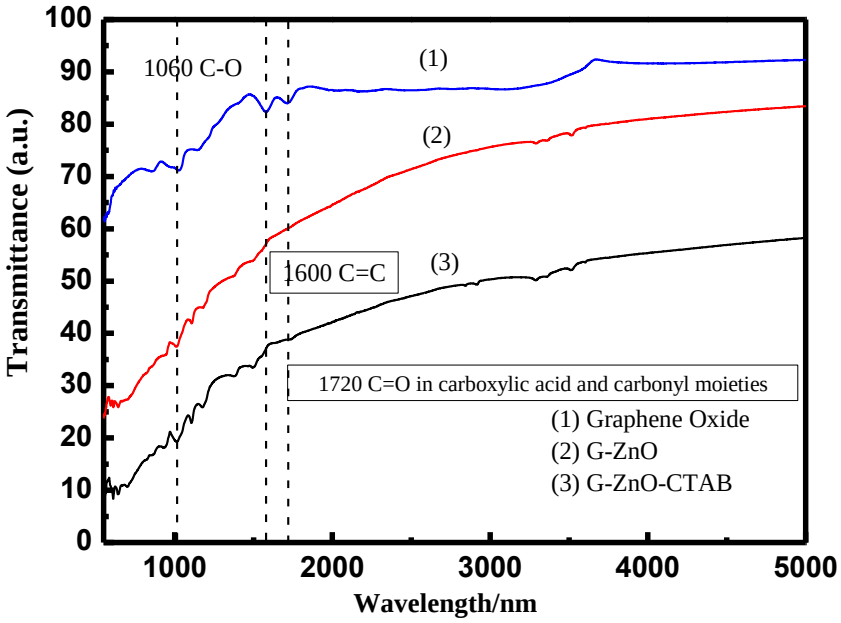

Figure 4. 3 FTIR spectra of GO, G-ZnO, G-ZnO-CTAB.

FTIR spectra of GO, G-ZnO and G-ZnO-CTAB are presented in Figure 4.3. For GO, strong O–H stretching at 3600 cm^{-1}, C-O stretching at 1020 cm^{-1}, and the C-OH stretching at 1160 cm^{-1} were clearly observed, suggesting the presence of hydroxyl, carboxyl and oxygenation functional groups. The G-ZnO and G-ZnO-CTAB have the similar FTIR profiles. For G-ZnO and G-ZnO-CTAB samples, the bands associated with the oxygen functional groups were eliminated. G-ZnO-CTAB has a stronger stretching peak at 1060 nm^{-1} comparing with G-ZnO, which indicates a stronger Zn-O-C combination. To introduce the acidic environment and CTAB can improve the reduction potential of Zn metal[19].

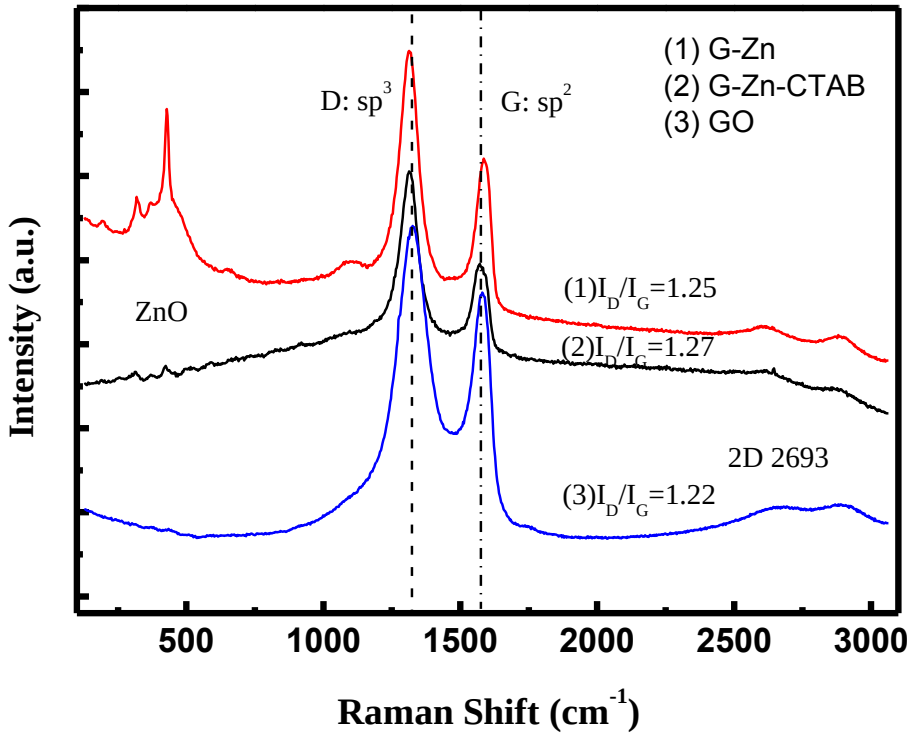

Figure 4. 4 Raman spectra of GO, RGO-Zn-CTAB, RGO-Zn.

Raman spectroscopy is widely used to study the ordered/disordered crystalline structures of carbonaceous materials. Figure 4.4 shows the Raman spectra of GO, G-ZnO-CTAB, and G-ZnO. The D and G bands arise at 1325 cm^{-1} and 1580 cm^{-1}, respectively on GO[28]. The tiny dislocation of G band of RGO-Zn and RGO-Zn-CTAB samples suggested more defects and heteroatom implanting. The increasing of peak intensity ratio of I_D/I_G indicated a decline in the average size of the sp2 domains [29] and more defect being created[30-32]. The similar 2D peaks of ZnO containing samples indicate that the graphene stack structure has not changed with or without CTAB[33].

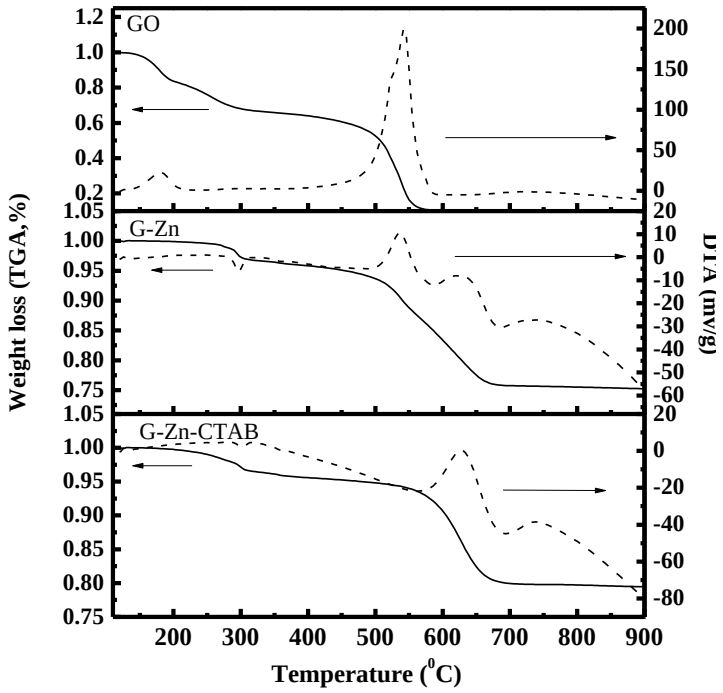

Figure 4. 5 TG-DTA spectra of GO, G-ZnO, G-ZnO-CTAB samples.

TGA is a widely used method to characterize particle thermal stability. Figure 4.5 reveals the TG-DTA curves of GO, G-ZnO and G-ZnO-CTAB. For GO, TG curve exhibited two steps of weight loss. The first one was due to the removal of oxygen-containing groups, which is accompanied by the liberation of CO_X and H_2O species at about 120 ℃[6]. The second step was owing to combustion of carbon structure; there is a sharp exothermic peak at 580 ℃ in DTA curve. In the curves of G-ZnO and G-ZnO-CTAB, there is about 20% weight loss in total and there are two mass-loss steps at different temperatures. The DTA curve of G-ZnO-CTAB did not demonstrate an exothermic peak at about 580 ℃, which appeared in G-ZnO sample.

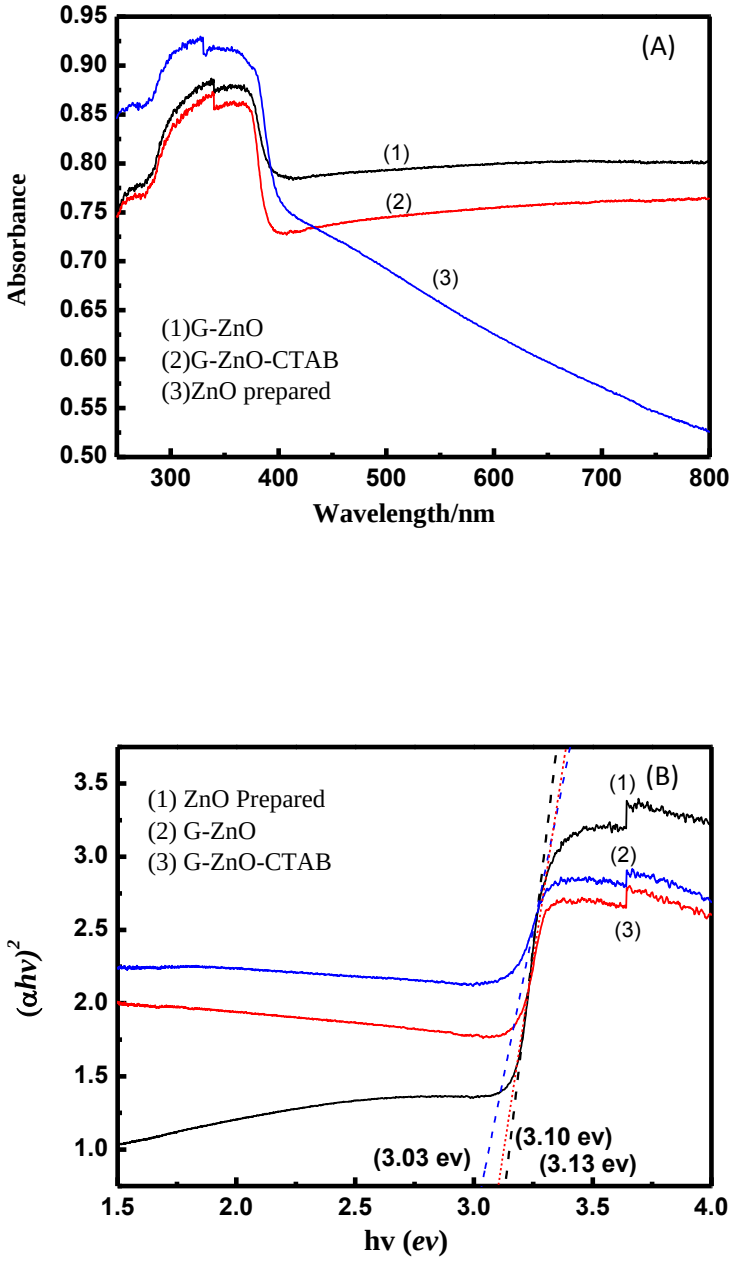

Figure 4. 6 UV-vis diffuse reflectance spectra (A) and the $(ahv)^2$ vs hv graph(B) of ZnO , G-ZnO, G-ZnO-CTAB .

Figure 4.6A reveals UV-vis diffuse reflectance spectra of synthesised ZnO and ZnO-graphene samples. All samples have a strong absorption edge before 400 nm. The ZnO

showed gradually reduced absorption in visible-light region while other two ZnO-graphene samples demonstrated strong and stable absorption in the visible region. The curves of $(\alpha h\nu)^2$ versus hv (Figure 4.6B) for band gap calculation indicated that the band gap of three samples did not change significantly. The band gap of ZnO is 3.13 ev. In contrast, G-ZnO photocatalysts exhibit slightly smaller band gaps energy. The band gap energies for G-ZnO-CTAB and G-ZnO are 3.10 and 3.03, respectively.

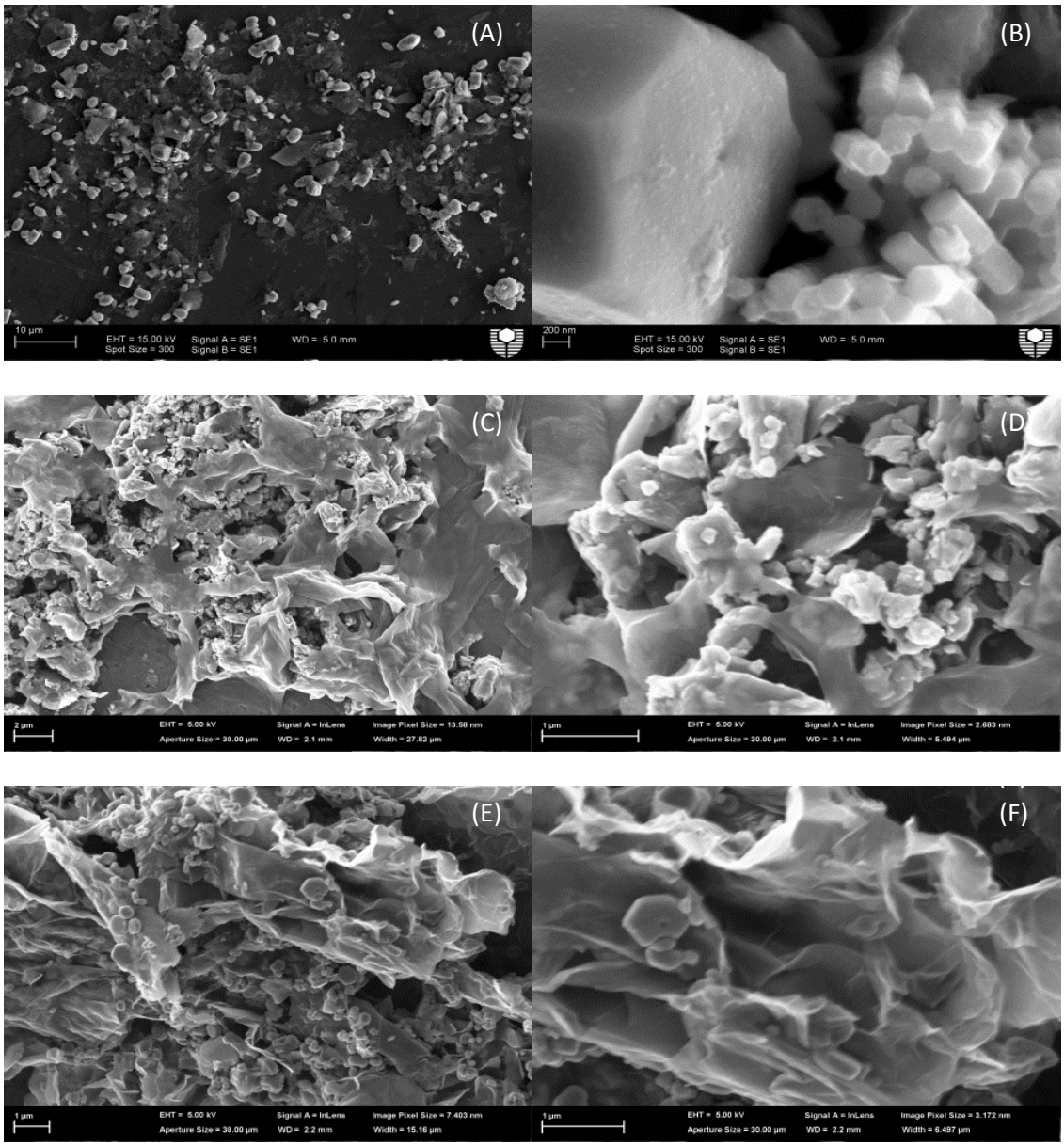

Figure 4. 7 SEM images of ZnO prepared (A, B), G-ZnO (C, D), and G-ZnO-CTAB (E, F).

The band-gap energy of ZnO was not modified significantly because of ZnO/RGO interposed structure [34], which restricts the interaction of ZnO and graphene. Fu [12] has found that ZnO and GO-Zn particle have similar absorption edge. It is also accepted that graphene sheet will enhance visible light absorption but weak absorption in ultraviolet light[35] .

Figure 4.7 shows SEM images of ZnO, G-ZnO and G-ZnO-CTAB. Figure 4.7 (A,B) shows that most of ZnO presents in hexagon with particle size at 200 nm. Few larger particles are also found. However, ZnO morphology changed on G-ZnO samples (Figure 4.7 C,D,E,F). Obviously many layers of graphene sheets can be found in G-ZnO samples, because GO could be well dispersed in aqueous solution of CTAB[36]. For G-ZnO and G-ZnO-CTAB, ZnO nanoparticles were anchored onto the surface of RGO sheets and they were intercalated between the graphene "Sandwich" aggregations. There are some hexagonal ZnO particles appeared in G-ZnO-CTAB (Figure 4.7E, F), which means CTAB can effectively help ZnO growth on graphene sheets.

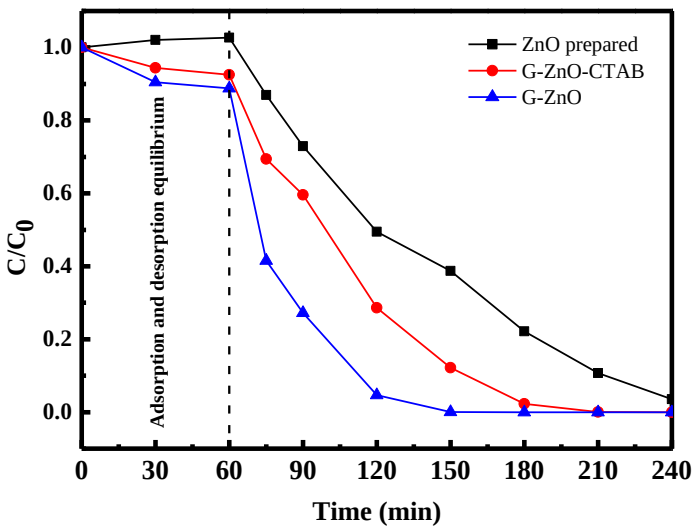

Figure 4. 8 Photodegradation of MB solutions under solar irradiations

Graphene loaded ZnO nanoparticles were tested for MB degradation under UV-visible illumination (Figure 4.8). Zinc oxide demonstrated no MB adsorption but activity in MB degradation. About 98% MB degradation was achieved in 4 h. Meanwhile, G-ZnO and G-ZnO-CTAB showed slight adsorption of MB due to the presence of graphene sheets. MB degradation would be 100% at 150 min for G-ZnO catalyst, and G-Zn-CTAB could decompose MB at 100% in 180 min. The surface will play an important role for G-ZnO photocatalyst to degrade MB. MB molecules were easier to transfer from the solution to the catalysts' surface with offset face-to-face orientation via π-π conjugation. Meanwhile graphene enhances particles to collect photo energy from light, which accelerates the decomposition process.

4.4 Summary

A one-step hydrothermal method has been successfully adopted to synthesize graphene- ZnO composites with high photocatalytic performance under UV-visible light. Zn powder could be simultaneously employed as reducing agent for GO reduction and Zn-source for ZnO formation. G-ZnO catalysts presented higher MB reduction under UV-visible light than ZnO. The G-ZnO catalyst without CTAB exhibited the best efficiency in degradation.

4.5 References

[1] Q. Xiang, Graphene-based semiconductor photocatalysts, Chemical Society reviews, 41 (2012) 782.

[2] R. Leary, A. Westwood, Carbonaceous nanomaterials for the enhancement of TiO2 photocatalysis, Carbon, 49 (2011) 741-772.

[3] P.V. Kamat, Graphene-based nanoarchitectures. Anchoring semiconductor and metal nanoparticles on a two-dimensional carbon support, The journal of physical chemistry letters, 1 (2010) 520.

[4] C. GÃ³mez Navarro, N. Gómez, Electronic transport properties of individual chemically reduced graphene oxide sheets, Nano letters, 7 (2007) 3499.

[5] G. Eda, G. Fanchini, M. Chhowalla, Large-area ultrathin films of reduced graphene oxide as a transparent and flexible electronic material, Nat Nano, 3 (2008) 270-274.

[6] S. Stankovich, Synthesis of graphene-based nanosheets via chemical reduction of exfoliated graphite oxide, Carbon, 45 (2007) 1558.

[7] D. Luo, G. Zhang, J. Liu, X. Sun, Evaluation Criteria for Reduced Graphene Oxide, The Journal of Physical Chemistry C, 115 (2011) 11327-11335.

[8] Z.S. Wu, Synthesis of high-quality graphene with a pre-determined number of layers, Carbon, 47 (2009) 493.

[9] X. Mei, J. Ouyang, Ultrasonication-assisted ultrafast reduction of graphene oxide by zinc powder at room temperature, Carbon, 49 (2011) 5389-5397.

[10] S. Park, R.S. Ruoff, Chemical methods for the production of graphenes, Nat Nano, 5 (2010) 309-309.

[11] J. Wu, X. Shen, L. Jiang, K. Wang, K. Chen, Solvothermal synthesis and characterization of sandwich-like graphene/ZnO nanocomposites, Applied Surface Science, 256 (2010) 2826-2830.

[12] D. Fu, The synthesis and properties of ZnO–graphene nano hybrid for photodegradation of organic pollutant in water, Materials Chemistry and Physics, 132 (2012) 673.

[13] B. Li, ZnO/graphene-oxide nanocomposite with remarkably enhanced visible-light-driven photocatalytic performance, Journal of Colloid and Interface Science, 377 (2012) 114.

[14] G. Williams, Graphene− Semiconductor Nanocomposites: Excited-State Interactions between ZnO Nanoparticles and Graphene Oxide†, Langmuir, 25 (2009) 13869.

[15] H. Zhang, X. Lv, Y. Li, Y. Wang, J. Li, P25-graphene composite as a high performance photocatalyst, ACS nano, 4 (2010) 380-386.

[16] O. Akhavan, Graphene Nanomesh by ZnO Nanorod Photocatalysts, ACS nano, 4 (2010) 4174-4180.

[17] Y. Fan, H.-T. Lu, J.-H. Liu, C.-P. Yang, Q.-S. Jing, Y.-X. Zhang, X.-K. Yang, K.-J. Huang, Hydrothermal preparation and electrochemical sensing properties of TiO2-graphene nanocomposite, Colloids and Surfaces B: Biointerfaces, 83 (2011) 78-82.

[18] O. Akhavan, Photocatalytic reduction of graphene oxides hybridized by ZnO nanoparticles in ethanol, Carbon, 49 (2011) 11-18.

[19] Z.J. Fan, Facile synthesis of graphene nanosheets via Fe reduction of exfoliated graphite oxide, ACS nano, 5 (2011) 191.

[20] G. Wang, Synthesis and characterisation of hydrophilic and organophilic graphene nanosheets, Carbon, 47 (2009) 1359.

[21] H. Nishizawa, T. Tani, K. Matsuoka, Crystal Growth of ZnO by Hydrothermal Decomposition of Zn-EDTA, Journal of the American Ceramic Society, 67 (1984) C-98-C-100.

[22] X.M. Sun, X. Chen, Z.X. Deng, Y.D. Li, A CTAB-assisted hydrothermal orientation growth of ZnO nanorods, Materials Chemistry and Physics, 78 (2003) 99-104.

[23] W.S. Hummers Jr, Hummers, Preparation of graphitic oxide, Journal of the American Chemical Society, 80 (1958) 1339.

[24] J.Y. Jang, M.S. Kim, H.M. Jeong, C.M. Shin, Graphite oxide/poly(methyl methacrylate) nanocomposites prepared by a novel method utilizing macroazoinitiator, Composites Science and Technology, 69 (2009) 186-191.

[25] H. Zhang, D. Yang, Y. Ji, X. Ma, J. Xu, D. Que, Low Temperature Synthesis of Flowerlike ZnO Nanostructures by Cetyltrimethylammonium Bromide-Assisted Hydrothermal Process, The Journal of Physical Chemistry B, 108 (2004) 3955-3958.

[26] N. Li, Battery Performance and Photocatalytic Activity of Mesoporous Anatase TiO2 Nanospheres/Graphene Composites by Template-Free Self-Assembly, Advanced functional materials, 21 (2011) 1717.

[27] M. Khenfouch, M. Baïtoul, M. Maaza, White photoluminescence from a grown ZnO nanorods/graphene hybrid nanostructure, Optical Materials, 34 (2012) 1320-1326.

[28] A.C. Ferrari, J.C. Meyer, V. Scardaci, C. Casiraghi, M. Lazzeri, F. Mauri, S. Piscanec, D. Jiang, K.S. Novoselov, S. Roth, A.K. Geim, Raman Spectrum of Graphene and Graphene Layers, Physical Review Letters, 97 (2006) 187401.

[29] Q.P. Luo, Reduced graphene oxide-hierarchical ZnO hollow sphere composites with enhanced photocurrent and photocatalytic activity, The journal of physical chemistry. C, 116 (2012) 8111.

[30] S. Zhu, J. Zhang, X. Liu, B. Li, X. Wang, S. Tang, Q. Meng, Y. Li, C. Shi, R. Hu, B. Yang, Graphene quantum dots with controllable surface oxidation, tunable fluorescence and up-conversion emission, RSC Advances, 2 (2012) 2717-2720.

[31] X. Zhou, Hydrothermal preparation of ZnO-reduced graphene oxide hybrid with high performance in photocatalytic degradation, Applied surface science, 258 (2012) 6204.

[32] A. Eckmann, A. Felten, A. Mishchenko, L. Britnell, R. Krupke, K.S. Novoselov, C. Casiraghi, Probing the Nature of Defects in Graphene by Raman Spectroscopy, Nano Letters, 12 (2012) 3925-3930.

[33] Z. Ni, Y. Wang, T. Yu, Z. Shen, Raman spectroscopy and imaging of graphene, Nano Research, 1 (2008) 273-291.

[34] B. Li, T. Liu, Y. Wang, Z. Wang, ZnO/graphene-oxide nanocomposite with remarkably enhanced visible-light-driven photocatalytic performance, Journal of Colloid and Interface Science, 377 (2012) 114-121.

[35] L. Jia, Highly durable N-doped graphene/CdS nanocomposites with enhanced photocatalytic hydrogen evolution from water under visible light irradiation, The journal of physical chemistry. C, 115 (2011) 11466.

[36] Z. Gu, C. Li, G. Wang, L. Zhang, X. Li, W. Wang, S. Jin, Synthesis and characterization of polypyrrole/graphite oxide composite by in situ emulsion polymerization, Journal of Polymer Science Part B: Polymer Physics, 48 (2010) 1329-1335.

5

5 Ta_2O_5 photocatalyst with graphene dopant for methylene blue decomposition

Abstract

Carbon or nitrogen element was successfully doped into the lattice of tantalum pentoxide photocatalyst using three different compounds: ammonia, graphene and C_3N_4. Those catalysts were analysed by X-ray diffraction; UV–vis diffuse reflectance spectra and Fourier transform infrared spectroscopy (FTIR). Their photocatalytic behaviour was investigated in methylene blue decomposition. Under UV-visible illuminations, the modified catalysts could decompose methylene blue, showing better activity than undoped Ta_2O_5. However, only N-doped Ta_2O_5 showed activity under visible light.

5.1 Background Introduction

Since 1967, photocatalytic reaction is successfully adopted to spilt water into H_2 and O_2 (Honda-Fujishima Effect), and ever since photocatalysis has been extensively studied. The most common photocatalyst TiO_2 with a wide band gap (about 3.2 eV) can only be stimulated under ultraviolet (UV) illumination. To hunt for photocatalysts with visible light response more and more researchers focus on photocatalyst modification [1]. A photocatalyst, Ta_2O_5, with a high refractive index and high hydrophilicity has also been extensively studied. Due to the high oxidation potential for excitation at near- ultraviolet (UV) to infrared (IR) spectra [2, 3] this material demonstrates better performance than TiO_2 [4]. However owing to its high band gap (3.7 eV), it merely responds to visible radiation [5], and the high thermal stabilization (it decomposes only at temperatures >1470 °C) makes its modification rather difficult. There are some reports in photocatalytic performance of $Ta_2O_{5-x}N_x$ particles under visible light [2] [6] [7] [8, 9]. For N-modification, Ta_2O_5 particles or precursors have to be calcined in ammonia gas for more than 24 hours. But the gas leaking into the environment restricts this method for a wide adoption.

Graphene is a single layer of carbon atom, tightly stacking into a two-dimensional honeycomb sp^2 carbon lattice. It possesses a large surface area, chemical stability, and very high electron transfer, which make it as a good candidate for catalyst carrier, carbon dopant and photo-electron accepter [10-12]. There are many reports on graphene doped/coupled TiO_2 compositions for organic/inorganic degradation with visible light [13-15].

Since the single atomic layer graphene has been found, the graphene-liked single lay lattice compounds stimulated the intensive studying. Graphitic carbon nitride (g-C_3N_4) (Figure 5.1) is a stable, metal-free photocatalyst showing visible light response. The g-C_3N_4 possesses

dislocation in π states, different from graphene. The band gap is 2.7 eV with conduction band at -1.3 eV and valence band at 1.3 eV[16].

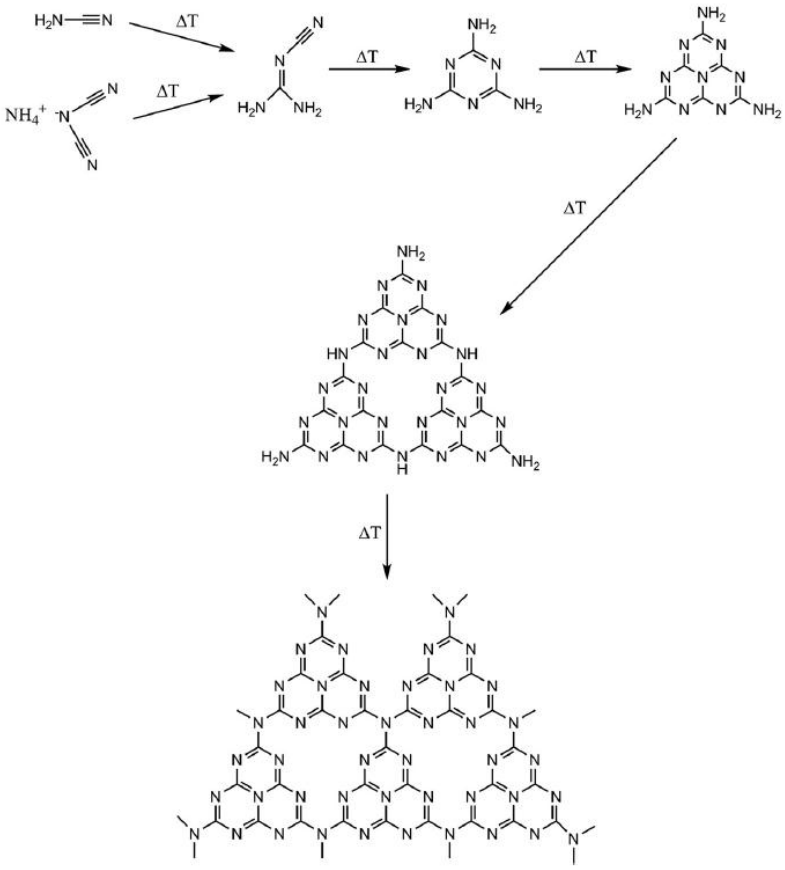

Figure 5. 1 The g- C_3N_4 chemical structure[17]

In this study, we prepared several composites based on Ta_2O_5. A commercial Ta_2O_5 subjected to ammonia treatment; reduced graphene oxide (RGO) and g-C_3N_4 doping were conducted. The photocatalytic behaviour was examined in decomposition of methylene blue (MB) under simulated sunlights and visible lights.

5.2 Catalyse Synthesizing

1. Materials and reagents

Natural graphite powders (AF99, 325 meshes, 99.995% carbon content) were used for GO synthesis. All other reagents, sulphuric acid (95–98%, Shcarlau), $KMnO_4$ (Fluka), H_2O_2 (30%, Biolab), were used as received. Hexadecyltrimethylammonium (CTAB), commercial Ta_2O_5 (> 99.99%) and melamine were obtained from Sigma–Aldrich.

2. Preparation of G-Ta_2O_5 and g-C_3N_4-Ta_2O_5 samples

Graphene oxide (GO) was prepared by a modified Hummers method [18, 19] and reduction of exfoliated GO was obtained by hydrothermal solvation using hydrazine hydrate. Typically, GO (100 mg) was loaded in a 250 mL round bottom flask with 100 mL deionized water and subjected to ultrasonic treatment for 2 h, yielding a homogeneous yellow-brown dispersion. Hydrazine hydrate (1.00 mL) was then added in and the solution was heated at 100 ℃ for 24 h. The reduced GO (RGO) was gradually precipitated as a black solid. This product was separated by filtration and washed with ethanol and water several times and then dried at 80 ℃.

The g-C_3N_4 was prepared by melamine decomposition. Typically, 5 gram melamine were calcined in a semi-closed crucible in air at 500 ℃ for 30 min, and then a slight yellow product was grinded into powder.

For synthesis of G-Ta_2O_5, RGO powder, hexadecyltrimethylammonium bromide (CTAB, 0.5 g, which was used to accelerate exfoliation process of RGO[20]) and 30 mL ethanol were placed in a 100 mL beaker with stirring for 30 min. Then a commercial Ta_2O_5 sample was

added into the solution. The suspension was stirred for 8 h and dried at 80 ℃. After that, the solid was calcined in a muffle furnace at 500 ℃ for 5 min and cooled down to 25 ℃ immediately.

For a comparison, the commercial Ta_2O_5 sample was also treated in a mist of ammonia/N_2 for 30 h at 700 ℃ to obtain N-Ta_2O_5 particles.

To obtain g-C_3N_4-Ta_2O_5 photocatalyst, the commercial Ta_2O_5 and g-C_3N_4 particles were mixed in 200 mL methanol with vigorous stirring for 24 hours and then dried in air and calcined at 700 ℃ in nitrogen gas.

3. Characterization of materials

The crystalline structure of samples was analyzed by powder X-ray diffraction (XRD) using a Bruker D8-Advance X-Ray diffractometer with Cu Kα radiation (λ = 1.5418 Å) operated at 40 kV and 30 mA. FTIR analysis was performed on a Perkin-Elmer FTIR-100 with a MIR detector. UV–vis diffuse reflectance spectra (DRS) of samples were recorded on a JASCO V670 spectrophotometer with an Ø 60 mm integrating sphere, and $BaSO_4$ was used as a reference material. Thermogravimetric-differential thermal analysis (TG-DTA) was carried out on a TGA/DSC-1 instrument of Mettler-Toledo under air flow at a heating rate of 10 ºC/min.

4. Photocatalytic tests

Photocatalytic performances of various catalysts were evaluated by the photodegradation of methylene blue (MB) under either artificial solar light or visible light. In a typical process, aqueous solution of MB (10 mg/L, 200 mL) and the photocatalysts (100 mg) were put into a 1- L double-jacket cylindrical reactor with cycled cooling water (25 ℃) and stirring. The photoreaction vessel was positioned 30 cm away from the radiation source with a cut-off

filter. Two light sources were applied. One is UV-vis light with intensities at 2.31 μW/cm^2 (220-280 nm), 6.94 mW/cm^2 (315-400 nm), 129.3 mW/cm^2 (400-1050 nm). The other is visible light with an intensity of 84 mW/cm^2 at 400-1050 nm. The reaction solution was firstly kept in dark and stirred for 30 min. The photocatalytic reaction was started by turning on the halogen lamp. At given time intervals, the dispersion was centrifuged and the MB solution was analyzed by a JASCO UV-vis spectrophotometer at a wavelength of 664 nm.

5.3 Catalysis Reaction Evaluation

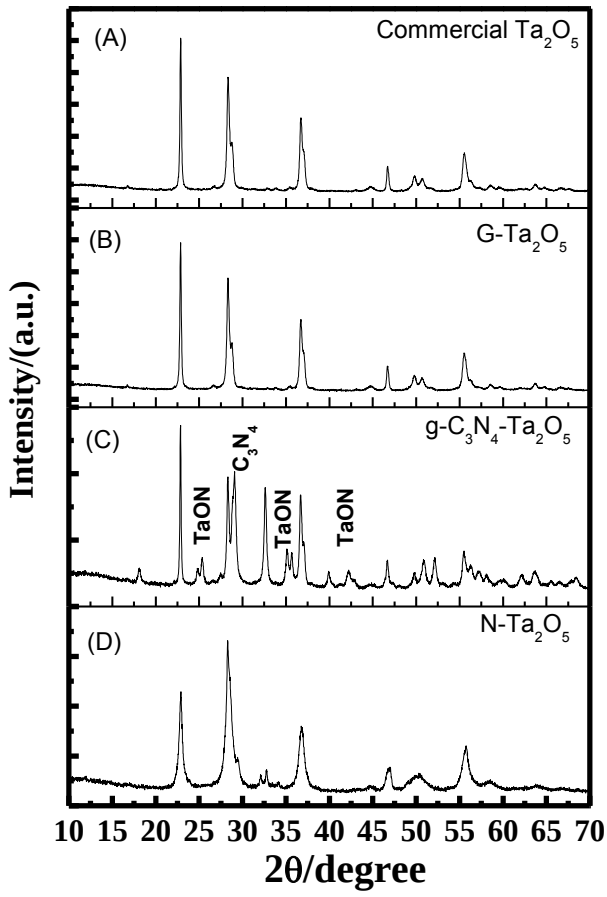

Figure 5. 2 XRD patterns of (a) undoped commercial Ta_2O_5, (b) Graphene doped Ta_2O_5 (c) g-C_3N_4 doped Ta_2O_5 and (D) nitrogen doped Ta_2O_5 .

Figure 5.2 reveals X-ray diffraction (XRD) patterns of commercial Ta_2O_5, graphene doped Ta_2O_5, g-C_3N_4 doped Ta_2O_5 and nitrogen doped Ta_2O_5 photocatalyst (N-Ta_2O_5). It is observed that graphene dopant could not affect the XRD pattern of commercial Ta_2O_5. N-Ta_2O_5 curve shows difference from Ta_2O_5. Some weak peaks of TaON were detected in the XRD analysis. Strong C_3N_4 peaks can be found in g-C_3N_4-Ta_2O_5 sample[21], and TaON peaks can also be found in the patterns.

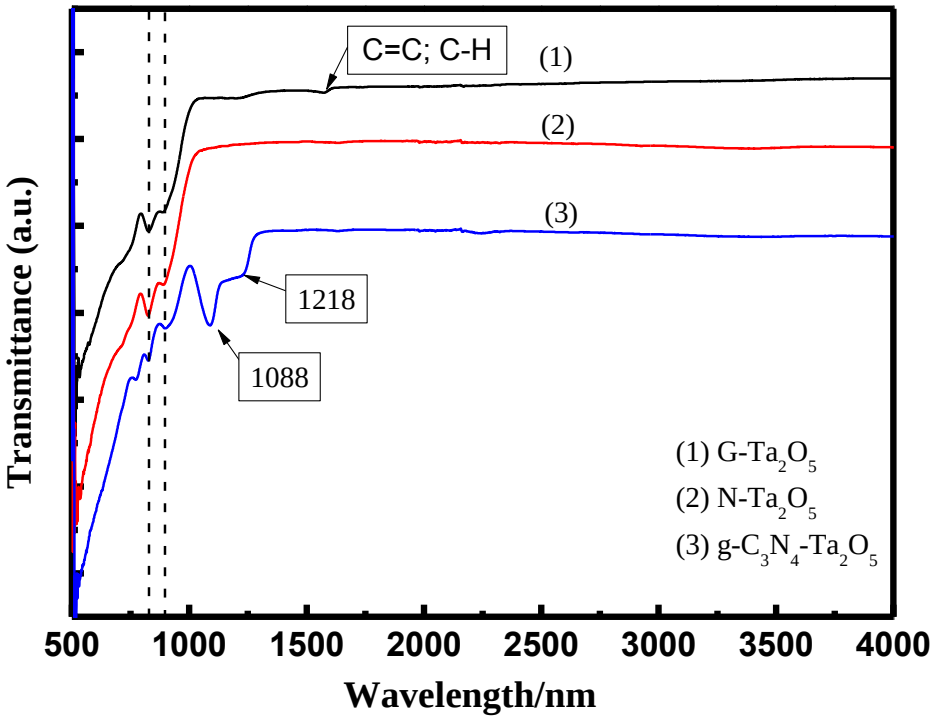

Figure 5. 3 FTIR spectra of (1) G-Ta_2O_5, (2)N-Ta_2O_5 and g-C_3N_4 –Ta_2O_5

FTIR spectra (Figure 5.3) indicate the presence of strong absorption peaks around 820 cm^{-1} to 900 cm^{-1} corresponding to Ta-O-Ta lattice. In graphene doped Ta_2O_5 pattern the absorption band near 1640 cm^{-1} can be found, which is attributed to C–H and C=C stretching. There is no other peak in N-Ta_2O_5. In g-C_3N_4-Ta_2O_5 sample, absorption peaks could be found near 1088 cm^{-1} to 1220 cm^{-1} which represents the aromatic C − N stretching of g-C_3N_4 layer.

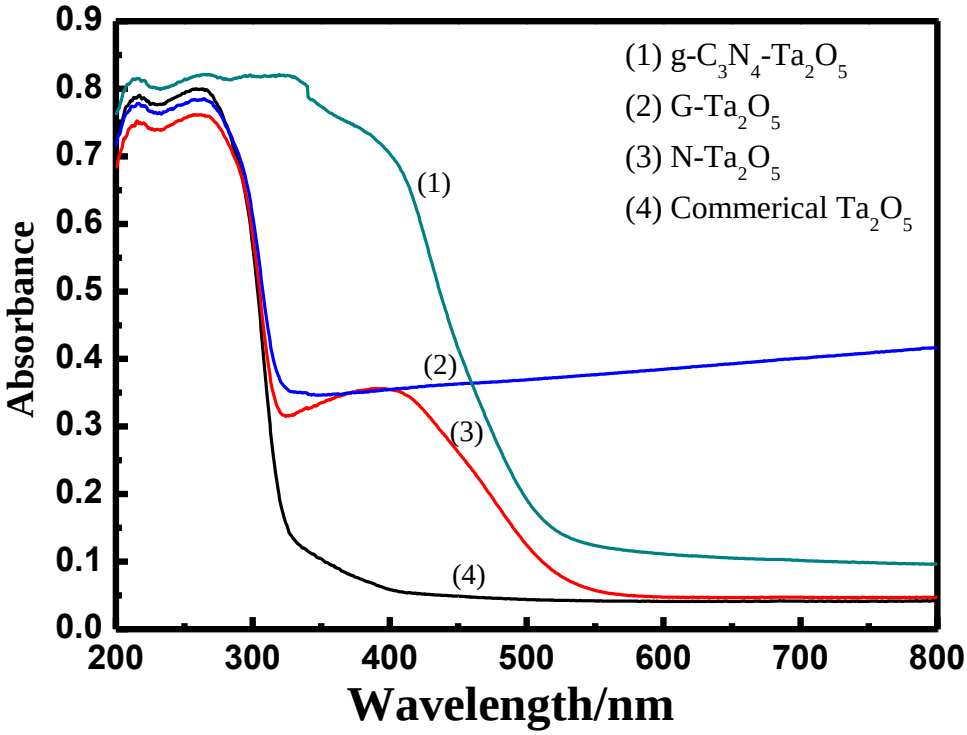

Figure 5. 4 Diffuse reflectance spectroscopy of (1) g-C_3N_4 doped Ta_2O_5, (2) RGO doped Ta_2O_5, (3) Nitrogen doped Ta_2O_5 and (4) naked commercial Ta_2O_5.

Figure 5.4 shows the spectra of UV-vis diffuse reflectance spectroscopy of g-C_3N_4 doped, graphene doped, nitrogen doped and naked Ta_2O_5 samples, which clearly indicates the effect of doping on the optical absorption of Ta_2O_5. The g-C_3N_4 dopant can shift the maximum absorption shape edge of Ta_2O_5 from about 300 nm to 450 nm, which is in the visible light region. Graphen could not make a shift of edge but it could absorb light in all region[22] and it also could enhance of radiation absorption of Ta_2O_5 in visible light. The N-doped commercial Ta_2O_5 has two absorption onsets at 330 nm and 550 nm, which suggests it could be excited at over 400 nm wavelengths. The naked Ta_2O_5 could absorb the radiation of UV before 300 nm.

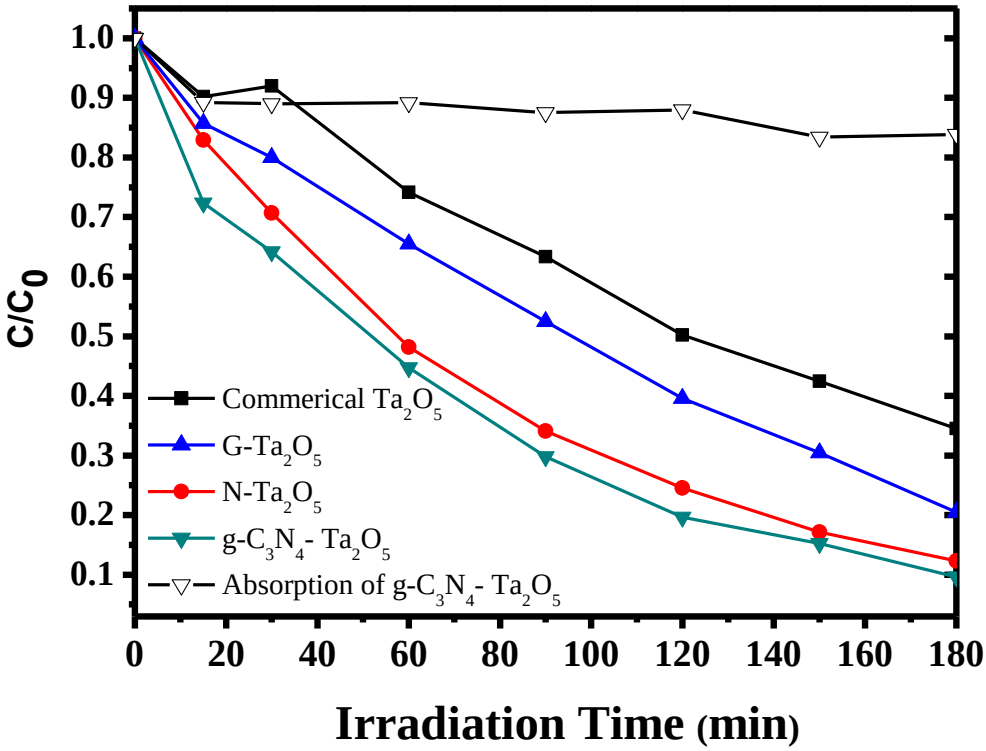

Figure 5. 5 Photocatalytic degradation of MB with Commerical Ta_2O_5, G- Ta_2O_5, N- Ta_2O_5, g-C_3N_4-Ta_2O_5 under UV-visible radiation; and the the MB absorption of g-C_3N_4-Ta_2O_5 particle.

In the photocatalytic reaction investigation, all samples firstly have been tested under UV-visible radiation. Figure 5.5 shows that all catalysts have a potential to mineralize the aromatic dye, methylene blue, in 3 hours. About 65% of MB could be eliminated by commercial Ta_2O_5. The catalyst, g-C_3N_4-Ta_2O_5 has the most powerful ability to degrade MB while it showed weak adsorption. N-doped Ta_2O_5 presented slightly lower activity than g-C_3N_4-Ta_2O_5. The graphene doped Ta_2O_5 sample could decompose 85% MB in 3 hours due to the strong adsorption of graphene single layer toward aromatic structure of MB[23, 24].

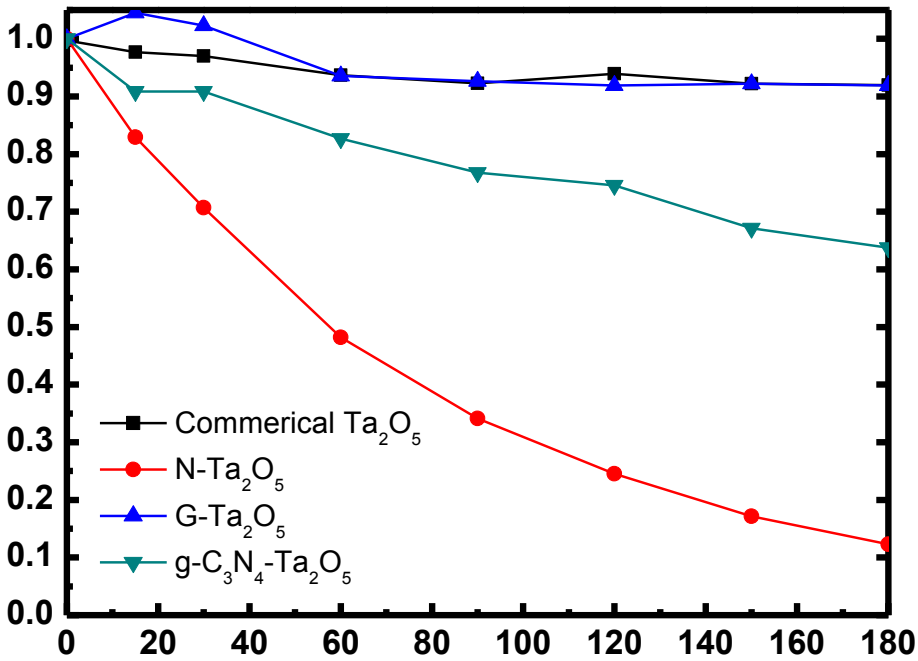

Figure 5. 6 Photocatalytic degradation of MB with Commerical Ta_2O_5, G-Ta_2O_5, N-Ta_2O_5, g-C_3N_4-Ta_2O_5 under visible radiation.

The Ta_2O_5 based samples were further studied under visible light (Figure 5.6), Ta_2O_5 and graphene doped sample have merely no activity under visible illumination. The nitrogen doped Ta_2O_5 has the similar MB degradation under UV-vis and visible radiation. The g-C_3N_4 doped sample has weak MB degradation in 3 hours.

The N-Ta_2O_5 having significant photocatalytic performance can be contributed by absorption edge at 550 nm in UV-vis diffuse reflectance spectroscopy which extends the absorption range of radiation in visible area. G-Ta_2O_5 has not been excited under visible light which indicates that there is no interaction between commercial Ta_2O_5, however graphene sheet has strong light absorption in all range but it does not have new band gap by its own. The g-C_3N_4 could enhance the Ta_2O_5 performance under visible weakly which was assumed that the photo electron from nitrogen is emitted in carbon states directly not to the orbit of tantalums.

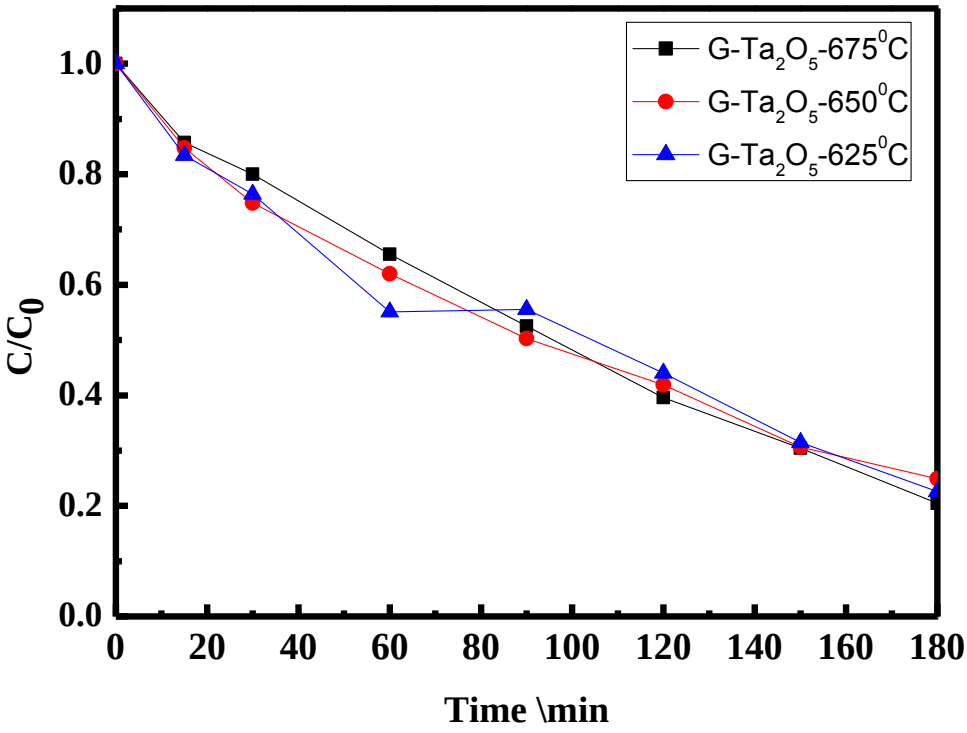

Figure 5. 7 Photocatalytic degradation of MB with Commercial Ta_2O_5, G-Ta_2O_5, N-Ta_2O_5, g-C_3N_4-Ta_2O_5 under visible radiation.

We also investigated the effect of calcinations temperature on catalytic performance of graphene doped commercial Ta_2O_5. The photocatalytic decomposition of MB at UV-vis light was demonstrated in Figure 5.7. There are no differences in activity among three samples. After 3 h radiation, about 80％ MB has been decomposed.

5.4 Results and Conclusion

Three dopants were adopted to modify a commercial Ta_2O_5 in this study. Nitrogen doped Ta_2O_5 has the best performance under visible or UV-vis radiation. Graphene doped Ta_2O_5 photocatalyst could not decompose MB pollutant under visible light radiation though graphene can enhance the light absorption at visible range of the catalyst. The g-C_3N_4 doped Ta_2O_5 works under UV-vis radiation but not effective as N-Ta_2O_5 under visible light.

5.5 Reference

[1] A. Fujishima, Titanium dioxide photocatalysis, Journal of photochemistry and photobiology. C, Photochemistry reviews, 1 (2000) 1.

[2] G. Hitoki, T. Takata, J.N. Kondo, M. Hara, H. Kobayashi, K. Domen, An oxynitride, TaON, as an efficient water oxidation photocatalyst under visible light irradiation ($\lambda \leq 500$ nm), Chemical Communications, (2002) 1698-1699.

[3] K. Harata, H. Akasaka, T. Endo, H. Nagase, H. Ueda, X-Ray structure of the [small delta]-cyclodextrin complex with cycloundecanone, Chemical Communications, 0 (2002) 1968-1969.

[4] W.-J. Chun, A. Ishikawa, H. Fujisawa, T. Takata, J.N. Kondo, M. Hara, M. Kawai, Y. Matsumoto, K. Domen, Conduction and Valence Band Positions of Ta2O5, TaON, and Ta3N5 by UPS and Electrochemical Methods, The Journal of Physical Chemistry B, 107 (2003) 1798-1803.

[5] R. Nashed, W.M.I. Hassan, Y. Ismail, N.K. Allam, Unravelling the interplay of crystal structure and electronic band structure of tantalum oxide (Ta2O5), Physical Chemistry Chemical Physics, (2013).

[6] M. Hara, G. Hitoki, T. Takata, J.N. Kondo, H. Kobayashi, K. Domen, TaON and Ta3N5 as new visible light driven photocatalysts, Catalysis Today, 78 (2003) 555-560.

[7] T. Murase, H. Irie, K. Hashimoto, Visible Light Sensitive Photocatalysts, Nitrogen-Doped Ta2O5 Powders, The Journal of Physical Chemistry B, 108 (2004) 15803-15807.

[8] Y. Takahara, J.N. Kondo, T. Takata, D. Lu, K. Domen, Mesoporous Tantalum Oxide. 1. Characterization and Photocatalytic Activity for the Overall Water Decomposition, Chemistry of Materials, 13 (2001) 1194-1199.

[9] M. Hara, J. Nunoshige, T. Takata, J.N. Kondo, K. Domen, Unusual enhancement of H2 evolution by Ru on TaON photocatalyst under visible light irradiation, Chemical Communications, (2003) 3000-3001.

[10] J. Yan, T. Wei, W. Qiao, B. Shao, Q. Zhao, L. Zhang, Z. Fan, Rapid microwave-assisted synthesis of graphene nanosheet/Co3O4 composite for supercapacitors, Electrochimica Acta, 55 (2010) 6973-6978.

[11] X. Li, Y. Zhu, W. Cai, M. Borysiak, B. Han, D. Chen, R.D. Piner, L. Colombo, R.S. Ruoff, Transfer of large-area graphene films for high-performance transparent conductive electrodes, Nano Letters, 9 (2009) 4359-4363.

[12] T. Mueller, F. Xia, P. Avouris, Graphene photodetectors for high-speed optical communications, Nature Photonics, 4 (2010) 297-301.

[13] M. Wojtoniszak, B. Zielinska, X. Chen, R.J. Kalenczuk, E. Borowiak-Palen, Synthesis and photocatalytic performance of TiO 2 nanospheres–graphene nanocomposite under visible and UV light irradiation, Journal of Materials Science, (2012) 1-6.

[14] H. Zhang, X. Lv, Y. Li, Y. Wang, J. Li, P25-graphene composite as a high performance photocatalyst, Acs Nano, 4 (2009) 380-386.

[15] O. Akhavan, E. Ghaderi, Photocatalytic reduction of graphene oxide nanosheets on TiO2 thin film for photoinactivation of bacteria in solar light irradiation, The Journal of Physical Chemistry C, 113 (2009) 20214-20220.

[16] J. Zhang, J. Sun, K. Maeda, K. Domen, P. Liu, M. Antonietti, X. Fu, X. Wang, Sulfur-mediated synthesis of carbon nitride: Band-gap engineering and improved functions for photocatalysis, Energy & Environmental Science, 4 (2011) 675-678.

[17] H. Yan, Y. Chen, S. Xu, Synthesis of graphitic carbon nitride by directly heating sulfuric acid treated melamine for enhanced photocatalytic H2 production from water under visible light, International Journal of Hydrogen Energy, (2011).

[18] W.S. Hummers Jr, Hummers, Preparation of graphitic oxide, Journal of the American Chemical Society, 80 (1958) 1339.

[19] J.Y. Jang, M.S. Kim, H.M. Jeong, C.M. Shin, Graphite oxide/poly(methyl methacrylate) nanocomposites prepared by a novel method utilizing macroazoinitiator, Composites Science and Technology, 69 (2009) 186-191.

[20] N. Li, Battery Performance and Photocatalytic Activity of Mesoporous Anatase TiO2 Nanospheres/Graphene Composites by Template-Free Self-Assembly, Advanced functional materials, 21 (2011) 1717.

[21] H. Yan, TiO2–gC3N4 composite materials for photocatalytic H2 evolution under visible light irradiation, Journal of alloys and compounds, 509 (2011) L26.

[22] F. Xia, D.B. Farmer, Y. Lin, P. Avouris, Graphene field-effect transistors with high on/off current ratio and large transport band gap at room temperature, Nano Letters, 10 (2010) 715-718.

[23] H. Zhang, P25-graphene composite as a high performance photocatalyst, ACS nano, 4 (2010) 380.

[24] Q. Xiang, J. Yu, M. Jaroniec, Graphene-based semiconductor photocatalysts, Chemical Society reviews, 41 (2012) 782-796.

6 Conclusion and future work

6.1 Concluding remarks

The major objectives of this research were to synthesize graphene and to fabricate graphene doped nanoparticles (TiO_2, ZnO and Ta_2O_5) as photocatalysts in order to test their activities in decomposition of methylene blue dye under visible illumination. The exfoliated graphene was obtained from chemical oxidation of a natural graphite powder. The graphene-like compound, graphitic carbon nitride (g-C_3N_4), was synthesized by thermal treatment of melamine. TiO_2 was either obtained from a commercial nano TiO_2 particle (P25) or synthesized from titanium (IV) isopropoxide by a sol-gol method. Graphene-doped TiO_2 was prepared by a sol-gel synthesis. For graphene doped ZnO, zinc powder was used as ZnO precursor and GO reducing agent in one step synthesis. Ta_2O_5 modification was carried out using ammonia, RGO and g-C_3N_4 to obtain N-doped and carbon doped Ta_2O_5. Photocatalytic evaluations indicate that all these photoparticles could degrade organic dye MB under visible light or UV-visible light in aqueous solution.

6.2 Effect of graphene doping on TiO_2

Graphene doped tatiana with high photocatalytic performance under visible light has been successfully prepared by a sol-gel method. Graphene dopant results in a strong red shift of UV-spectra on G-TiO_2. The G-TiO_2 catalysts exhibited higher efficiency in degradation of methylene blue under visible light than G-P25 photocatalyst.

Three different oxidants were also used with G-TiO_2 photocatalyst for catalytic reaction. Peroxymonosulphate (PMS), peroxydisulphate (PDS) and hydrogen peroxide (H_2O_2) could

enhance MB decomposition process. H_2O_2 presented the best catalytic performance and complete MB decomposition reaction could achieve in 20 min at 10 ppm MB.

6.3 One step synthesis of RGO doped ZnO photocatalysts

One-step hydrothermal method has been successfully employed to synthesize graphene-ZnO composites to decompose MB dye under artificial solar illumination. Zn powder was a reducing agent for graphene oxide and source for ZnO. The G-ZnO catalysts exhibited better efficiency than the artificial ZnO under the same conditions.

6.4 NH_4OH, RGO and g-C_3N_4 modified commercial Ta_2O_5 photocatalysts

The elements, nitrogen, carbon or nitrogen/carbon, were doped to commercial Ta_2O_5 particles by ammonia gas, RGO and g-C_3N_4. Nitrogen doped Ta_2O_5 particle has the best performance under UV-vis or visible radiation. Graphene doped Ta_2O_5 photocatalyst could not decompose MB under visible light radiation but graphene can enhance the light absorption of the new catalyst. The g-C_3N_4 doped Ta_2O_5 works under both UV-vis radiation and visible light but the degradation of MB was lower.

6.5 Recommendation for future work

All the studies were focused on photocatalyst modification by graphene or graphene-like dopants for aromatic organic water pollutant (MB) treatment with UV/Visible illumination.

All catalysts could decompose MB solution. However detailed study is further required to comprehensively investigate the mechanism of photocatalytic efficiency and role of carbon doping and its electronic property on photocatalysis. Future research is suggested as presented below.

It is widely accepted that graphene could be obtained via natural graphite with strong oxidation agents such as H_2SO_4, $HClO_4$, K_2MnO_4. However, laboratory routes involved are high cost, high energy consumption and safety/environment hazard. It was believed that some novel hydrothermal technologies could reduce the GO synthesis requirements and enhance the natural graphite separation in liquid. This path will greatly reduce raw material consumption; further study will focus on substitution of strong oxidation agents.

In the study of SEM, graphene single sheet was merely found in our samples. It is widely accepted that GO particle tends to aggregate in its suspension even after a long time ultrasonic treatment and it is difficult to make single layer graphene sheet. Numerous methods were applied to separate block GO, such as microwave, vacuum evaporation and so on. In the studies of UV-visible spectra, block GO or RGO has strong absorption in all region of radiation. It is found that graphene particle is easy to cover semiconductor particles and impede radiation absorption over the catalyst. Also the different graphene contents did not affect the ZnO and commercial Ta_2O_5 on MB degradation under visible light. So the way to obtain single layer GO or thin block GO is required. Chemical vapor deposition method (CVD) is one of efficient methods. In further study CVD will be adopted to produce single/thin layer GO which maybe improve the photocatalytic performance.

FTIR study showed three functional groups could be found on GO sheet: hydroxyl, carboxy and epoxy groups. Several studies indicate that oxygen content affects the band gap energy of graphene oxide which will affect the activity of graphene doped photocatalysts under visible light. Different reduction agents will greatly affect the oxygen content of RGO such as NaOH, KOH, hydrazine hydrate and so on. In future, RGO from different reduction methods will be used in order to study the interaction between catalyst and graphene.

Many studies indicate there are two types of defects around graphene sheet; zig-zag and armchair. Defects have different electronic properties which will affect pollutant adsorption and reaction. The chemical tailoring should be applied to produce epical defects on graphene sheet, and requires more investigation in the future.

In our study, three photocatalysts were modified to improve their photocatalytic performance. G-TiO_2 demonstrates the best performance in MB decomposition under UV and visible light. G-ZnO and G-Ta_2O_5, however, exhibited activity only under UV light. In this case the photocatalytic material selection plays a significant role and alternative materials with solar energy responsive, high reaction performance and environment compatible should be developed using co-doping precursor such as g-C_3N_4.